Development of a Dual-Modal Microfluidic Paper-Based Analytical Device for the Quantitative and Qualitative Detection of The Total Hardness of Water.

Oyejide Damilola Oyewunmi

A Thesis

In the Department of

Mechanical and Industrial Engineering

Presented in partial fulfilment

of the requirements for the degree

Master of Applied Science (Mechanical Engineering) at

Concordia University

Montreal, Quebec, Canada.

November 2020

CONCORDIA UNIVERSITY

School of Graduate Studies

This is to certify that the thesis prepared,

By: Oyejide Damilola Oyewunmi

Entitled: **Development of a Dual-Modal Microfluidic Paper-Based Analytical Device for the Quantitative and Qualitative Detection of The Total Hardness of Water.**

And submitted in partial fulfilment of the requirements for the degree of

Master of Applied Science (Mechanical Engineering)

Complies with the regulations of the University and meets the accepted standards with respect to originality and quality.

Signed by the Final Examination Committee:

_____ Chair

_____ Examiner 1
Dr. Alex De Visscher

_____ Examiner 2
Dr. Farjad Shadmehri

_____ Supervisor
Dr. Sana Jahanshashi Anbuhi

Approved by: _____
Dr. Mamoun Medraj Graduate Program Director

Date: 30th November 2020 _____Dean of Faculty
Dean Mourad Debbabi

Abstract

Development of a Dual-Modal Microfluidic Paper-Based Analytical Device for the Quantitative and Qualitative Detection of The Total Hardness of Water.

Oyejide Damilola Oyewunmi

A dip-and-read microfluidic paper-based analytical device (μPAD) was developed for the qualitative and quantitative detection of the total hardness of water. To create well-defined hydrophobic barriers on filter paper, a regular office printer and a commercially available permanent marker pen were utilized as a quick and simple technique with easily accessible equipment/materials to fabricate μPAD in new or resource-limited laboratories without sophisticated equipment. After a wettability and barrier efficiency analysis on the permanent marker colors, the blue and green ink markers exhibited favorable hydrophobic properties and were utilized in the fabrication of the developed test devices. The device had five reaction and detection zones modeled after the classification given by the World Health Organization (WHO), so qualitatively it determined whether the water was 'soft', 'moderately hard', 'hard', or 'very hard' by changing color from blue to pink in about 3 min. The device was also used to introduce an alternative colorimetric reaction for quantitative analysis of the water hardness without the need for ethylenediaminetetraacetic acid (EDTA) and without compromising the simplicity and low cost of the device. The developed μPAD showed a calculated limit of detection (LOD) of 0.02 mM, which is at least 80% less than those of commercially available test strips and other reported μPADs, and the results of the real-world samples were consistent with those of the standard titration (with EDTA). In addition, the device exhibited stability for 2 months at room and frigid condition (4 °C) and at varying harsh temperatures from 25 to 100 °C. The results demonstrate

that the developed paper-based device can be used for rapid, on-site analysis of water with no interferences and no need for a pipette for sample introduction during testing.

A mathematical estimation of the flow of liquid water and blood serum on the fabricated paper device was computed using a geometrically modified version of the Lucas-Washburn equation to predict the signal time of the paper sensor during each test. The estimation correlated excellently with experimental data and observation, hence making the modification of the Lucas-Washburn equation valid specifically for the fabricated μPAD.

Finally, all-inclusive pullulan tablets were fabricated as an alternative analytical platform to detect the total hardness of water. The assay was used to compute a calibration curve which can be used to quantify the total hardness of water in about five minutes by just dropping the required number of tablets in the water sample, and a limit of detection of 0.0140 mM was achieved.

List of publications and conference contributions

The following list of publications and conference proceedings show my contribution to the annals of research in the course of this thesis. The last two publications are not presented in this thesis.

- **Oyejide Damilola Oyewunmi**.; Seyed Hamid Safiabadi-Tali; Sana Jahanshahi-Anbuhi. Dual-Modal Assay Kit for the Qualitative and Quantitative Determination of the Total Water Hardness Using a Permanent Marker Fabricated Microfluidic Paper-Based Analytical Device. *Chemosensors* **2020**, *8*, 97. https://doi.org/10.3390/chemosensors8040097
- **Oyejide Damilola Oyewunmi**, Sana Jahanshahi-Anbuhi. "Paper-Based Analytical Devices: A Tool to Monitor the Hardness Level of Water", CQMF-QCAM Student Symposium, Montreal, Canada, November **2019**
- **Oyejide Damilola Oyewunmi**, Sana Jahanshahi-Anbuhi. "Microfluidic Device for Detection of Water Hardness", Alembic Study Tour, Montreal, Canada, July **2019**
- **Oyejide Damilola Oyewunmi**, Sana Jahanshahi-Anbuhi. "Paper-Based Microfluidic Device for Detection of Water Hardness", Chemical engineering research day, Montreal, Canada, March **2019**
- Amir Esfahani, Zubi Sadiq, **Oyejide Damilola Oyewunmi**, Ndifreke Usen, Daria Camilla Boffito, Sana Jahanshahi-Anbuhi. Portable, stable and sensitive assay to detect phosphate in water with gold nanoparticles (AuNPs) and dextran tablet. Analyst, 2020, (Under review)
- Seyed Hamid Safiabadi Tali, Jason J. LeBlanc, Zubi Sadiq, **Oyejide Damilola Oyewunmi**, Carolina Camargo Buritica, Bahareh Nikpour, Narges Armanfard, Selena M. Sagan, Sana Jahanshahi-Anbuhi. Overview and Outlook on Diagnostic methods for SARS-CoV-2, Clinical Microbiology Reviews, 2020, (Under review)

Acknowledgment

This research work was supervised by Dr. Sana Jahanshahi-Anbuhi, and I will like to express my sincere gratitude to her for believing in me and giving me the opportunity to be part of her amazing research group. I have immensely learnt from not only the invaluable scientific input and academic advice, but also from the aspiring life lessons, creativity, compassion and commitment. Also, I want to thank her for the support in terms of funding invested towards this project - which was provided through the Natural Sciences and Engineering Research Council of Canada discovery grant and the Concordia University FRDP grant for Development of Paper-Based Microfluidic Analytical Device (μPADs) for Diagnostic and Environmental Application. All these have made this project a success.

I wish to thank my colleagues and friends at the Concordia University, and the entire Anbuhi Research Group members for the great teamwork and their dear friendship. Special thanks to Jude Akinnawonu, Paul Unwana, Hamid Safiabadi-Tali, Amir Esfahani, and Zubi Sadiq.

Furthermore, many thanks to all the faculty members and staff that have impacted my development during this thesis. I am extending a heartfelt gratitude to Dr. Alex de Visscher, Dr. Ge li, and Harriet Laryea for their advice, encouragement and inspiration.

Lastly, I would like to express my greatest gratitude to my parents -Mr & Mrs Oyewunmi, siblings - Oyegbenga, Oyefunbi, Oyeniyi, & Oyeniran, and my fiancée – Mary Adegunloye for their continuous support and advice over the years.

Table of Contents

List of Figures

List of Tables

Abbreviations

µPAD	Microfluidic Paper-Based Analytical Device
EBT	Eriochrome Black T
EDTA	Ethylenediaminetetraacetic acid
CAPS	3- (Cyclohexylamino) propanesulphonic acid
3-D	Three Dimensional
2-D	Two Dimensional
HPLC	High performance Liquid Chromatography
PDMS	Polydimethylsiloxane
PMMA	Polymethyl methacrylate
OTS	Trichloro(octadecyl)silane
TMOS	Tetramethyl orthosilicate
qnt	Quantitative
Mn^{2+}	Manganese ion
Fe^{2+}	Iron II ion
NH^{4+}	Ammonium ion
Cl^{-}	Chloride ion
F^{-}	Fluoride ion
Cu^{2+}	Copper II ion

D	Detection zone
R	Reaction zone
C	Control zone
S	Soft water
MH	Moderately hard water
H	Hard water
VH	Very hard water
ppm	Part per million
CTS	Commercial test strip
MAC	Maximum allowable concentration
μ	Viscosity of liquid [Pa.s]
γ	Surface tension of liquid [N/m]
L	Height of the rising liquid font in the paper [m]
θ	The contact angle of liquid with the paper substrate [deg.]
t	Time taken for liquid to rise the capillary tubes [s]
D_c	Capillary pore diameter [m]
D_h	Hydraulic pore diameter [m]
D_e	Effective pore diameter [m]

r	Effective radius [m]
Ψ	Geometric correction factor [-]

1.1 Background

Water is a valuable resource for humanity. The various usage of water knows no bounds—from industrial usage to domestic and drinking purposes, to agricultural purposes, which in the end supply food for humanity. In all, there are water quality control specifications being set by regulatory organizations for the safety of humanity and the environment. Hardness of water is one of such water quality control specifications that is often considered before its usage. The hardness of water is defined as the amount of metallic ion present in water. And due to the relatively high concentration of calcium ion (Ca^{2+}) and magnesium ion (Mg^{2+}) in natural water as compared to other metallic ions, the hardness of water is defined basically as the total amount of calcium and magnesium ion in water reported as a calcium carbonate equivalent (Abeliotis et al., 2015; World Health Organization, 2010). The World Health Organization (WHO) grouped total hardness of water into four classes based on concentration as shown in Table 1.1 (World Health Organization, 2010).

Table 1.1 World health organization classification of total hardness of water by concentration of equivalent calcium carbonate(World Health Organization, 2010).

Concentration of Calcium carbonate (mM)	Total Hardness level
<0.61	Soft
0.61-1.20	Moderately hard
1.21-1.80	Hard
>1.80	Very hard

* *The equivalent calcium carbonate indicates the concentration of magnesium and calcium ions together.*

Hardness of water is also known as the measure of the ability of water to react with soap, and the more the hardness of the water, the larger the amount of soap needed to form lather. This generates a big issue in domestic and industrial washing, as the hard water needs to be made soft or a large amount of soap will be required for the washing operation (Abeliotis et al., 2015). Hard water also creates stain on glassware, ring deposit on bathtubs and toilet bowls. Also, it causes clogs in municipal water pipe network as well as industrial connections because of scale build-up which eventually lead to breakdown and ultimately costly repairs or overhauling (Liang et al., 2014). Excessive hardness affects the aesthetic appearance of water, which limits its acceptability by many at that level and hence water hardness is a major factor at swimming pools and other artificial water recreation centers. According to Health Canada (2019), the acceptable level of hardness in water is 80-100 mM to provide a balance between corrosion and incrustation. Moreover, excessive intake of hard water by people suffering from renal insufficiency or milk alkali syndrome causes hypercalcemia, which is due to the inability to eliminate excess nutrients in the body. This may lead to total kidney failure or death, if not properly checked (World Health Organization, 2010; Leurs et al., 2010; Sengupta, 2013). Furthermore, exposure to hard water has been reported to aggravate eczema, particularly in children (Cotruvo et al., 2017). In addition, dissolved minerals in water affects the taste, which is relative for everyone based on preference and familiarity (Cotruvo et al., 2017; Health Canada, 2019; World Health Organization, 2010). These issues have led to various investigations and innovations on how to detect the level of hardness of water and how to make hard water soft.

1.2 Motivation

The common means of determining the level of hardness of water has been the traditional titration method, the ion selective electrode analysis (Bakker, 2018), the Inductively Coupled Plasma

Atomic Emission Spectroscopy (ICP- OES) (Butcher, 2010), and Raman Spectroscopy characterization (Yang et al., 2014). These methods, though give accurate results, require bulky instruments and apparatus, need an external power source and a large amount of sample for operation, and do not allow for dynamic and point-of-use testing. These properties limit the use of these testing methods in remote areas and in some developing countries. However, testing can be made easy and readily available by fabricating simple, portable, and cheap devices that can also perform the required test with high accuracy, hence the development of microfluidic paper-based analytical device.

Microfluidic paper-based analytical devices are micro-scale instruments consisting of interconnection of micro-channels and micro-tanks, of which operating principle involves the use of some traditional separation process techniques- sedimentation, chromatography, filtration, etc.- in conjunction with physical laws- capillarity, surface tension, and wettability- to separate desired products for analysis and analyte detection on paper substrate (Almeida et al., 2018; Cate et al., 2013; Liu et al., 2019; Myers et al., 2015). The concept of operation of paper-based analytical device is to create hydrophobic barriers on paper that will limit the flow regime of liquid samples and cause flow in a well-defined way. Therefore, the best substances to create such barriers are those that are hydrophobic and can also withstand enough liquid pressure exerted by the liquid flow. Hence, creating hydrophobic barriers and hydrophilic channels.

To provide low-cost analytical testing platforms for point-of-use analysis, paper-based analytical devices (μPADs) have, over the last decade, become popular in the research community. These devices use paper as substrate, which are impregnated with reagents for systematic testing of analytes through colorimetric or other methods such as electrochemistry (Channon et al., 2018; de Oliveira et al., 2019; Jahanshahi-Anbuhi et al., 2014a, 2014b, 2012; Nantaphol et al., 2019; Sicard

et al., 2015). Many researchers have developed μPADs to detect various metals in water, such as lead (Satarpai et al., 2016), copper (Wu et al., 2019), mercury (Chen et al., 2014), iron (Marquez et al., 2019), calcium and magnesium (Jarujamrus et al., 2019; Karita and Kaneta, 2016), chromium (Rattanarat et al., 2013), zinc (Kudo et al., 2017), and nickel (Yamada et al., 2018). However, most of these μPADs either required the use of a volume calibrated tool for sample introduction or did not perform both qualitative and quantitative detection simultaneously.

To allow defined flow of liquid along defined paths on papers, the principle of hydrophobicity and hydrophilicity is used to create well-defined channels and barriers. Several methods of μPAD fabrication have been investigated, such as Teflon stamping (Sun et al., 2018), technical drawing pen writing (Nuchtavorn and Macka, 2016), micro-embossing (Juang et al., 2019), filtration-assisted screen printing (Juang et al., 2017), chemical functionalization of papers (Devadhasan and Kim, 2018), 3D wax printing (Chiang et al., 2019), photoresist utilization (Mora et al., 2019), and direct ink writing (Ching et al., 2019). The commonest way of creating hydrophobic barriers for μPAD has been wax printing (Carrilho et al., 2009). However, as of the year 2019, the manufacturing of all the employed solid ink printers -Xerox ColorQube 8580 (Chabaud et al., 2018), ColorQube 8880 (Tan et al., 2020), ColorQube 8700 (Yehia et al., 2020), etc.- have been discontinued by Xerox – the manufacturer (Xerox Inc., n.d.). Hence, the need to look into a generally accepted method as the wax printers.

1.3 Principle of Complexometric Chelate Titration.

In the complexometric titration, water containing the unknown concentration of Ca^{2+} and Mg^{2+} is titrated against Ethylenediaminetetraacetic acid (EDTA). The reaction between Ca^{2+} and EDTA is done at a pH 10, hence a buffer with a pH 10 is added to the water sample to be analysed.

Just as in any titration experiment which requires an indicator, a metal ion indicator is used for this analysis. The choice metal ion indicator must be able to give up its metal ion to EDTA. Several metal ion indicators exist but calmagite and Eriochrome black T have been used to detect water hardness specifically (Bhattacharjee et al., 2013). Firstly, little portion of the metal ion indicator is added to the water sample, producing a wine-red/pink complex as shown by the equation 1.1 below;

$$Ca^{2+} + \underset{\text{Blue}}{In^{2-}} \rightarrow \underset{\text{Wine-red}}{CaIn} \quad (1.1)$$

Afterwards, the EDTA is titrated against the sample mixture, and the end point is indicated at the instant the red wine/pink color changes to blue, as shown by equation (1.2);

$$\underset{\text{Wine-red}}{CaIn} + EDTA^{4-} \rightarrow CaEDTA^{2-} + \underset{\text{Blue}}{In^{2-}} \quad (1.2)$$

Finally, on getting the volume of EDTA and water sample used for the titrations, the amount of $CaCO_3$ equivalent present in the sample is calculated through stoichiometry analysis and compared with approved regulated standard as shown by equation 1.3 and Table 1.1;

$$ppm\ CaCO_3 = \frac{mL\ of\ EDTA\ used\ in\ titration}{mL\ of\ water\ sample} \times 1000\ ppm \quad (1.3)$$

1.4 Pullulan tablets

It is undeniably true that paper substrates are an amazing platform for analytical assay. However, paper being used as a substrate comes with some disadvantages including; (1) the difficulty of immobilizing analytes on paper, (2) irregular patterns of paper surface matrix which causes

irregularity in result output, (3) the inconsistent lightning exposure issue when capturing detection zones for colorimetric assay.

To tackle these issues, an all-inclusive tablet-based sensor was investigated by fabricating mixtures of EBT-CAPs buffer-pullulan tablets for the detection of the total hardness of water. Pullulan is a natural polysaccharide which readily dissolves in water and solidifies on drying. Due to the water dissolving and re-solidifying phenomenon, pullulan has been employed in the pharmaceutical and food industry to manufacture food additives, breath strips, oxygen barriers and food adhesive. Also, pullulan as been reported to give stability to labile biomolecules (Jahanshahi-Anbuhi et al., 2014c), reagent immobilization (Kannan et al., 2015a), solvent barrier (Jahanshahi-Anbuhi et al., 2015), RNA protection (Hsieh et al., 2017), and Vaccine stability (Leung et al., 2019).

1.5 Objective of Thesis

The goal of this research was to fabricate portable analytical platforms for the determination of the total hardness of water. The use of commercially available permanent marker (Sharpie©) to create hydrophobic barriers and hydrophilic channels was thoroughly investigated as well. Permanent marker inks contain hydrophobic pigments, color pigments and resins which gives the water resistance strength of the pen. The pigments and resins are mostly non-polar in nature. Examples of such pigments, surfactants and resins are alkylphenol ethyoxylate, fluorocarbon, silicone, polymethyl methacrylate, octalphenol, ethoxylate and other alcohol group compounds (Mott and Walnutport Pa., 1992; Sanborn and Loftin, 1998). The fabricated μPAD was systematically designed to determine qualitatively and quantitatively the total hardness of water through the complexometric titration reactions (Figure 1.2a and b). Using the water hardness classification given by the world health organization (Table 1.1), the device qualitatively indicated if the water

sample was soft, moderately hard, hard, or very hard (Figure 1.2c). This approach makes it easy for the final consumers to get a quick and easy eye-observed result of the water hardness level. In addition, a control zone for the quantitative determination of the total hardness of water was incorporated into the design for more precise analysis (Figure 1.2d). The following sections present experiments and data leading to a simple and ready-to-use assay kit for the determination of the total hardness of water.

Furthermore, all-inclusive pullulan tablets were fabricated to test for the total hardness of water, as another analytical testing platform without the limitation of paper as substrate.

Finally, an estimation of the time it takes to get the result of the total hardness test by using the fabricated μPAD was also investigated by manipulating the properties of the Whatman® grade 4 filter paper and the reaction rate of the complexometric titration on the paper substrate.

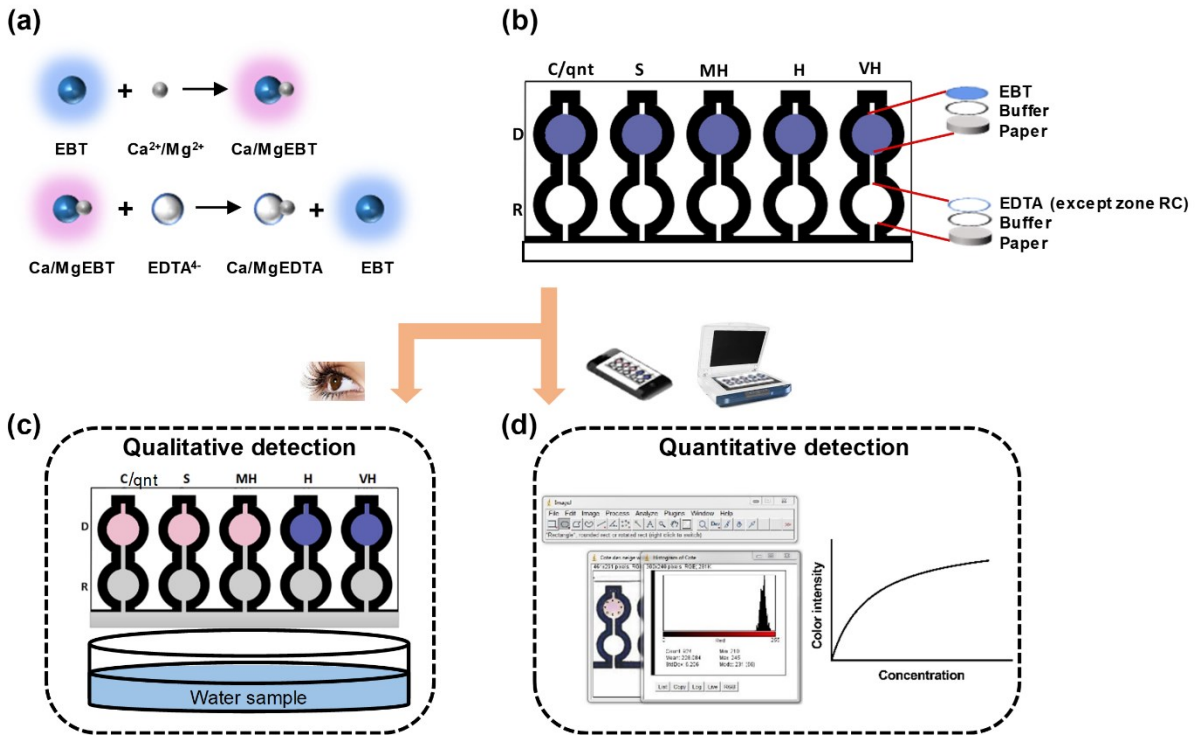

Figure 1-1 Schematic of the microfluidic paper-based analytical device (µPAD) for the detection of the total hardness of water. (a) The principle of the complexometric titration reactions; (b) the multi-layered deposition of the analytes on the µPAD; (c) the qualitative detection of the total hardness of water; (d) the quantitative detection of the total hardness of water.

1.6 Thesis organisation

The content of this thesis is outlined into five chapters. Chapter 1 provides an introduction platform which includes the background knowledge, motivation, and objectives. Chapter 2 gives a comprehensive literature review on the fabrication techniques for paper-based analytical devices, the detection procedures incorporated into such devices, and water contamination. Chapter 3 focuses on the preparation of the reagents that were used during the experiments, the experimental techniques that were employed and the fabrication procedures that were utilized for the analytical testing flatforms. Chapter 4 outlines the results obtained from each experiment and discussed in detail the fabricated of the µPAD, the all-inclusive tablet-based sensor, and the estimation of the

response time of the μPAD using the Lucas-Washburn equation. Finally, Chapter 5 gives a conclusion on the research work and future recommendations.

2.1 Introduction

Microfluidics paper-based analytical devices (μPAD) emerged in the research scene when a group of researchers at Harvard University lead by Professor George M. Whiteside's reported the use of hydrophobic polymers to create well defined hydrophilic channels on paper substrate, which was used for simultaneous detection of glucose and protein in urine sample (Martinez et al., 2007). However, the concept of paper patterning had existed for decades since Muller and Clegg reported the patterning of paper substrate with paraffin in 1949 (Müller and Clegg, 1949). These μPAD are functionalized paper substrate and micro-scale instruments consisting of interconnection of micro-channels and micro-tanks, of which the operating principle involves the use of some traditional separation process techniques- sedimentation, chromatography, filtration, etc.- in conjunction with physical laws- capillarity, surface tension, and wettability- to separate, immobilize, and store desired reagents for analysis and analyte detection (Akyazi et al., 2018; Nguyen et al., 2018; Xia et al., 2016).

Paper is an excellent substrate for the fabrication of these devices because of its properties which are particularly attractive for the manufacturers, the final consumer and the environment. Paper is know to be cheap, readily available, flexible, light weight, low thickness, and environmentally biodegradable (Akyazi et al., 2018; Credou and Berthelot, 2014; e Silva et al., 2020; Tabani et al., 2020). Paper is made of cellulose fibers in dilute aqueous suspension state which are processed by sieving, pressing, and drying to produce sheets of paper made of randomly entwined cellulose

fibers (Credou and Berthelot, 2014). These fibrous and porous configuration makes the paper to; allow the movement of fluid along the paper matrix through capillary force without the need for external forces; remove air bubble easily from the paper matric hence effecting air permeability; posses a high surface area to volume ratio which allows the possibility of analyte immobilization and storage (Henares et al., 2017; Rahbar et al., 2019; Yu et al., 2011b; Zhu et al., 2018). With the abovementioned properties, μPAD are promising tools for point-of-use monitoring of the quality of domestic tap water and large water bodies to ascertain strict compliance with laws and regulations enacted by regulatory organisations.

The current surge in population growth, urbanization and industrialization in most countries around the world has deteriorated drastically the quality of water, hence putting the fate of aquatic environment in critical conditions globally. This surge has led to enormous demand and pressure on the water resources (Almeida et al., 2018). In addition, negligence in the management of industrial and agricultural waste and other anthropogenic pollution activities have been the major contributing factors to the deterioration in water quality (Koop and van Leeuwen, 2017). These issues have led to various socioeconomic reforms and political measures on the proper management and control of water quality in other to provide safe and healthy water for human consumption and at the same time preserve our aquatic environment. To ensure adequate compliance to the reforms in the form of laws and regulations, the need for testing platforms which incorporate high accuracy and sensitivity, rapid detection and simplicity with low-cost and portability, for regulatory organisations, scientists and also the general populace who are interested in personally monitoring water quality in their jurisdiction.

Microfluidic paper-based devices have been researched and used for various medical and environmental diagnostics over the decade. And various fabrication methods have been reported

based on usage, functionality and cost. These devices provide promising advantages in terms of low-cost and portability, sensitivity and accuracy, with rapid detection and simplicity, therefore making them appropriate for point-of-use water quality monitoring. Hence, the remaining body of this review will be on the various fabrication techniques and detection procedures, and the issue of water contamination.

2.2 Fabrication Techniques

Microfluidic paper-based analytical devices can be fabricated using the two-dimensional geometry (2D) or the three-dimensional geometry (3D). The 2D geometry basically involves the functionalization of some specific areas of paper substrate to be hydrophobic or the cutting of undesired area, therefore leaving the pristine area hydrophilic. This functionalization causes well-defined hydrophilic channels or spot to be created for flow and detection of analytes with specific hydrophobic barriers (Nguyen et al., 2020; Rattanarat et al., 2013; Yamada et al., 2018). The 3D geometry on the other hand involves the stacking and assembly of different layers of functionalized paper substrate which are amalgamated with adhesives to allow flow of liquid and analytes through the interconnected channel caused by the stacking (Li and Liu, 2014; Mora et al., 2019; Santhiago et al., 2014; Tan et al., 2020). Overall, many fabrications technique have been reported in the literature for the fabrication of microfluidic paper-based analytical devices which includes : (1) Cutting, (2) Photo – Lithography, (3) Flexography printing, (4) Ink-jet etching, (5) Wax dipping, (6) Polydimethyl-siloxane (PDMS) printing, (7) Screen printing, (8) Ink-jet printing, (9) Vapour phase deposition, (10) Stamping, (11) Wax printing, (12) Plasma treatment, (13) Wet etching, (14) Hand-held corona treatment.

2.2.1 Cutting

The paper cutting technique involves the patterning of hydrophilic channels on paper by literally cutting away specific areas of the paper substrate. The cutting process is often done with a paper craft cutter, knife modified X-Y plotters, or CO_2 laser cutter (Figure 2.1). With these instruments, a well-defined pattern is achieved which is a great advantage over some other manual techniques. For example, Fenton et al. fabricated a 2D microfluidic paper-based analytical device using a computer-controlled X-Y plotter which was modified with a knife instead of a traditional pen (Fenton et al., 2009). Multiple designs and pattern of μPAD's were made with this cutting technique by manipulating the number of passes of the knife through the paper substrate. It was reported that the X-Y plotter could produce a full device in less than 30 seconds which makes it a viable technique for mass production.

Cassano and Fan also reported the use of a commercially available paper craft (Graphtec craft Robo-S, Graphec corporation) for fabricating a μPAD just like the way a regular identification card is made (Cassano and Fan, 2013). This method required the use of the AutoCAD software to make the design which was then transferred to the software page of the Graphtec craft Robo-S (Robo master Pro). Afterward, the craft cutter was utilized to shape the paper substrate into the desired design and laminated.

Furthermore, Spicar-Mihalic et al. reported the use of commercially available CO_2 laser cutter (M360, Universal Laser systems) for the manufacturing of well-defined paper based devices (Spicar-Mihalic et al., 2013). Nitrocellulose membrane was used as the substrate, which is combustible, hence it was coated between polymer sheets during the cutting operation to prevent ignition. This laser cutting technique produced well-defined devices in so little time, therefore its promising potential for mass production and commercialization.

One major disadvantage of the cutting technique is the extra cost involved in the purchase of the cutting instruments. Basic CO_2 Laser cutters, paper craft instruments and their corresponding computer software cost between $300 – $10,000 per device, which adds a huge amount to the overall cost of production of each µPAD.

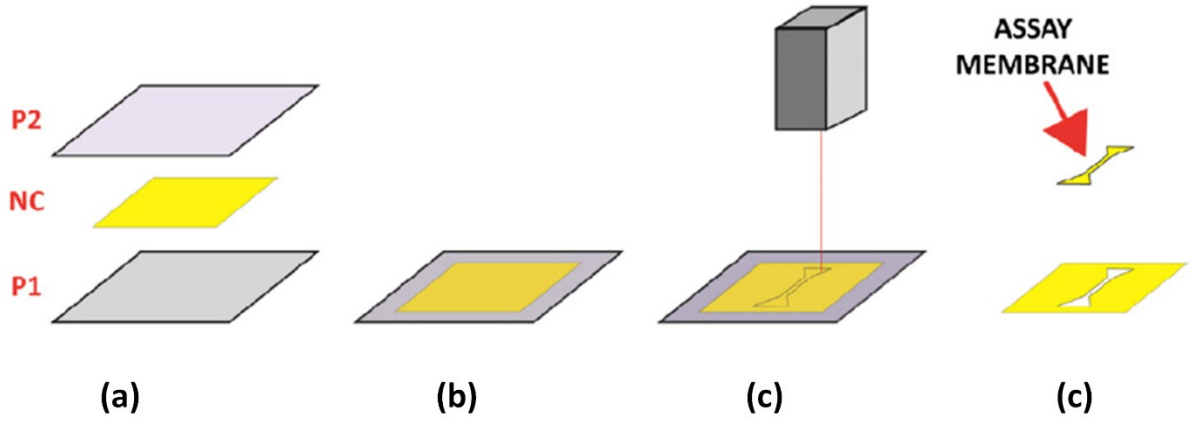

Figure 2-1 Schematic diagram showing the process of the cutting techniques used the fabrication of paper-based analytical device. (a) and (b) Sandwiching of the nitrocellulose (NC) between two polymers (P1 and P2). (c) Cutting using CO2 laser to selectively carve patterns. (d) Removal of the final paper device ready to analysis. Adapted from Spicar-Mihalic et al. (Spicar-Mihalic et al., 2013).

2.2.2 Photolithography

Photolithography involves the patterning of µPAD's by transferring desired pattern from photomasks to the light sensitive negative photoresist on the paper substrate, which gives a defined hydrophilic channel with hydrophobic barriers after exposure to UV light and the chemical washing process (Figure 2.2). This method involves the use of a photoresist chemical, an etching or washing chemical and a UV light source. The first use of this method for fabrication of µPAD was reported by Professor Whiteside's research group (Martinez et al., 2007). In that study, Martinez et al. soaked paper substrate in the SU-8 2010 photoresist, which was afterwards exposed to UV light through a photomask. Then, the unpolymerized photoresist was washed by soaking

and washing with propylene glycol monomethyl ether acetate and propan-2-ol respectively. The resulting patterned paper was then exposed to oxygen plasma to increase the hydrophilicity of the channels.

In addition, Sones et al. reported the use of photolithography to fabricate μPAD (Sones et al., 2014). However, in their approach, a laser-based direct write (LBDW) was employed to cause the polymerization of the desired photoresist pattern. This LBDW was advantageous since it incorporates a mask-less patterning procedure (a photomask was not needed), and its contactless deposition prevents contamination of paper substrate during fabrication.

The major disadvantages of the photolithography method are the requirement of expensive equipment, the presence of complex and delicate steps which needs to be painstakingly achieved, and the need for expensive reagents (the photoresist reagent and the unpolymerized photoresist cleansing reagents) (He et al., 2015, 2013; OuYang et al., 2014).

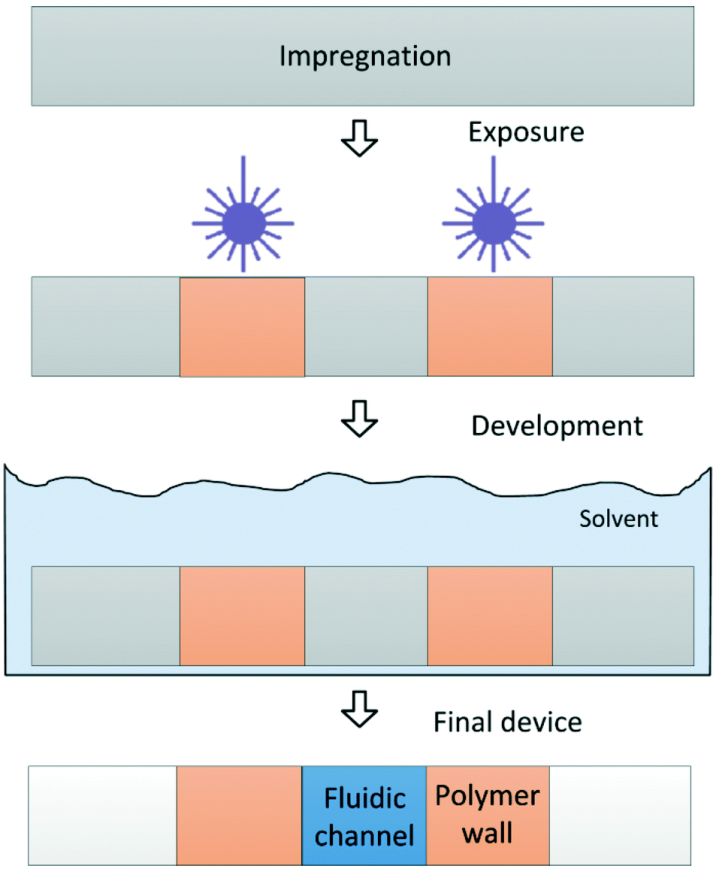

Figure 2-2 Procedure for the use of the photolithography technique in the fabrication of paper-based analytical devices. Adapted from Sones et al. (Sones et al., 2014)

2.2.3 Flexographic Printing

Flexographic printing is a technique for making µPAD in one step using a flexography unit which allows predesigned pattern to be printed on paper substrate with polystyrene or other nonpolar reagents. This method is a one-step printing process with control on the amount of polystyrene deposited on the paper substrate by the amount of pass through the flexography Unit (Figure 2.3). Olkkonen et al. reported the use of a flexographic for creating paper devices that were used as glucose indicators (Olkkonen et al., 2010). The Flexography unit consist of five main components; the impression roll which holds the paper substrate, the plate roll that holds different cells of patterns to be printed on the paper substrate, the Ink reservoir, the dock plate that aids in spreading and scrapping of excess ink from the plate roll, and the anilox roll that carries the ink from the

reservoir to the plate roll and ultimately to the impression roll. These units are mechanically fixed together, making the µPAD fabrication fast with high throughput for mass production.

The major advantages of the flexographic printing technique are the avoidance of heat treatment of the paper substrate and the easy direct roll-to-roll mechanism which is already incorporated into pre-existing printing instruments. However, the disadvantages of this technique includes it high cost, and need for constant surface cleaning to prevent contamination (Akyazi et al., 2018).

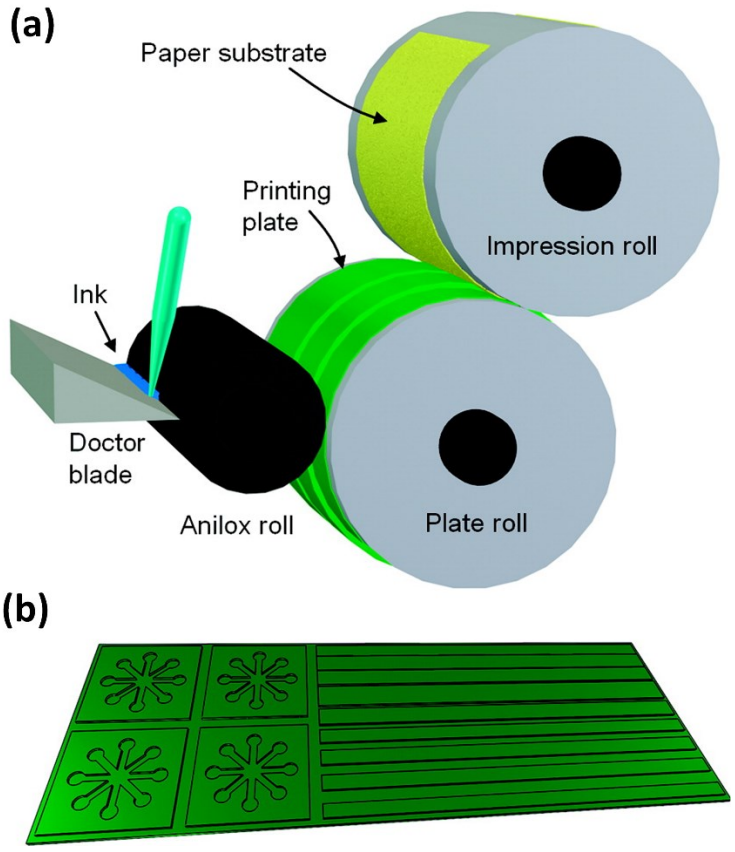

Figure 2-3 Schematic of the use of flexographic printing in the fabrication of paper-based analytical devices. (a) The flexographic unit and procedure. (b) The fabricated paper-based analytical devices. Adapted from Olkkonen et al (Olkkonen et al., 2010).

2.2.4 Ink-jet etching

Ink-jet etching is a µPAD fabrication technique which involves the soaking of the paper substrate in a polystyrene solution, which is etched according to the desired pattern with an inkjet printer

modified with toluene solvent (Figure 2.4). Abe et al. reported the use of the ink-jet etching technique to fabricate a paper device for the simultaneous detection of pH, total protein, and glucose (Abe et al., 2008). In that report, Abe et al. dipped paper substrates in 1.0 wt% polystyrene in toluene. Afterwards, an inkjet printer (PicoJet – 2000) modified with toluene solvent was used to eject toluene in a patterned fashion to dissolve the polystyrene, and the same printer was later used to eject the testing reagents on the paper device. The technique produced μPAD with four detection zones and the corresponding hydrophilic channels leading to the zones. In about a year later, Abe et al. also reported the use of the inkjet etching technique to fabricate a μPAD for immune-chemical sensing, which detects the human IgG concentration down to 10 μL in less than 20 minutes (Abe et al., 2010).

Overall, one major advantage of the inkjet printing is the low cost, since only a single printer instrument is needed to fabricate the paper device and print testing reagents on the zones. However, the multiple printing step involving customization of the printing apparatus is a major drawback for this technique (Abe et al., 2010, 2008; Akyazi et al., 2018).

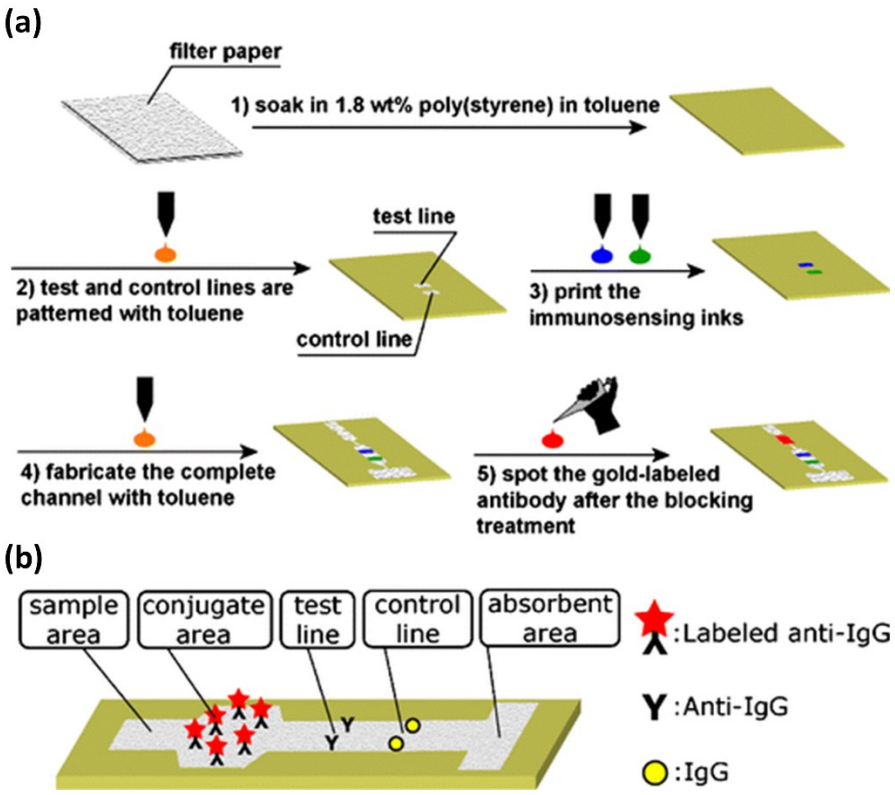

Figure 2-4 The schematics of the fabrication procedure for paper-based analytical devices using ink-jet etching. (a) The fabrication procedure. (b) The ready-to-use device. Adapted from Abe et al. (Abe et al., 2010).

2.2.5 Wax dipping

Wax dipping is a very fast and cheap technique for fabricating µPAD which involves the dipping of pre-masked paper substrate into melted wax for a specific time in order to allow the wax to penetrate the unmasked areas and cause a hydrophobic barrier for well-defined liquid flow. This technique often requires a heating source in order to melt the solid wax mass (Figure 2.5). Songjaroen et al. reported a µPAD fabricated by dipping of paper substrate into white bee wax after been masked with a metal mask (Songjaroen et al., 2012). In that report, white bee wax was melted by heating at 125 °C on a hotplate. Afterwards, the sized paper substrate and a blood separation membrane was overlapped on a glass slide with patterned metal mask on the paper and a permanent magnet under the glass slide for firm grip of the metal mask. This setup was then

dipped in the melted white bee wax for 1 second and the resulting device was used to test for protein concentration in blood plasma.

Overall, the wax dipping technique is advantageous because it is cheap and simple, quick, and has a greener impact on the environment. However, the inconsistency in the pattern on the μPAD due to the variation in dipping is a draw back for mass production (Songjaroen et al., 2012, 2011).

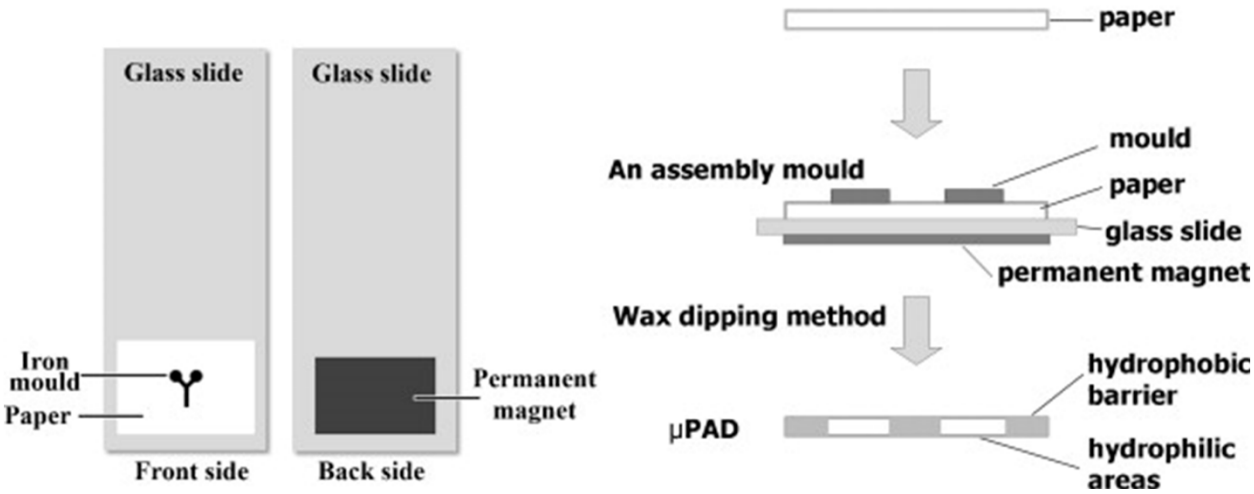

Figure 2-5 Schematics of the use of wax dipping for the fabrication of paper-based analytical devices. Adapted from Songjaroen et al. (Songjaroen et al., 2012).

2.2.6 Polydimethyl-siloxane (PDMS) printing

The polydimethyl-siloxane printing technique involves the use of a desktop plotter with a modified pen to pattern paper using PDMS as the hydrophobic ink (Figure 2.6). Bruzewicz et al. reported the fabrication of a μPAD with PDMS printing which was used for the detection of glucose and protein (Bruzewicz et al., 2008). In that report, a desktop plotter (Hewlett-Packard 7550A) was modified with a pen containing an ink of PDMS diluted with hexane in ratio 3:1. The use of the desktop plotter was preferred over desktop printers because; the desktop plotter can print on different kinds of paper types and grades and other different porous materials, the plotter does not fold the paper while printing which makes it compatible with inks that dry over time, the plotter

doesn't require any pre-built software, and it allows for ink modification. PDMS was specifically chosen as the printing solution because; PDMS is a common material to researchers working on microchannels, the elastomer property of PDMS allows it to be bent and folded without damage, and the very low toxicity to human health. Test reagents were impregnated into the detection zones with micropipettes and the device was used to detect glucose, pH and protein.

In all, polydimethyl-siloxane printing technique is advantageous due to the cheap patterning agent (PDMS), the flexible devices it generates and automatic means of depositing the patterning agent on the paper substrate. Conversely, this technique has an irregular control over the hydrophobic barrier patterning which makes it a poor candidate for mass production (Akyazi et al., 2018; Bruzewicz et al., 2008).

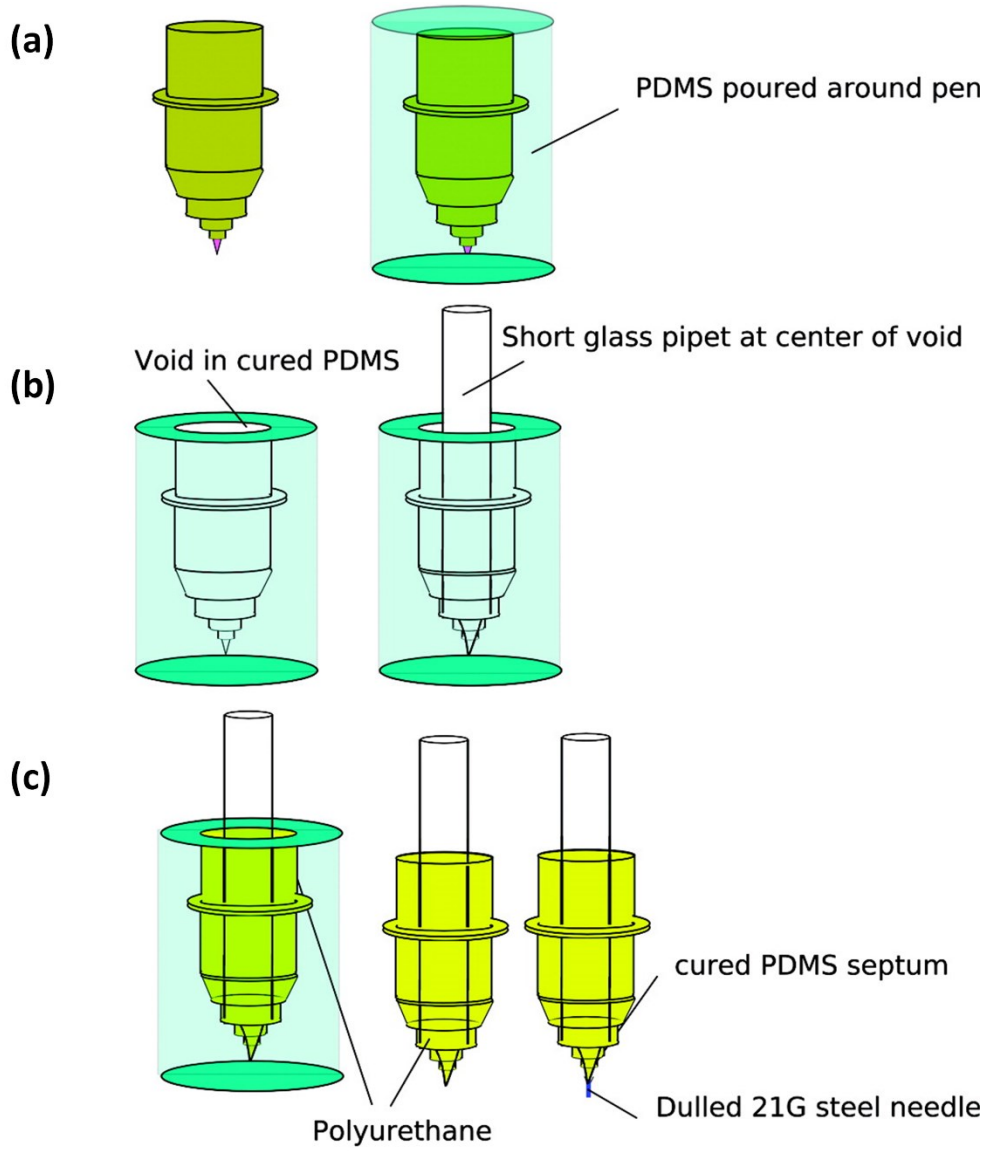

Figure 2-6 Schematics of the pen modification utilized for PDMS printing for the fabrication of paper-based analytical device. (a) Original pen embedded in PDMS. (b) Inclusion of pen in mold. (c) The molded plotter pen. Adapted from Bruzewicz et al. (Bruzewicz et al., 2008).

2.2.7 Screen Printing

Screen printing is a technique for the fabrication of µPAD which utilizes a pressure-based approach and desired patterns are printed on paper substrate with the aid of a hydrophobic ink through a layer of mesh incorporated with an ink blocking stencil, which is a mirror image of the desired pattern (Figure 2.7). This technique is often used also in printing of design and patterns on

clothes and other varieties of substrates. Various inks reported to have been used for the screen printing technique includes; solid wax (Dungchai et al., 2011), polydimethyl-siloxane (Mohammadi et al., 2015), Polymethyl methacrylate (Juang et al., 2017), vanishing paints and roof sealant (Sun et al., 2015), and polystyrene (Tasaengtong and Sameenoi, 2020). In addition, Jarujamrus et al. reported the use of cis-1,4- polyisoprene gotten from rubber latex as the hydrophobic ink for the fabrication of a μPAD for detection of magnesium ion (Jarujamrus et al., 2019). In that report, the design pattern was after the similitude of a barcode and an android phone software application was developed to quantify the amount of magnesium ion present in the water sample.

More recently, Aksorn and Teepo reported the use of polylactic acid as the hydrophobic ink for the fabrication of a μPAD for the multiplex detection of sucrose, maltose and fructose (Aksorn and Teepoo, 2020). The patterned screen used to create the device was made from 100 mesh polyester with a thickness of 290 μm on a wooden frame. On patterning the paper substrate, the screen was placed on the paper and a 10% w/v polylactic acid solution was poured on the screen and squeezed to allow thorough penetration.

Generally, one major advantage of the screen-printing technique is its low cost for the fabrication of μPAD. However, the notable disadvantages include the low resolution and rough trimming of the μPAD barriers, and the negative environmental impact of the hydrophobic inks utilized (Aksorn and Teepoo, 2020; Jarujamrus et al., 2019; Mohammadi et al., 2015; Tasaengtong and Sameenoi, 2020).

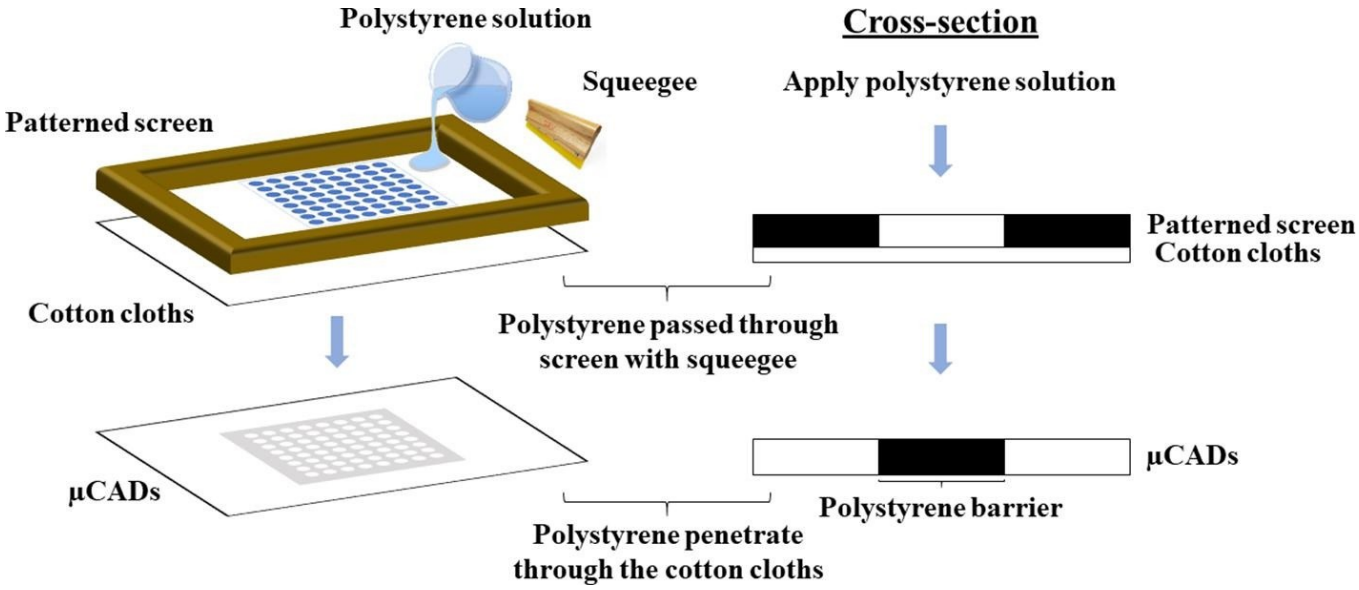

Figure 2-7 Schematics of the fabrication of paper-based analytical device using the screen-printing technique. Adapted from Tasaengtong and Sameenoi, 2020 (Tasaengtong and Sameenoi, 2020).

2.2.8 Ink-jet Printing

Ink-jet printing is a technique for the fabrication of µPADs which involves the modification of the ink of commercially available inkjet printers with Alkenyl ketene dimer (AKD) or other compatible nonpolar compounds for the patterning of paper substrate to create hydrophobic barriers and hydrophilic channels (Figure 2.8). In addition, a heating step is needed to allow the complete penetration of the AKD or other compatible ink through the paper matrix. For example, Delaney et al. reported the fabrication of a µPAD with an inkjet printer which was modified with AKD and used for electro-chemiluminescent detection (Delaney et al., 2011). In that report, the inkjet printer used was the Canon Pixma ip4500, which was modified with a 2% v/v AKD-heptane solution.

Alternatively, Wang et al. reported the use of hydrophobic sol-gel derived methylsilsesquioxane (MSQ) as the modified ink for the inkjet printer used for the fabrication of µPAD (Wang et al., 2014). In that report, the MSQ solution efficiency was compared with that of wax and AKD, and

it was concluded that the MSQ provided better barrier efficiency against surfactant solutions (Triton x-100, CTAB, SDS) and aggressive cell lysing solutions.

Generally, the advantages of the inkjet printing technique include the high resolution in the fabrication of µPAD which requires only a desktop device for µPAD fabrication and testing reagent deposition. However, the disadvantages of the technique includes the requirement for ink modification which must be done with care and skill, and the need for a heating step which is costly (Li et al., 2010a; Maejima et al., 2013; Xu et al., 2015; Abe et al., 2010).

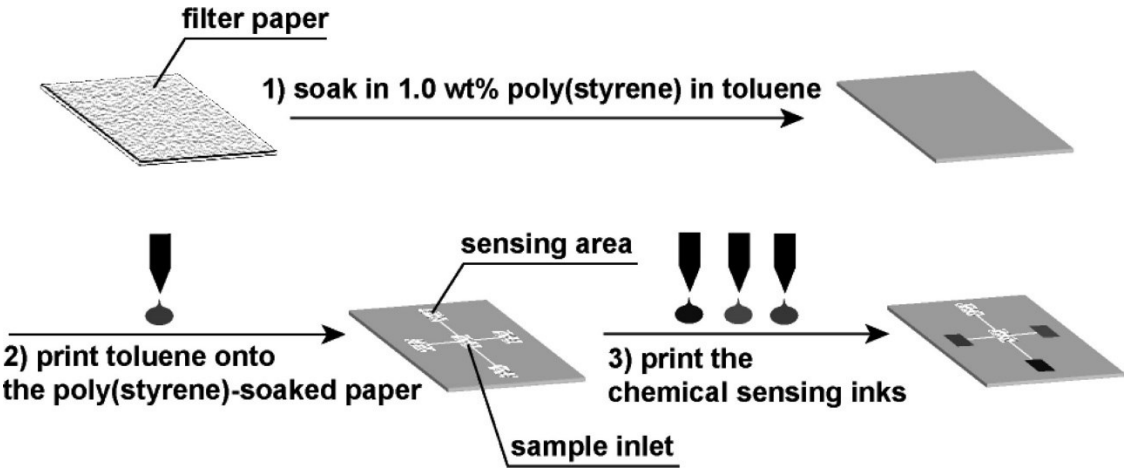

Figure 2-8 Schematics of the fabrication of paper-based analytical devices using ink-jet printing technique. Adapted from Abe et al (Abe et al., 2010)

2.2.9 Vapor Phase deposition

The Vapour phase deposition is a technique which is been utilized in the fabrication of µPAD for the creation of hydrophilic channels and hydrophobic barriers on paper substrates. This technique involves the use of the initiated chemical vapor deposition polymerization process to deposit hydrophobic reagents on paper substrates, which are afterwards masked and etched to reveal the hydrophobic barrier and the hydrophilic channels on the substrate. All the deposition takes place

in vapor phase in a deposition chamber (Figure 2.9). For example, Deminel and Babur reported the fabrication of a paper device with the vapor-phase deposition of polymers which was afterwards used for the detection of glucose, protein, uric acid, alanine aminotransferase (ALT) and aspartate aminotransferase (AST) (Demirel and Babur, 2014). In addition, Haller et al. also used the vapor phase deposition method to make a 3D μPAD which provided a formidable hydrophobic barrier when tested with liquid dye along the hydrophilic channel (Haller et al., 2011).

Altogether, the vapor phase deposition method allows for complex patterns to be designed on μPAD in a very simple and environmentally friendly manner. Nonetheless, the high cost of purchasing the deposition chamber and other equipment are disadvantages attributed to this technique (Akyazi et al., 2018; Haller et al., 2011; Kwong and Gupta, 2012).

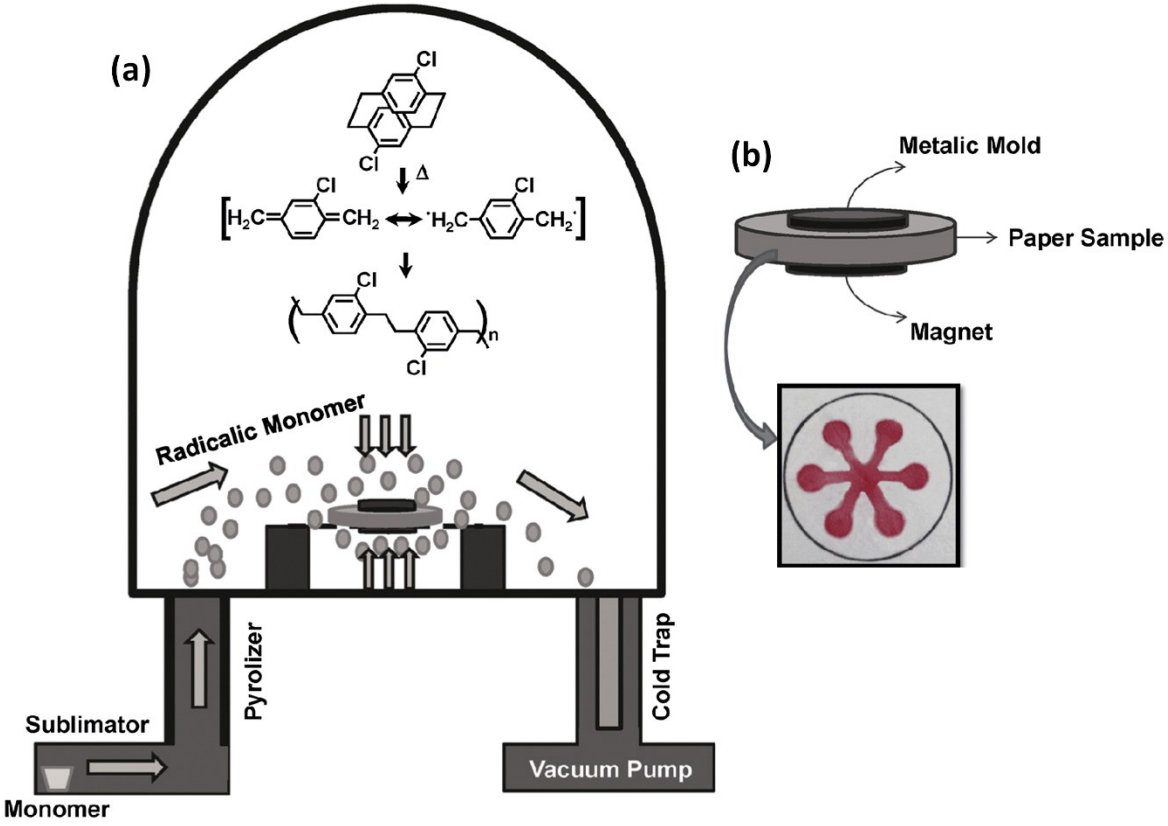

Figure 2-9 Schematics of the fabrication of paper-based analytical devices using vapour phase deposition technique. (a) The vapour deposition chamber. (b) Masking and etching operation Adapted from Demirel and Babur (Demirel and Babur, 2014).

2.2.10 Stamping

The stamping technique is a method for fabrication of μPAD which involves the use of a prepatterned stamp to pick up hydrophobic polymers and afterwards applied with some pressure on the paper substrate to print the desired pattern. A heating step is then applied to allow the penetration of the hydrophobic polymer through the paper matrix (Figure 2.10). Various kinds of hydrophobic polymers have been utilized while using the stamping technique to fabricate μPAD. For instance, Sun et al. reported the fabrication of a μPAD with the stamping technique which was used to detect lead (II) ion in liquid through a suspension droplet mode (Sun et al., 2018). In that report, PDMS was utilized as the hydrophobic polymer which was stamped using a Teflon stamp on the paper substrate for patterning purpose. The Teflon stamp was designed to have gaps to be filled by the PDMS polymer, therefore the stamp was kept in a vacuum chamber until the PDMS polymer fills up the gaps. The paper substrate was heated for some time after the stamping process to allow the PDMS polymer to penetrate the paper matrix.

Alternatively, De Tarso Garcia et al. reported that use of a heated metal stamp to transfer paraffin wax from a paraffin wax laden paper to a normal paper, therefore creating hydrophobic barriers on the normal paper (de Tarso Garcia et al., 2014). That technique eliminates the need to heat the paper substrate, which prevents potential burning that causes the color change of the paper and ultimately affecting the colorimetric accuracy of assays.

Overall, the stamping method is quite cheap and easy to manipulate. Howbeit, the existence of the heating step is a major disadvantage due to the high cost of heating and the potential hazard of

burning of the paper substrate (Akyazi et al., 2016; Curto et al., 2013; de Tarso Garcia et al., 2014; Sun et al., 2018).

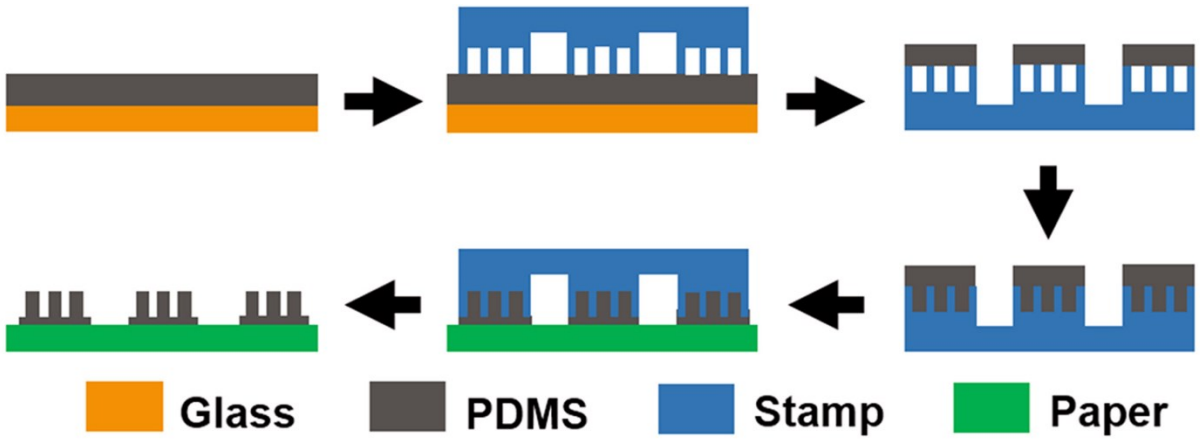

Figure 2-10 Schematics of the fabrication of paper-based analytical devices using the stamping technique. Adapted from Sun et al (Sun et al., 2018).

2.2.11 **Wax printing**

Wax printing is a technique for the fabrication of µPAD with specific solid ink printers which dispenses hydrophobic wax on paper substrate to create well defined hydrophobic barriers and hydrophilic channels (Figure 2.11). The commonest set of solid ink printers are made by Xerox® which includes the Xerox ColorQube 8580, ColorQube 8880, ColorQube 8700 and the ColorQube 8900. These printers have been used by several µPAD investigators and have become the generally accepted technique (Carrilho et al., 2009; Chabaud et al., 2018; Tan et al., 2020; Yehia et al., 2020). Lu et al. reported the first use of the solid ink technology to fabricate paper devices (Lu et al., 2009). In that report, three methods were proposed, namely (1) wax pen handwriting, (2) inkjet printer printing followed by wax painting, (3) total wax printer printing. However, only the total wax printer printing technology was widely accepted. In the total wax printing technique, a FUJIXEROX Phaser 8560 DN printer was utilized which has a resolution of 2400dpi × 2400dpi.

After the wax printing process, the printed paper substrate was then placed to a hotplate at a steady temperature to allow the penetration of the wax through the thickness of the paper.

Recently, Xerox has discontinued the sale of the solid ink printers due to the various clogging complains received by customers (Xerox Inc., n.d.). This discontinuation has put a great limitation to the future of using wax printing for μPAD fabrication since new solid ink printers and the hardware components will not be available in the market in the nearest future.

Overall, the wax printing technique is advantageous because it produces well-defined devices with fast (5-10 minutes) and simple processes. However, the additional heating step is a major disadvantage of this technique since heating is quite costly (Jeong et al., 2015; Kannan et al., 2015b; Leung et al., 2010; Mace and Deraney, 2014).

Figure 2-11 Schematics of the fabrication of paper-based analytical devices using the wax printing technique. Adapted from Carrilho et al (Carrilho et al., 2009)

2.2.12 Plasma Treatment

Plasma treatment is a technique for the fabrication of μPAD which involves paper substrate been made hydrophobic by dipping into hydrophobic polymers, and later incorporated with a patterned mask in order to make the unmasked area fully hydrophilic through plasma exposure (Figure 2.12). For instance, Li et al. reported the fabrication of a μPAD through plasma treatment, and used the

device as a miniaturized reactor for acid-base titration (Li et al., 2008). In that report, the paper substrate was first dipped into Akyle ketene dimer (AKD) to make the paper substrate fully hydrophobic and cured in an oven. Afterwards, a metal mask was incorporated on the paper substrate and put in a vacuum plasma reactor (K1050X plasma asher (Quorum Emitech, U.K.)) to make the unmasked areas hydrophilic.

In all, plasma treatment is advantageous because of the automated technique of creating hydrophilic channels on paper substrate therefore limiting manual errors. However, the high cost of equipment (the plasma reactor) needed for the process is a major drawback (Kao and Hsu, 2014; Li et al., 2010b).

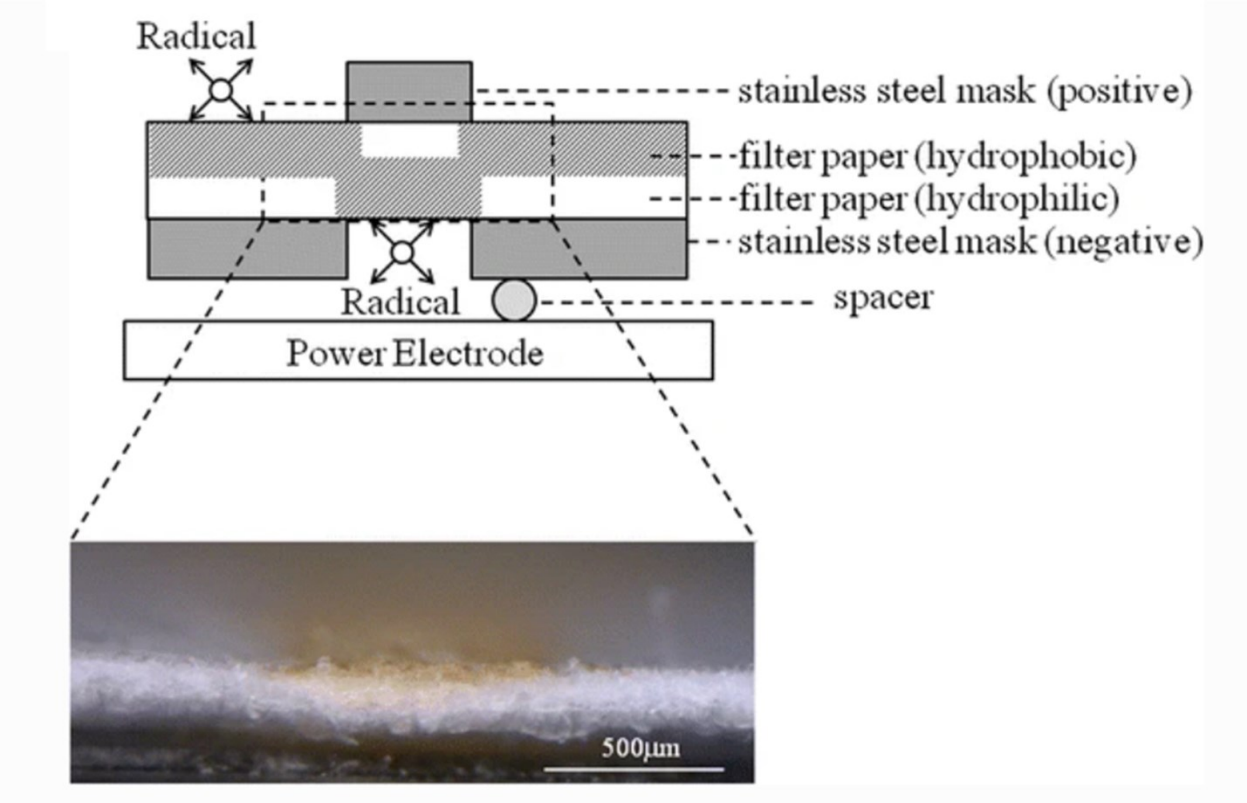

Figure 2-12 Schematics of the fabrication of paper-based analytical devices using the plasma treatment technique. Adapted from Kao and Hsu (Kao and Hsu, 2014)

2.2.13 Wet etching

Wet etching is a technique for the fabrication of μPAD which involves the etching of an already fully hydrophobic paper substrate with another patterned and wet paper in order to make the paper substrate hydrophilic along the area exposed to the etching paper. Due to the wet nature of the etching paper, the name 'wet etching' was derived (Figure 2.13). For example, Cai et al. reported the fabrication of a paper-based sensor with the wet etching technique (Cai et al., 2014). Here, a paper substrate was made hydrophobic by dipping in Trimethoxyoctadecylsilane (TMOS). Afterwards, a paper masked penetrated with sodium hydroxide was aligned to the paper substrate and etched with the etching reagent (sodium hydroxide).

This wet etching technique is advantageous since it requires no expensive equipment or reagents, fast and simple. However, it use for fabricating μPAD with complex designs is questionable (Akyazi et al., 2018; Cai et al., 2014).

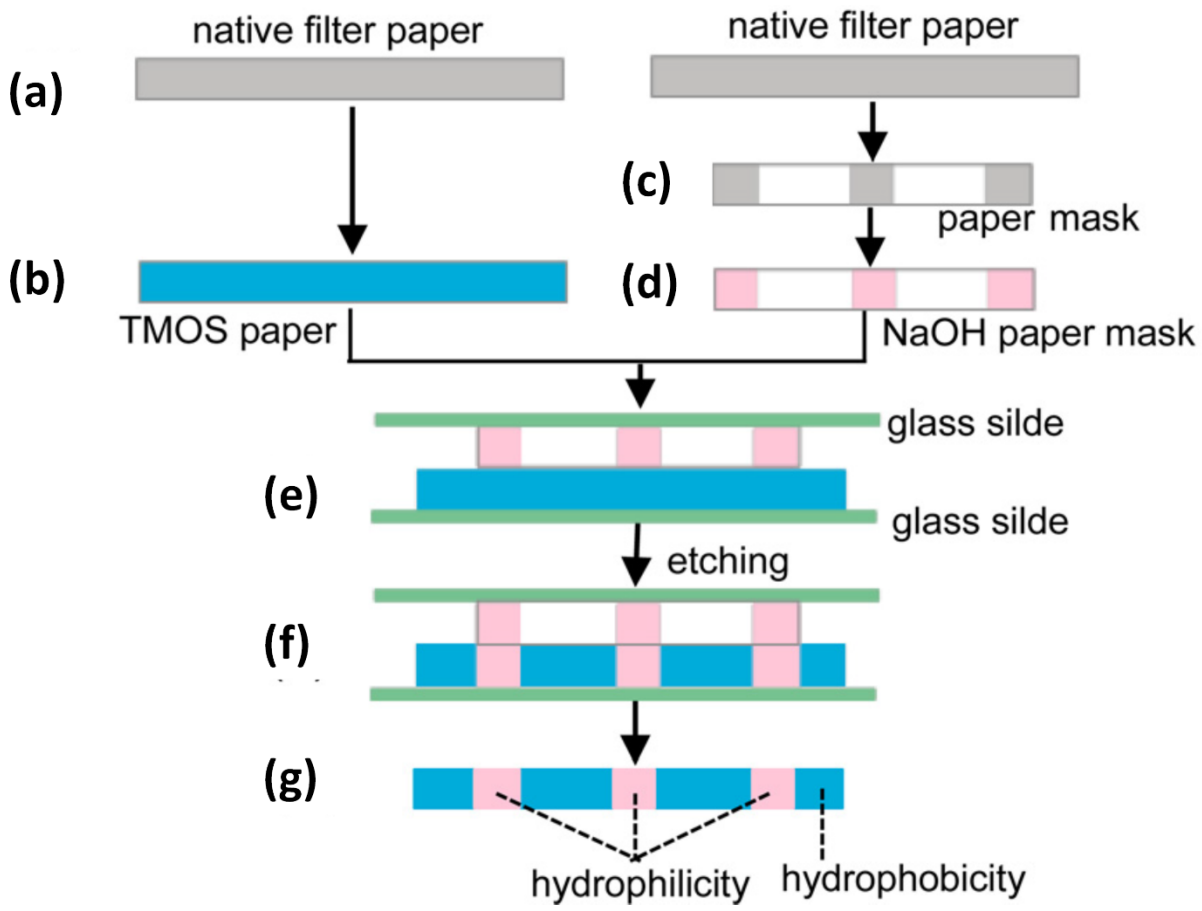

Figure 2-13 Schematics of the fabrication of paper-based analytical devices using the wet etching technique. (a) Pristine filter paper. (b) Filter paper soaked in tetramethyl orthosilicate (TMOS) to make hydrophobic. (c) Filter paper mask. (d) Filter paper mask soaked in NaOH. (e) Glass slide sandwiched paper mask and hydrophobic filter paper for the etching operation. (f) Paper assembly after etching (g) Hydrophobic and hydrophilic variation on paper. Adapted from Cai et al (Cai et al., 2014).

2.2.14 Hand-held corona treatment

Hand-held corona treatment is a technique for fabrication of µPAD which involves making hydrophilic an already fully hydrophobic paper substrate with an easy-to-use and portable corona generator (Figure 2.14). For instance, Jiang et al. reported the use of a portable corona generator to make well defined hydrophilic channels and hydrophobic barriers on paper substrate (Jiang et al., 2016). In that report, the paper substrate was made hydrophobic by dipping in octadecyltrichlorosilane (OTS). Afterwards, the hydrophobic paper substrate was aligned with a

patterned plastic mask and was exposed to the corona. Therefore, the masked area of the hydrophobic paper substrate remained hydrophobic, while the exposed portion returned to the original hydrophilic state of the paper.

Overall, the hand-held corona treatment technique a is a very simple and low-cost method. However, the safety consideration when using a corona generator requires constant reminder and policing of the operator in order to prevent fatal accidents (Akyazi et al., 2018; Jiang et al., 2016).

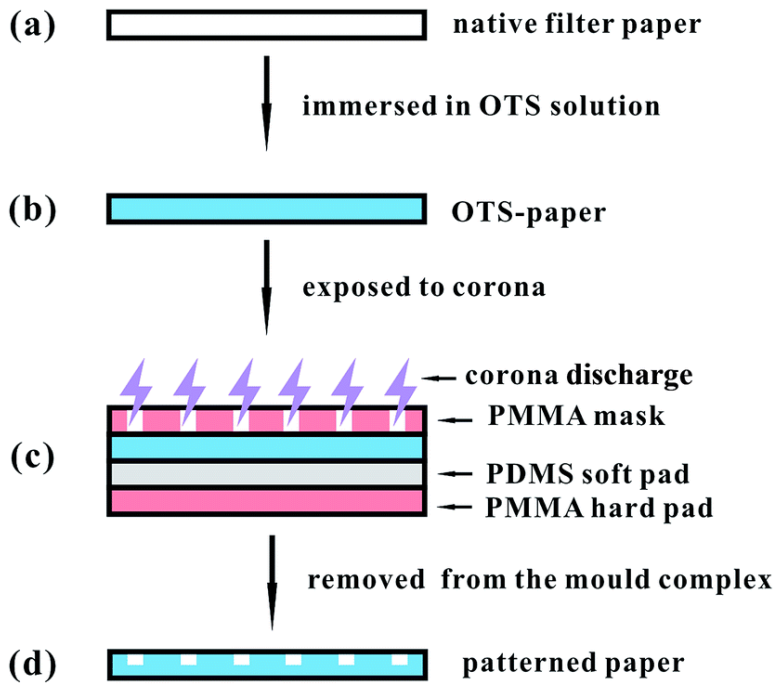

Figure 2-14 Schematics of the fabrication of paper-based analytical devices using the hand-held corona treatment technique. (a) Pristine filter paper. (b) Filter paper soaked in trichloro(octadecyl)silane (OTS). (c) Corona discharge on masked paper. (d) Patterned paper. Adapted from Jiang et al (Jiang et al., 2016).

2.3 Detection Procedure

Numerous methods have been reported in literature concerning the detection mechanism of assays on a µPAD. These detection mechanisms are the main feature of the µPAD which contributes greatly to the sensitivity, selectivity and the user friendliness. The detection methods include

colorimetric detection, electrochemical detection, fluorescence detection, chemiluminescence detection and electrochemiluminescence detection. The fundamentals, advantages, and limitations of these detection methods will be discussed going forward.

2.3.1 Colorimetric detection

Colorimetric detection is the commonest detection means employed in μPAD. This detection method involves the use of visual observation and inspection, photometric readout, and reflectometric readout of desired endpoint of a reaction from the detection zone of the μPAD (Akyazi et al., 2018; Almeida et al., 2018). The visual inspection occurs by comparing the color of the detection zone with it previous color or the color of the control zone to determine if the presence of specific analytes exist. The visual inspection method is often used to get a yes or no output or a semi-quantitative output (Jayawardane et al., 2012; Karita and Kaneta, 2016; Nogueira et al., 2019), which is what is employed in the most off-the-shelf pregnancy test kits.

Alternatively, the photometric and the reflectometric readout involves the use of electrical gadgets (Mobile phone, portable paper scanner, office paper scanner, camera etc.) to capture the image of the detection zone for color intensity analysis. The color intensity analysis is often been done using the free Image J software (Evans et al., 2014; Firdaus et al., 2019; Kim et al., 2017).

The colorimetric detection method is simple and very user friendly, therefore the reason for its widespread usage in μPAD analysis. However, the inhomogeneity in the color formation output often displayed at the detection zone to form the coffee-ring phenomenon and reading errors due to light source and contrast are major drawbacks to this method (Arciuli et al., 2013; Chabaud et al., 2018; Devadhasan and Kim, 2018; Nguyen et al., 2018).

2.3.2 Electrochemical Detection

Electrochemical detection involves the use of electrodes on μPAD to generate electrochemical signals in order to determine the presence of specific analytes. The electrodes often include a working electrode, a counter electrode, and a reference electrode which are used to perform amperometry, stripping and cyclic voltammetry, and coulometry. In order to improve electrochemical signal during assay, the working electrode is sometimes treated with conducting polymers or nanomaterials like graphene oxide, carbon nanotubes, and metal nanoparticles (Silveira et al., 2016). The electrodes are usually attached to the paper substrate by screen printing or inkjet printing using metal inks or conductive carbon (Cao et al., 2020; e Silva et al., 2020), or by hand writing with pencil (Dornelas et al., 2015; Dossi et al., 2013; Santhiago et al., 2014) - since pencil is made of graphite which conducts electricity.

Microfluidic paper-based analytical devices which use the electrochemical detection method have recently been called “paper-based electrochemical devices (PED)” due to their compatibility (Maxwell et al., 2013). PED have been applied to a variety of diagnostic analysis like DNA and nucleosides (Cunningham et al., 2014; Lu et al., 2012), metals (Apilux et al., 2010; Chaiyo et al., 2016; Ruecha et al., 2015), immunoassays (Szűcs and Gyurcsányi, 2012; Wang et al., 2016; Wu et al., 2012), glucose (W. Li et al., 2016), and cholesterol (Shih et al., 2009).

Generally, electrochemical detection method gives very accurate and precise result reading in comparison with the colorimetric detection. However, the electrochemical method still uses auxiliary instruments to perform the stripping and cyclic voltammetry or other analysis, which reveals a need for further work on miniaturization (Akyazi et al., 2018; Almeida et al., 2018).

2.3.3 Fluorescence detection

Fluorescence detection is a method of detection in μPAD which involves the measurement of the light intensity emitted by analytes that have previously absorbed light and other electromagnetic radiation (Akyazi et al., 2018). This method provides a higher sensitivity and achieves very low limit of detection in comparison with the colorimetric method (Xia et al., 2016). However, since paper substrate contains some additives that are self-florescence, it may cause some errors in result reading.

The fluorescence detection method has been utilized in μPAD by various researchers to achieve excellent detection output. For example, the detection of protein (Liu and Crooks, 2011; Rosa et al., 2014; Yamada et al., 2014), DNA (Allen et al., 2012; H. Li et al., 2016), cancer cells (Liang et al., 2016) and drugs (Caglayan et al., 2016).

Overall, the major drawbacks of the fluorescence detection method is the need for the often bulky fluorescent instrument and the existence of large interference between competing metal ions (Xia et al., 2016).

2.3.4 Chemiluminescence and electrochemiluminescence detection

Chemiluminescence detection is a method of detection in μPAD which involves the measurement of the light emitted as a result on chemical reactions taking place on the paper substrate. This method is reported to be more sensitive than the colorimetric and fluorescence detection method because of the absence of an excited light signal which causes a low background signal (Almeida et al., 2018). This method is also compatible with micromachining technologies which is the reason for its wide range of application by skilled and unskilled persons (Nuchtavorn and Macka, 2016). A portable chemiluminescence reader is needed as an auxiliary tool for result reading. This method

has been applied to glucose and uric acid detection (Yu et al., 2011a), hormone detection (Zangheri et al., 2015), metal detection (Alahmad et al., 2016), and pesticide detection (Liu et al., 2014).

Electrochemiluminescence detection on the other hand involves the generation of luminescence due to electrochemical reaction. This method is particularly advantageous due to its ability to be applied for both luminescence and electrochemical method. Electrochemiluminescence detection has been used in numerous μPAD detection analysis like for tumour marker detection (Gao et al., 2015; Ge et al., 2012; Wang et al., 2012), chemical contaminant (Mani et al., 2013), and cancer cells (Li et al., 2015).

Overall, the chemiluminescence and the electrochemiluminescence detection method are categorized to be more sensitive than the colorimetric and the fluorescence detection method. However, the need for auxiliary equipment for signal reading, adds additional cost to the μPAD which is a major drawback (Akyazi et al., 2018; Almeida et al., 2018; Xia et al., 2016).

2.4 Water contamination

Water contamination is caused basically by the presence of abundance or limited amount of nutrients, heavy metals and organic contaminants in water. The variation of these parameters in water have specific information to tell about the quality of the water source. The source of a water sample can often be used to get a rough estimate of the concentration of these parameters. For example, ocean water is known for being salty, which is due to the openings in the ocean floor and runoffs from the land. These parameters are being measured regularly and acceptable standards have been enacted for various water body and usage purposes. These acceptable standards are policed strictly with heavy repercussion to persons, organisations, or companies that go against such standards in their activities. The standard measuring technique for detecting the parameters

in water includes spectrophotometry, Atomic absorption spectroscopy, laboratory biological assay (for some organic contaminants) etc. Going forward, the water parameters will be elucidated and discussed.

2.4.1 Nutrients

Nutrients are essential molecules which are present in water bodies for aquatic life. These nutrients include nitrogen, phosphorus, nitrite, nitrate, ammonia and reactive phosphate. Even though these nutrients are important to aquatic life, excessive amount can cause serious havoc to the aquatic ecosystem. For example, excessive amount of nitrogen and phosphorus in water can cause eutrophication, which is the boom of aquatic plant on the surface of water causing too much competition for dissolved oxygen with other aquatic life. This is a life-threatening situation for aquatic life, which may ultimately lead to death. Various μPAD have been fabricated to detect these nutrients in water sample, for example phosphorus detection, nitrite and nitrate detection (Jayawardane et al., 2014a, 2014b, 2012) etc.

2.4.2 Heavy metal

Heavy metals are part of the parameters monitored to determine the quality of water. Examples of such metals include mercury, cadmium, lead, copper, nickel, zinc, manganese, iron etc. Even though some heavy metals are needed in trace amount by living organisms, excessive amount in water bodies is catastrophic to the ecosystem. For example, excessive amount of lead in drinking water can cause lead poisoning which leads to abnormal growth development in children and memory losses in adults (Chaiyo et al., 2016). Various μPAD have been fabricated to detect these metals in water sample, for example lead (Satarpai et al., 2016), copper (Wu et al., 2019), mercury (Chen et al., 2014), iron (Marquez et al., 2019), calcium and magnesium (Jarujamrus et al., 2019;

Karita and Kaneta, 2016), chromium (Rattanarat et al., 2013), zinc (Kudo et al., 2017), and nickel (Yamada et al., 2018).

2.4.3 Organic contaminants

Organic contaminants are one of the parameters/compounds measured in water to determine the quality. Examples of these compounds include pesticides, polycyclic aromatic hydrocarbons, plastics, microplastics etc. These organic compounds are replete in many domestic household products and cosmetic products which has led to major environmental issues due to their presence in aquatic habitats (Almeida et al., 2018). These organic contaminants have been reported to be found in the stomach of aquatic animals and humans which has the potential to cause fatal harm (Kelly et al., 2004). Various µPAD have been fabricated to detect these nutrients in water sample, for example, organophosphate (Sicard et al., 2015), pentachlorophenol (Sun et al., 2014), p-nitrophenol (Santhiago et al., 2014) etc.

Some water quality parameters do not fall into the categories listed above, and they are as equally important. Such parameters include pH measurement, hydrogen sulphide measurement, water hardness measurement, and halogens measurement.

2.5 Water hardness: Definition and detection technique

Water hardness is one of the measured parameters in water to determine its quality. Water hardness is simply the amount of metallic ion (often calcium and magnesium ions) present in water, measured as a calcium carbonate equivalent. As stated earlier in section 1.2, the commonest means of detection of total hardness of water over the years have been the traditional titration method, the ion selective electrode analysis (Bakker, 2018), the Inductively Coupled Plasma Atomic Emission Spectroscopy (ICP- OES) (Butcher, 2010), and Raman Spectroscopy characterization

(Yang et al., 2014). Interestingly, many other detection techniques apart from the earlier mentioned ones have been reported by various researchers. Going forward, these various detection techniques will be discussed.

2.5.1 Traditional titration

This detection technique is the commonest utilised means for the detection of the total hardness of water. It is also called complexometric titration. The method utilises the titration principle of the reaction between a titrant of know concentration and an analyte of unknown concentration in the presence of a metal ion indicator. In this case, the titrant often used is Ethylenediaminetetraacetic acid (EDTA) of known concentration and the analyte is the water sample to be detected. In order to allow the quantitative reaction of the metal ions with EDTA, a buffer with a pH of about ten is introduced into the solution. Ammonia buffer solution is commonly used, however, other buffer solutions like 3- (Cyclohexylamino) propanesulphonic acid (CAPS) are utilized. Examples of indicators used are eriochrome black T, patton reeder, murexide, mordant black II (Hildebrand and Reilley, 1957; Ostad et al., 2017; Tsunogai, 1968).

2.5.2 The ion selective electrode analysis

This detection mechanism for total water hardness utilizes an electrochemical electrode probe which gives specific voltage values depending on the type and concentration of ions present in the water sample, without perturbing the sample (Bakker, 2018). The electrode probe utilized for total water hardness detection is often a neutral carrier-based Mg^{2+}/Ca^{2+}-selective electrode without any supplementary complexing agent (Maj-Zurawska et al., 1989; Meier et al., 1980). This detection method is also employed for detecting a wide variety of ions in water, apart from does responsible for total water hardness (Criscuolo et al., 2018; Fan et al., 2020; Saleh et al., 2000; Tóth et al., 1993).

2.5.3 Spectroscopy characterization

This is a technique that generally uses the interaction between electromagnetic radiation and matter to detect the presence and concentration of specific elements as a function of corresponding wavelengths and frequency output. Often for water analysis, a measure of specified quantum energy is shot at the sample to cause an excitation of its atomic/metal constituents, and this effect the release of wavelengths or frequencies which are exclusive to specific atom/metals. Examples of spectroscopy analysis used for water hardness analysis include, inductively coupled plasma-atomic emission spectrometry (ICP-AES) (Bakker, 2018), raman spectroscopy characterization (Yang et al., 2014).

2.5.4 Other detection techniques

Apart from the aforementioned detection techniques used for the total hardness of water, other techniques have also been reported in literature. For example, Lerga and O'Sullivan (Lerga and O'Sullivan, 2008) reported the use of a fluorescent molecular aptamer beacon to detect the total hardness of water. In that report, a synthetic doubled labelled oligonucleotide was used as the fluorescent molecular aptamer beacon for the assay. The molecular beacon assay was reported to provide a sensitive, easy to use, replicable, cheap and low detection time (30 seconds). Also, Verissimo et al (Verissimo et al., 2007) reported the use an acoustic wave sensor for the detection of total hardness in tap water. In that article, two distinct piezoelectric quartz crystals were coated with poly(vinyl chloride) membranes and ionophore (Mg or Ca) respectively, therefore providing an alternative and effective testing platform.

More recently, Shariati-Rad and Heidai (Shariati-Rad and Heidari, 2020) reported the use of silver nanoparticles to classify and detect the total hardness of water. The assay is based on the color change of silver nanoparticles in water samples due to the presence of metallic ions. The assay was

reported to have a quantifying range between 116-248 mg/L. Furthermore, paper-based analytical devices have been employed in the detection of the total hardness of water (Karita and Kaneta, 2016; Ostad et al., 2017), however limitations regarding the use of auxiliary devices for analyte introduction, and semi-qualitative detection mechanisms have been major drawbacks.

3.1 Chemical and Materials

Ethylenediaminetetraacetic acid disodium salt dihydrate (EDTA) was purchased from Sigma Aldrich, Canada and was used as received without any alteration. The metal ion indicator Eriochrome blue-black B (EBT) was purchased from Sigma Aldrich, Canada, and was utilized without any purification.

The spiked metal ion solutions were prepared using Magnesium Sulfate and Calcium Chloride Dihydrate. The Calcium Chloride Dihydrate was purchased from Fisher Scientific, Canada, while the Magnesium Sulfate was purchased from Sigma Aldrich, Canada.

0.1M of Sodium hydroxide concentrate and 3-(Cyclohexylamino) propanesulphonic acid (CAPS) which were used in the buffer preparation were purchased from Sigma Aldrich, Canada and used with any purification.

The solvent HPLC (High Performance Liquid Chromatography) grade methanol with greater than 99.9% purity was bought from Sigma Aldrich Canada and was used as received. HPLC grade water was purchased from Concordia University central store, Montreal and was used as received.

The Grade 4 Whatman® filter paper, Grade 4 Whatman® Chromatography paper, Grade 1 Whatman® filter paper and the Grade 2 Whatman® filter paper were purchased from Fisher Scientific, Canada. Neon food color preparation and the Sharpie© permanent marker utilized were purchased from local grocery stores in Montreal.

Water samples of unknown concentrations were collected and tested for total hardness concentration using the traditional titration and with the device. The samples were gotten from Concordia University Hall building (Montreal, Canada), Abeokuta resident (Abeokuta, Nigeria) Cote des Neige resident (Montreal, Canada), St. Leonard resident (Montreal, Canada).

Manganese acetate tetrahydrate, ferrous sulphate, ammonium fluoride, ammonium chloride, copper dinitrate trihydrate used for getting the interference ions (Mn^{2+}, Fe^{2+}, NH^{4+}, F^{-}, Cl^{-}, and Cu^{2+}) for the interference analysis was purchased from Sigma Aldrich, Canada.

Calibrated Micropipettes (Sartorius) were used for every aliquot reagent transfer from liquid containers to paper substrate. The Contact Angle measurement was done using the Dropometer purchased from Droplet Smart Tech Incorporation, Canada.

3.2 Methods

3.2.1 Preparation of EDTA Solution

EDTA solution between 0.2 mM – 4 mM was prepared by initially making a stock solution of 10 mM. The 10 mM stock solution was prepared by dissolving 9.3060 g of EDTA with HPLC water in a 250 mL volumetric flask and filled up to the 250 mL mark. Further dilutions were done to get desired concentration.

3.2.2 Preparation of Buffer Solution

The buffer solution was prepared by dissolving 1.1066 g of CAPS in a 100 mL volumetric flask with HPLC water not up to the mark. The pH of the resulting solution was measured and increased to a pH of 10 with dropwise addition of 0.1 M of sodium hydroxide.

3.2.3 Preparation of Standard Metal Ion Solution

The spiked metal ion solution utilized all through the analysis were prepared by dilution and mixing of individual stock solutions of magnesium ion and calcium ion. To prepare 0.5 M stock solution of calcium ion, 1.8378g of Calcium Chloride Dihydrate was diluted with HPLC water in a 250 mL volumetric flask and filled up to the mark. To prepare 0.5 M solution of magnesium ion, 1.5046g of Magnesium Sulfate was diluted with HPLC water in a 250 mL volumetric flask and filled up to the mark. Further dilutions were done to get lower concentration of magnesium ion and calcium ion respectively.

25 mL of the 0.5 M calcium ion stock solution was mixed with 25 mL of the 0.5 M magnesium ion solution to give 50 mL of 0.5 M combined calcium ion and magnesium ion stock solution. Further dilutions were done to get lower concentration of combined magnesium and calcium ion solution.

3.2.4 Preparation of Metal Ion Indicator Solution

The metal ion indicator – EBT- utilized was prepared by dissolving 0.1000g of EBT with 20 mL of HPLC grade methanol in a 100 mL volumetric flask. After the EBT was dissolved completely, the HPLC grade methanol was added to the 100 mL mark. This mixture gave a 0.1w/v solution of EBT indicator.

3.2.5 Preparation of Interference Ions

100 µM of manganese ion (Mn^{2+}) solution was prepared by mixing 1.0723 mg of manganese acetate tetrahydrate in 50 mL of HPLC grade water. 100 µM of Iron II ion (Fe^{2+}) solution was prepared by mixing 1.3901 mg of ferrous sulphate heptahydrate in 50 mL of HPLC grade water. 100 µM of ammonium ion (NH^{4+}) solution was prepared by mixing 0.2675 mg of ammonium

chloride in 50 mL of HPLC grade water. 100 µM of chloride ion (Cl^-) solution was prepared by mixing 0.2675 mg of ammonium chloride in 50 mL of HPLC grade water. 100 µM of flouride ion (F^-) solution was prepared by mixing 0.1852 mg of ammonium flouride in 50 mL of HPLC grade water. 100 µM of copper II ion (Cu^{2+}) solution was prepared by mixing 1.208 mg of copper dinitrate trihydrate in 50 mL of HPLC grade water.

3.2.6 Fabrication of Paper-Based Analytical Device

The structure of the µPAD was designed using the Microsoft PowerPoint 2019 software. The design (Fig. 3.1a) contains five detection (D) and reaction zones (R); four for the different classes of water hardness including soft (S), moderately hard (MH), hard (H), and very hard (VH) and one for a control (C) section that is used for the quantification. In each section, a channel links each reaction zone to the detection zone called the transition zone. There is also a dip zone which is the part of the device that is inserted into the water sample. A channel also exists which connects the dip zone to the reaction zone. On top of the detection zone, there is a waste zone which aids in reducing the elution time (Nguyen et al., 2018). The boundaries of the device were designed doubled line in order to give space for the application of the permanent marker for creating the hydrophobic barriers. Afterward, the design was printed on the Whatman® Grade 4 filter paper (A4 paper dimension) with a Hewlett-Packard LaserJet P4015× Printer, using the EconoMode printer setting (Figure 3.1b). The diameter of both the detection and the reaction zone was 0.7 cm. The length and width of the transition zone were 0.54 cm and 0.1 cm, respectively. The waste zone had a length and width of 0.2 cm and 0.1 cm, respectively. Overall, the device had a dimension of 15.88 cm × 12.7cm.

To make the hydrophilic channels on the printed design, a commercially available permanent marker (Sharpie©) was applied in between the doubled line boundary of the design. This was done

by passing the marker between the boundary lines at most twice, in order to allow proper penetration of the ink through the paper matrix and at the same time prevent excessive ink deposit on the paper. Therefore, it took about 1 min to apply the permanent marker ink for one device and less than 30 s for the ink to dry. The device was ready for the next stage of the fabrication process almost immediately after the application of the hydrophobic pigment due to the volatile nature of the carrier solvent. Afterward, the reagents were systematically added to different zones and

allowed to dry completely for usage.

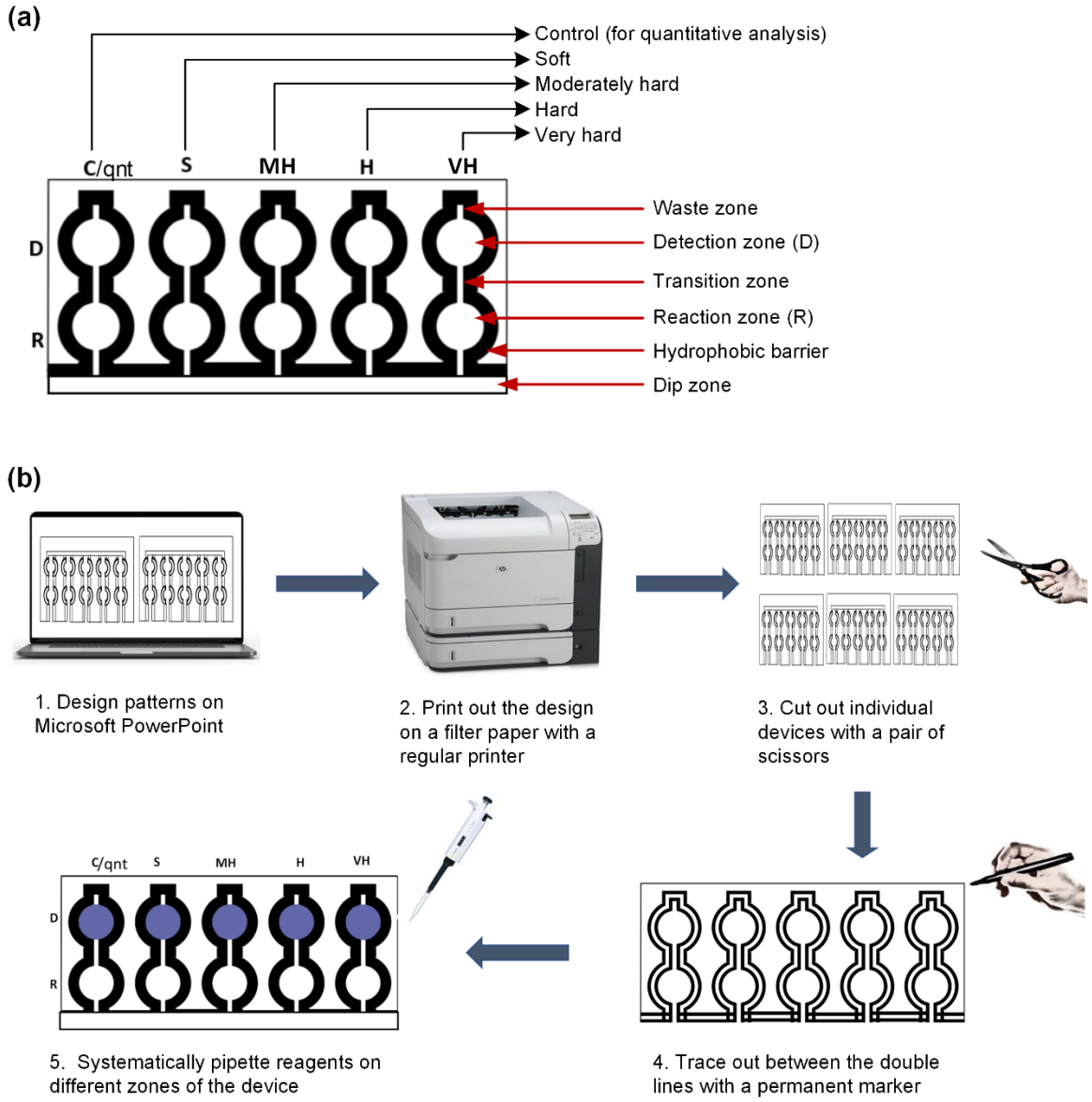

Figure 3-1 The paper-based analytical device's design and fabrication. (a) Schematic diagram of the lateral flow dip-and-read paper-based analytical device (D: detection; R: reaction; C: control; S: soft; MH: moderately hard; H: hard; VH: very hard). (b) Fabrication steps and procedures for the lateral flow dip-and-read paper-based analytical device.

3.2.7 Systematic Introduction of Reagents on The Fabricated Microfluidic Paper-Based Analytical Device

After the application of the permanent marker on the device to create the barriers and channels, reagents were systematically added to the device for the final preparation. 4.5 µL of the CAPS buffer at a pH of 10 was added to all the reaction and detection zones. The buffer solution dried completely on the paper after ~5 min at room ambiance. The presence of the buffer allowed all the zones to be conditioned to a pH of 10 as needed for the complexometric chelate titration. After the complete drying of the device, 3 µL of the EBT indicator was added to the detection zones, which turned from its original pink color to blue due to the conditioned pH of 10. Even though the EBT was dissolved in methanol during the solution preparation stage, it had no effect on the zone barriers since only an exact volume that filled the detection zone was applied. It was observed that 11 µL of liquid would fill up the device when completely dry, hence 5.5 µL of EDTA was added to the reaction zones (R.S.–R.VH.) except for the first reaction zone (R.C.). This volume selection of EDTA was chosen to model a systematic reaction concentration ratio of 1:2 of the concentration of the water sample to EDTA in each testing channel. Hence, the volume and the concentration balanced each other as EDTA and the water sample ions originally react in the ratio 1:1 as shown in figure 1.2a. 5.5 µL EDTA with the concentrations 0.40, 1.22, 2.42, and 3.62 mM was added to the reaction zones R.S. to R.VH., respectively. The concentration of EDTA added to the reaction zones was twice the lowest limit of the different ranges of water hardness given by the World Health Organization, excluding the first concentration (0.40 mM) which was chosen to affect a soft water characterization between 0.2–0.6 mM. The device was then allowed to dry completely and become ready to use. Therefore, for example, if the hardness concentration is higher than 0.2 mM, the calcium/magnesium ions will completely react with the 0.4 mM EDTA (volume ratio of 2:1 of water sample to EDTA) at the zone R.S., and the remaining hardness concentration will

move up to the corresponding detection zone causing a color change from blue to pink. This systemic titration and analyte cancelling on the paper will take place at other channels too.

3.2.8 Contact Angle Determination

The contact angle measurement was determined using the Dropometer (Droplet Smart Tech Incorporation, Toronto, ON, Canada). The Grade 4 Whatman filter paper was cut into square sheets of dimension 2×2 cm. The four colors of permanent marker are then applied on the square sheet. HPLC water was fed into the sample application syringe and an aliquot amount was ejected on each square sample. Afterwards, the image is captured and analysed using the installed Sessile mobile application.

3.2.9 Elution Velocity Determination

Different paper grades (Whatman® Grade 1 filter paper, Whatman® Grade 2 filter paper, Whatman® Grade 4 filter paper, and Whatman® Grade 4 chromatography paper) were cut into strip sizes of 0.5 cm × 4 cm. Afterward, the paper strips were dipped into the HPLC grade water and observed with respect to time as the water wicked up at room atmospheric conditions.

3.2.10 Leakage Analysis

The strength of the hydrophobicity of the permanent marker was investigated by using four different colors of the marker to fill up the boundaries of the device. The colors utilized were blue, green, black and red. Each of these devices are then dipped into colored water for four minutes. It takes about three minutes to fill up the device with liquid, hence the extra one minute is to test the resistance of the boundary.

3.2.11 Stability Test

The stability of the device was investigated over 8 weeks both at room temperature and at a temperature of 4 ºC. The devices were fabricated and stored for bi-weekly investigation. The residual activity of the device is then computed. Also, the device was introduced to temperature range from 25 – 100 ºC for 20 minutes using an oven, and the residual activity was analysed.

3.2.12 Real-Life Sample Analysis

Tap water samples were collected from Concordia University hall building in Montreal, Saint Leonard Montreal, Cote des Neige Montreal, and Abeokuta Nigeria. The sample solutions were kept in plastic centrifuge tubes and analysed in the laboratory. The samples were evaluated with the paper based analytical device and with the traditional EDTA titration for comparative analysis to evaluate the accuracy and precision of the device.

3.2.13 Interference Test

Common interference ions in water (Mn^{2+}, Fe^{2+}, NH^{4+}, Cl^{-}, F^{-}, and Cu^{2+}) was prepared at concentration of 100 µM each and tested with the µPAD. The 100 µM concentration was chosen since the maximum allowable concentration (MAC) given by Health Canada (Health Canada, 2019) for each of the investigated ions is less than 80 µM.

3.2.14 Creation of Pullulan Tablets

15 mL of Eriochrome Black T (0.1M) solution was mixed with 15 mL of CAPS buffer (0.1 M) in a 50 mL centrifuge tube and mixed. Then, 5g of pullulan is weighted and poured into the resulting solution and mixed vigorously until all the solutes are dissolved. This results in a slurry solution of Eriochrome Black T, CAPS buffer, and pullulan. The slurry is then cast on a cylindrical plastic mold which is 8mm in diameter and 1 mm in height using a manual syringe pump. The slurry in

the mold is air-dried for 24 hours at room temperature till the tablet is well-formed. The resulting tablets were stored in a cool and dry place. Figure 3.2 shows the fully formed all-inclusive tablets.

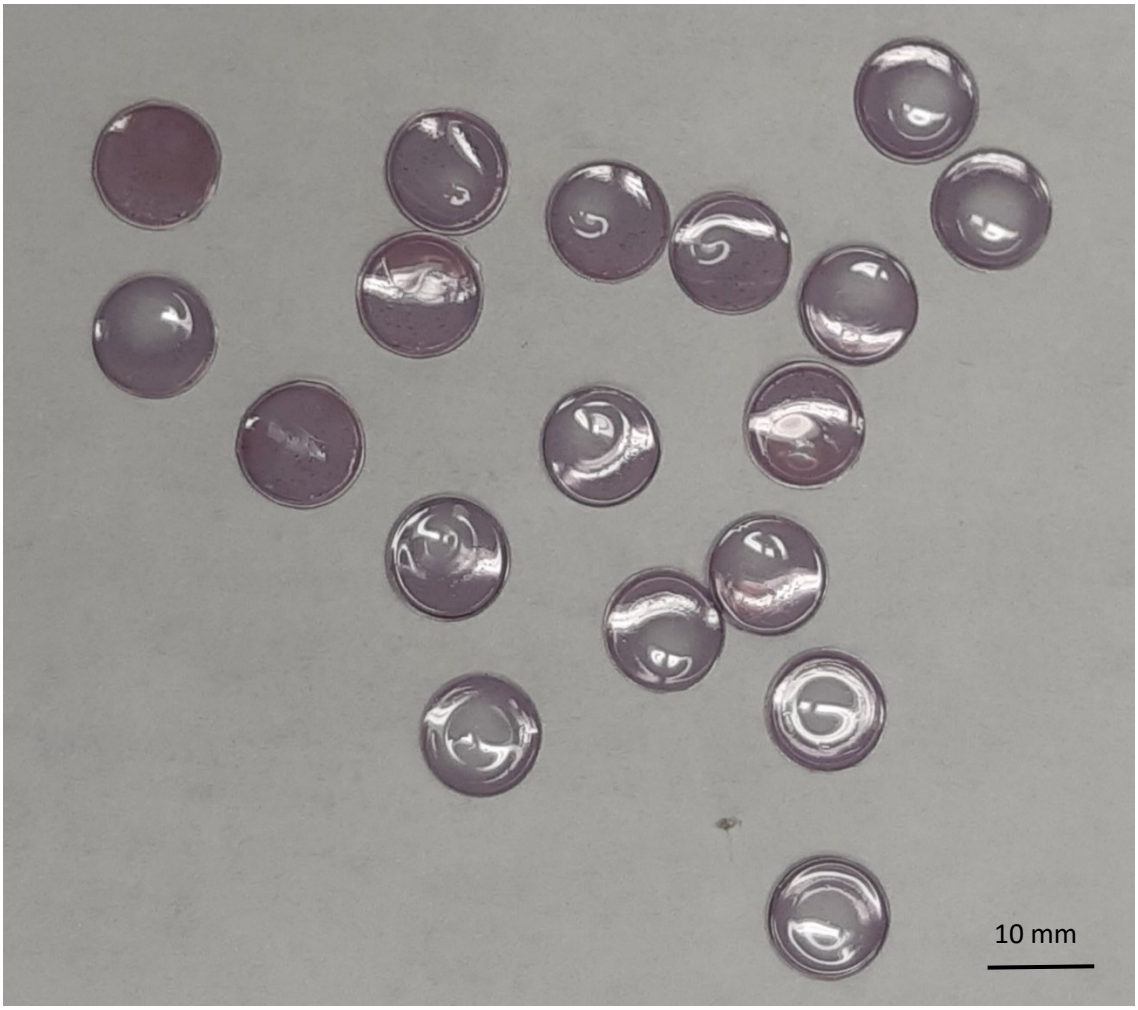

Figure 3-2 The all-inclusive pullulan tablets fabricated to determine the total hardness of water. The tablets are a mixture of eriochrome black T, CAPS buffer and pullulan powder.

4.1 Paper-based analytical device for the detection of the total hardness of water

4.1.1 Selection of The Paper Type and Marker Color for The Creation of Hydrophobic Barrier

Initial studies involved the optimization of the paper sensor in terms of the paper type and the selection of the permanent marker ink color for creation of the hydrophobic barrier to obtain the fastest detection and well-confined hydrophilic channels on paper (see Figures 4.1 and 4.2). The type of paper utilized was optimized in terms of wicking velocity. The most favorable color of permanent marker to be utilized also needed to be determined based on its barrier efficiency against water penetration, and this was investigated by using the water contact angle and leakage analysis. The permanent marker usage is quite promising for new and resource-limited laboratories on a low budget, particularly due to discontinuation of the solid ink printers by Xerox, which were the top candidate for creating hydrophobic barriers on paper substrate.

Elution velocity for four different types of Whatman paper was investigated and is shown in Figure 4.1a. The velocities of 66, 82, 241, and 270 μm/s were determined for Whatman Grade 2 filter paper, Whatman Grade 1 filter paper, Whatman Grade 4 chromatography paper, and Whatman Grade 4 filter paper, respectively. Therefore, the Whatman Grade 4 filter paper recorded the highest velocity. The observed higher velocity in Whatman Grade 4 filter paper was due to its higher pore size as compared the other paper types. The pore size of Whatman Grade 4 filter paper as given by the manufacturer is 20–25 μm, while for Whatman Grade 1 filter paper and Whatman Grade 2 filter paper, it is 11 and 8 μm, all at 98% efficiency, respectively. These results also follow excellently the Washburn equation (Masoodi and Pillai, 2010) of flow in porous media which gives

a directly proportional relationship between the velocity and pore size. Hence, due to the fast wicking velocity of the Whatman grade 4 filter paper, this paper type was selected for the fabrication of the μPAD.

In order to determine the best color of permanent marker appropriate for the fabrication of the μPAD, we analyzed the contact angle of the HPLC grade water on the different colors of permanent marker. To do this, the blue, black, green, and red permanent markers were applied thoroughly on the Whatman Grade 4 filter paper sheets. The contact angle measurements were performed after 10 seconds of dropping from the water droplet. The contact angles of 144 deg. for the black marker, 151 deg. for the blue marker, 145 deg. for the red marker, and 158 deg. for the green marker were observed as shown in Figure 4.1b. Therefore, the hydrophobic strength based on the water contact angle measurements was in the order green marker > blue marker > red marker ≈ black marker. In addition, an investigation of the contact angles of the four marker colors over 60 seconds showed similar results with those of the 10 seconds, indicating that the pigments in the marker pen had the potency to retain their hydrophobicity over time (Figure 4.1b).

Permanent markers contain non-polar solvents that are used in transporting the color pigment to the desired surfaces and have resins that cause the color pigment to stay on the surface (Mott and Walnutport Pa., 1992). The difference in contact angle for the different colors of marker may be linked to the difference in the concentration of resins, color pigments, and solvents utilized during manufacturing (Sanborn and Loftin, 1998). Particularly, the blue and green permanent markers are known to contain a large amount of the blue phthalocyanine pigment (van der Werf et al., 2011), which is a large organic compound that is insoluble in most solvents including water.

A leakage analysis of the 4 colors of permanent markers was conducted to further determine which color to use for the fabrication of the device. The device made with the 4 colors was dipped

into the colored HPLC grade water and investigated for leakages. After 4 min in the colored water, the device made with the green and the blue color markers did not show any sign of leakage, as they provided a formidable barrier against the pressure of the water molecules (Figure 4.2a and b). However, the black and the red marker fabricated devices leaked after 4 min in the colored water (Figure 4.2c and d). This leakage can be linked to the lower concentration of the non-polar resin and pigment (Mott and Walnutport Pa., 1992) in the red and black marker and hence the lower resistance.

Therefore, for the fabrication of the μPADs, the green and the blue markers were utilized to create hydrophobic barriers for the flow of water through the device.

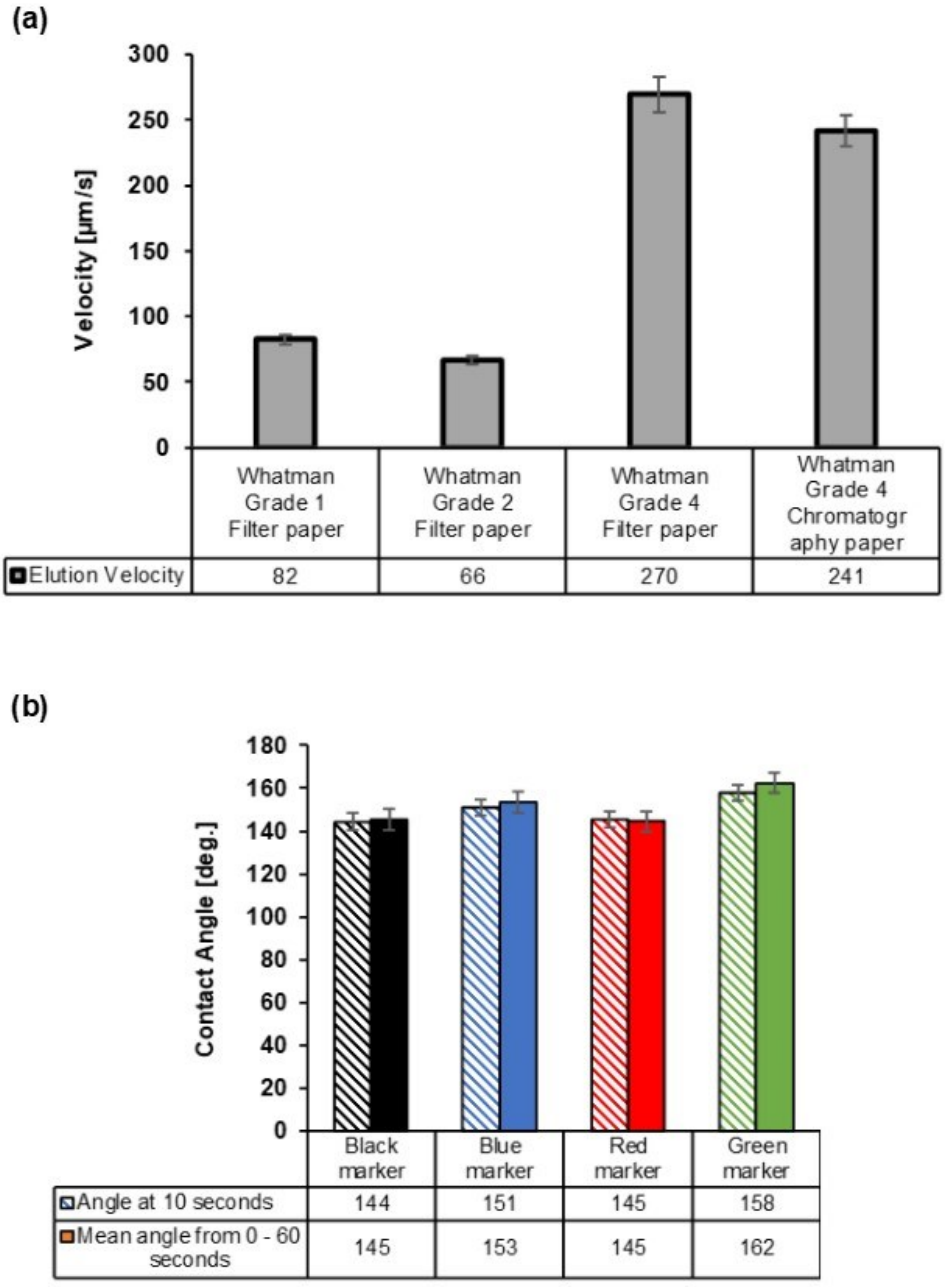

Figure 4-1 Optimization of the paper-based analytical device's fabrication with respect to the paper type and marker color. (a) The elution velocity of distilled water in different grades of paper. (b) The contact angle measurement over time for the black marker, blue marker, red marker and green marker on Whatman® Grade 4 filter paper (slanted shade is measurement at 10 s and full color shade is mean measurement over 60 s.). Each bar represents the mean of the three individual experiments ± standard deviation.

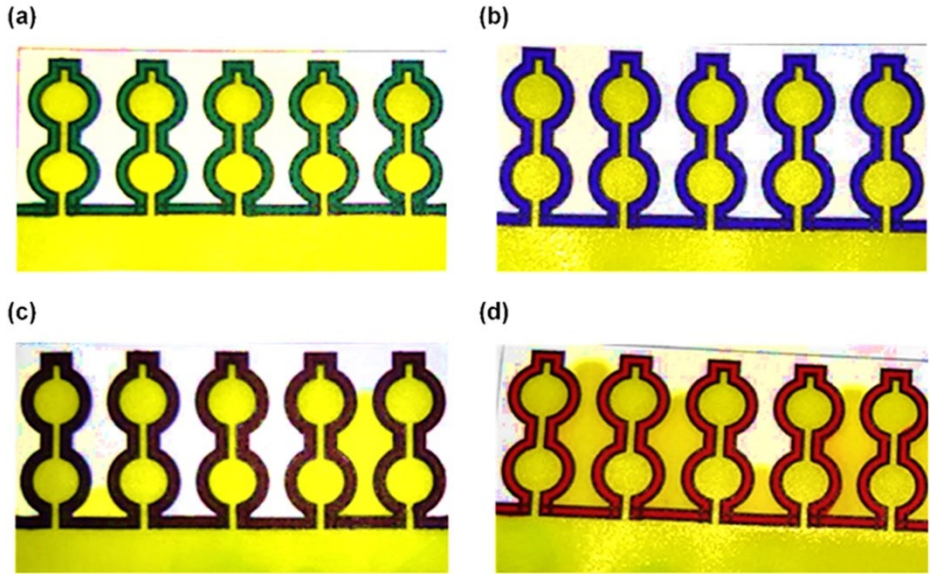

Figure 4-2 Leakage analysis for different marker colors on the device; (a) green marker (b) blue marker (c) black marker (d) red marker.

4.1.2 Selection of Appropriate Working Design for The Microfluidic Paper-Based Analytical Device

In the process of determining the best working design for the µPAD, several designs were considered, and their feasibility was analysed. A three-dimensional (3-D) µPAD (sandwiching two layers of paper substrate) as reported by Jayawardane et al. (Jayawardane et al., 2012) , was designed and investigated (Figure 4.3). The reaction zones and the detection zones were designed to be superimposed perfectly with adhesives on the paper surface. Hence, the detection zones housed the metals ion indicator (EBT), the reaction zone housed the EDTA, and the water sample is introduced through the reaction zones and moves down to the detection zone for the systematic detection of the total hardness of the water as shown in Figure 4.3. The corresponding reactions zones to the detection zones D1, D2, D3 and D4 contained dried analytes of 3 µL of 0.5mM, 0.61 mM, 1.21 mM and 1.8 mM of EDTA respectively. Therefore, 3 µL of 0.81 mM $CaCO_3$ equivalent of water hardness was introduced to each reaction zones and left for about 5 minutes for the complexometric reaction to take place and to cause the downward movement of the unreacted

solute in the sample to the detection zones. However, the design was impeded by mixing issues at the detection zones (D1 – D4) as shown in figure 4.3b, since only zones D1 and D2 is expected to turn pink while zones D3 and D4 should remain blue. The color change and formation in the detection zone was not uniform due to lack of uniformity in the distribution of analytes as the analytes move from the reaction zones to the detection zones. This caused a phenomenon called the Coffee Ring reported by Garcia-Cordero and Fan (Garcia-Cordero and Fan, 2017).

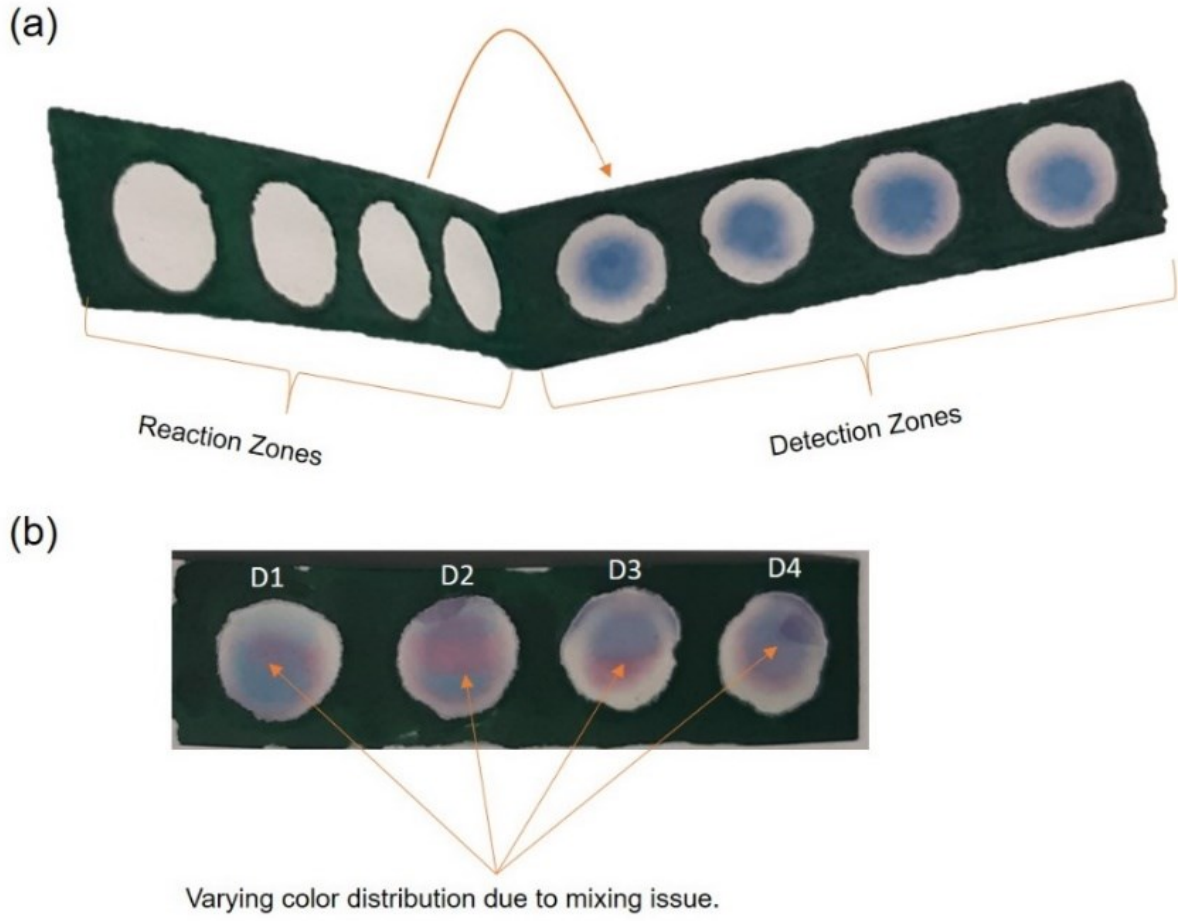

Figure 4-3 Proposed three-dimensional (3D) design for µPAD (a) description of the device (b) Outcome of the result after testing with unequal distribution of analytes and formation of output signal.

In order to solve the mixing and analyte distribution issue for the 3D model, a transition zone was in cooperated as shown in Figure 4.4a. This transition zone was included to cause a lag in time for

the complexometric reaction to take place before the analytes get to the detection zone. As shown in Figure 4.4b, this transition zone introduction approach didn't solve the mixing issues, as the poor mixing of analytes still exits.

Due to the mixing issues, the 3D design approach for the µPAD fabrication was dropped and the 2-D lateral flow design was adopted and used for the device fabrication as described in Figure 3.1b which ends with the application of the permanent marker pen on the printed device.

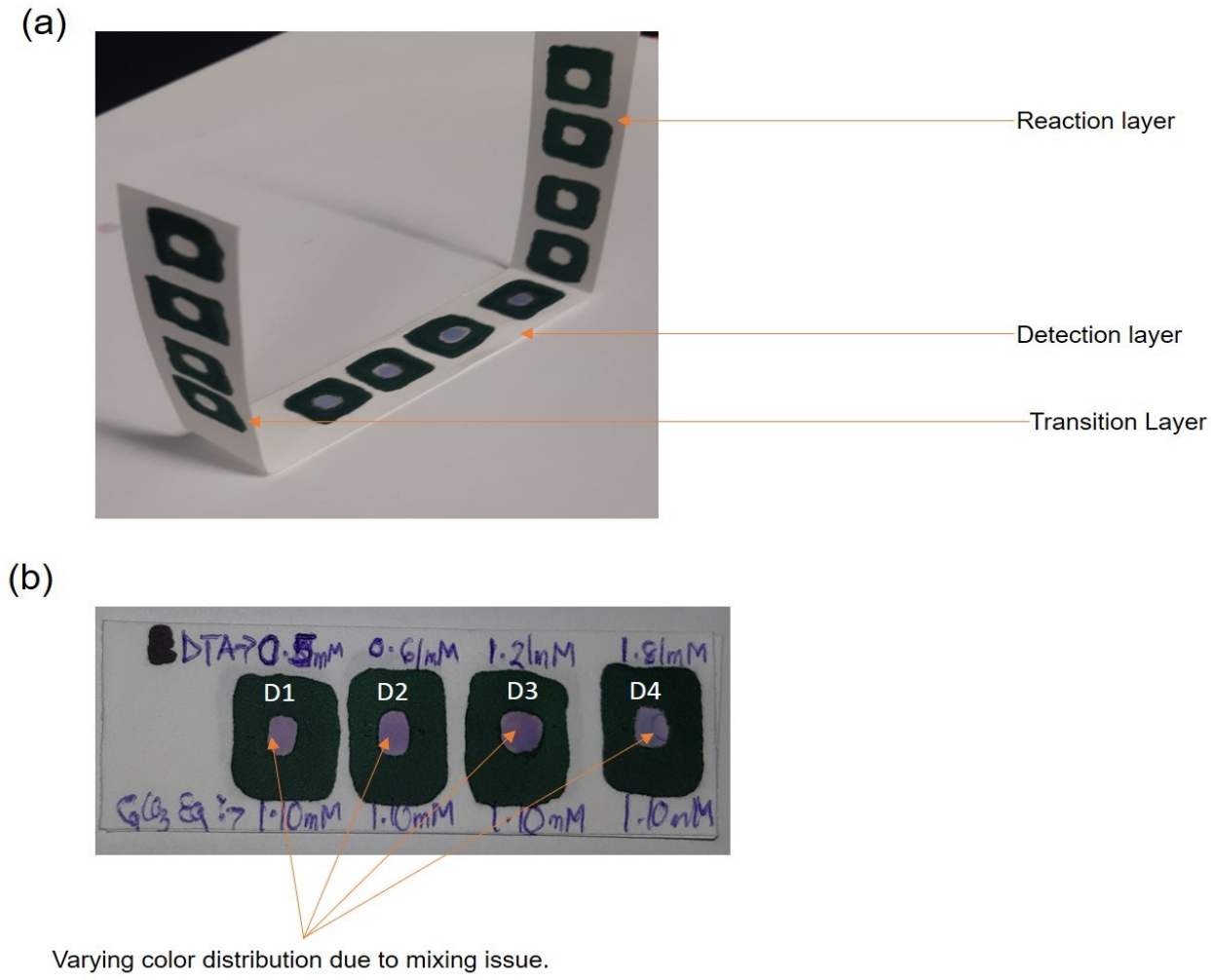

Figure 4-4 Proposed three-dimensional (3D) design with transition layer for µPAD (a) description of the device (b) Outcome of the result after testing with unequal distribution of analytes and formation of output signal.

4.1.3 Analysis of Water Sample Using the Microfluidic Paper-Based Analytical Device

After the selection of the Whatman grade 4 filter paper as the paper substrate and the green and the blue permanent markers as the marker type for creating hydrophobic barriers on the µPAD, the paper sensor was fabricated, and reagents were deposited on each zone.

The µPAD was used by inserting the dip zone into the water sample (as illustrated in Figure 4.5) and allowed to remain in the sample for about 3 min, which is the time taken to fill up the device completely. After the complete filling of the device, it was removed and read qualitatively or quantitatively depending on need.

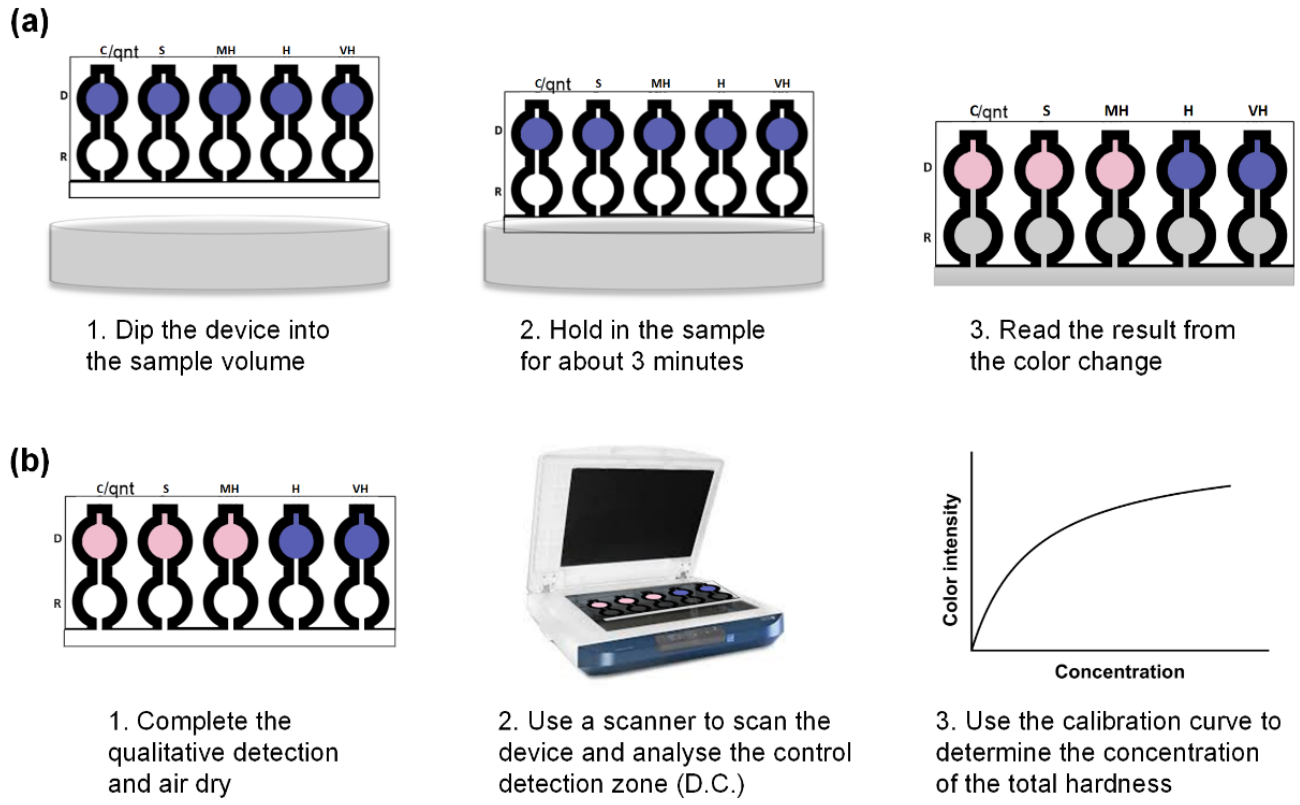

Figure 4-5 The application of the paper-based analytical device for water analysis. (a) Qualitative detection of total hardness using lateral flow dip-and-read paper based analytical device. (b) Quantitative detection of total hardness using lateral flow dip-and-read paper based analytical device.

4.1.4 Optimization of The Reagents on The Microfluidic Paper-Based Analytical Device, Stoichiometric Cancellation, and Expectations

The deposition of reagents was done in a way that mimicked the classification given by the World Health Organization and allowed for the selective cancelling of analytes at the reaction zones during testing. Therefore, excess analytes moved to the detection zones to produce a color change from blue to pink. For qualitative detection, the result was determined by the last color change signal from blue to pink at the detection zone starting from the leftmost detection zone D.C. Hence, if the last color change from blue to pink happens at the zones D.S., D.MH., D.H., or D.VH., it means the hardness of the water is either soft, moderately hard, hard, or very hard, respectively (see Table 4.1 and Figure 4.6).

Table 4.1 Calculations of the stoichiometric expectations for the test results of the spiked water samples with Mg^{2+} and Ca^{2+} using the paper-based device. (a) Soft water with the total hardness less than 60 mM; (b) moderately hard water with the total hardness between 0.61-1.20 mM; (c) hard water with the total hardness between 1.21-1.8 mM; (d) very hard water with the total hardness more than 1.81 mM.

Channel	Hardness of the water sample (mM) "Volume = 11 µL"	Concentration of the applied EDTA (mM) in the reaction (R) zone "volume = 5.5 µL"	Hardness of water moving to the detection (D) zones (mM)	Color output at the detection (D) zones
a) Soft water				
Channel 1 (C)	0.40	0.00	0.40	Pink
Channel 2 (S)	0.40	0.40	0.20	Pink
Channel 3 (MH)	0.40	1.22	0.00	Blue
Channel 4 (H)	0.40	2.42	0.00	Blue
Channel 5 (VH)	0.40	3.62	0.00	Blue
b) Moderately hard water				
Channel 1 (C)	0.81	0.00	0.81	Pink
Channel 2 (S)	0.81	0.40	0.61	Pink
Channel 3 (MH)	0.81	1.22	0.20	Pink
Channel 4 (H)	0.81	2.42	0.00	Blue
Channel 5 (VH)	0.81	3.62	0.00	Blue

c) Hard water				
Channel 1 (C)	1.40	0.00	1.40	Pink
Channel 2 (S)	1.40	0.40	1.20	Pink
Channel 3 (MH)	1.40	1.22	0.79	Pink
Channel 4 (H)	1.40	2.42	0.19	Pink
Channel 5 (VH)	1.40	3.62	0.00	Blue
d) Very hard water				
Channel 1 (C)	2.00	0.00	2.00	Pink
Channel 2 (S)	2.00	0.40	1.80	Pink
Channel 3 (MH)	2.00	1.22	1.39	Pink
Channel 4 (H)	2.00	2.42	0.79	Pink
Channel 5 (VH)	2.00	3.62	0.19	Pink

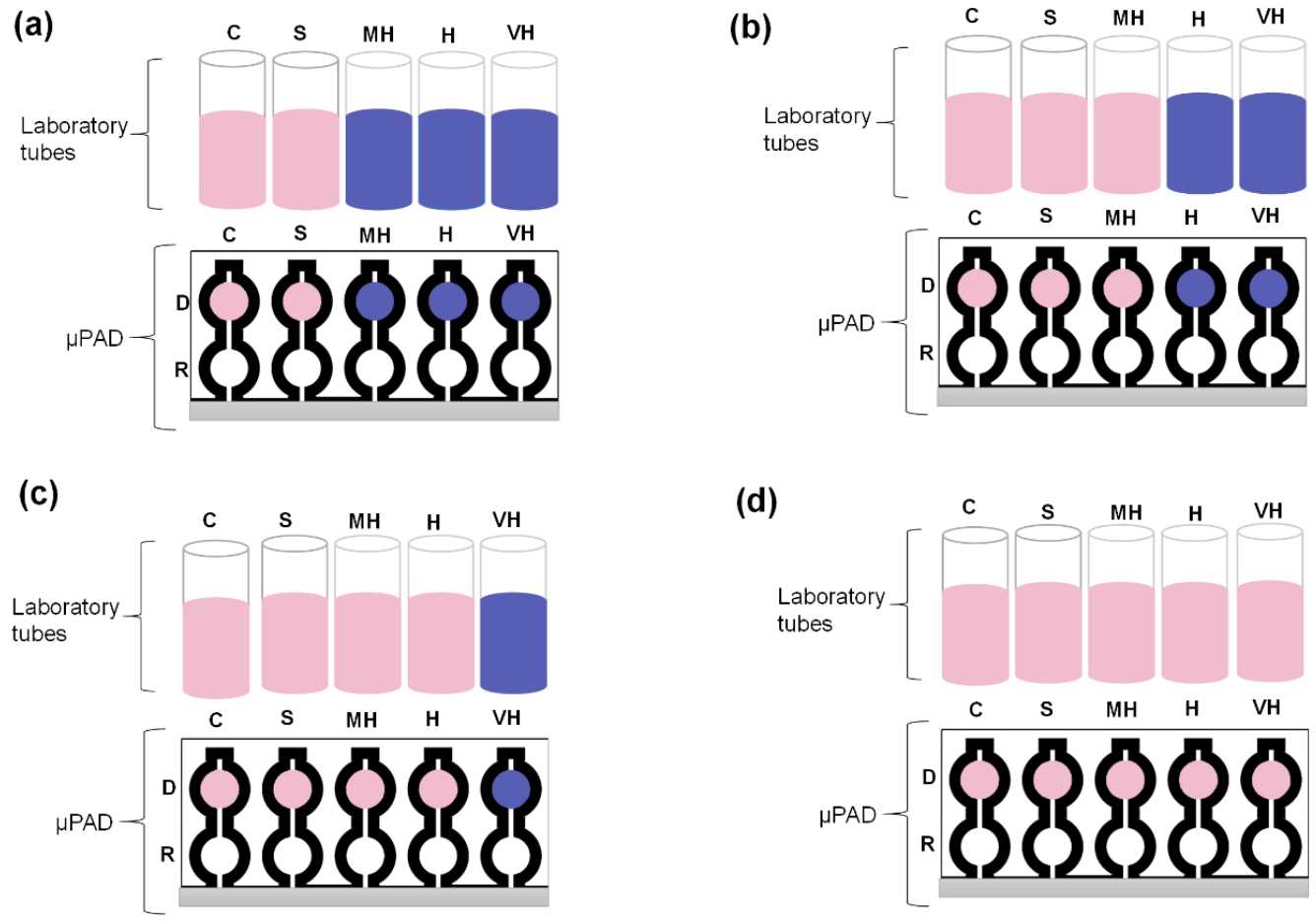

Figure 4-6 Schematic of the complexometric titration in the solution phase in laboratory test tubes and the expectations on the paper-based device according to the stoichiometric calculations which were presented in Table S1: (a) soft water, (b) moderately hard water, (c) hard water, and (d) very hard water (D: detection zone; R: reaction zone; C: control; S: soft; MH: moderately hard; H: hard; VH: very hard).

For the equivalent $CaCO_3$ concentration less than 0.61 mM (soft water), only the zones D.C. and D.S. were expected to turn from blue to pink (Fig. 4.6a). The stoichiometric relationship that happened when the μPAD detected soft water (0.4 mM total hardness) is tabulated in Table 4.1a to show the cancellation of analytes and the reason for the color change at the detection zones. For $CaCO_3$ concentration equivalent between 0.61–1.20 mM (moderately hard water), only the zones D.C., D.S., and D.MH. were expected to turn from blue to pink (Figure 4.6b), since only these zones had free analytes ready to react with the indicator as shown in the stochiometric table for 0.81 mM total hardness (moderately hard water) in Table 4.1b. For equivalent $CaCO_3$ concentration between 1.21–1.80 mM (hard water), only the zones D.C., D.S., D.MH., and D.HW. were expected to turn from blue to pink (Figure 4.6c), and for equivalent $CaCO_3$ concentration greater than 1.8 mM (very hard), all the detection zones (D.C.–D.VH.) were expected to turn from blue to pink (Figure 4.6d). The stoichiometric relationship for hard water (1.4 mM total hardness) and very hard water (2.0 mM total hardness) on the μPAD is tabulated in Table 4.1c and d, respectively, showing the progression of the analyte cancelation in the reaction zones and the moving of excess analytes to the detection zones to produce the color change.

4.1.5 Qualitative Determination of the Total Hardness of Water for Spiked Samples

To evaluate the performance of the developed paper sensors, Ca^{2+} and Mg^{2+} ions as $CaCO_3$ equivalent of the total hardness were spiked into the HPLC grade water samples at four different known concentrations and assayed using the paper device to evaluate if the color changes met the expectation. The color change expectations were based on the stoichiometry of the reactions for the total hardness of water that happened in the reaction and detection zones (see Table 4.1 and Figure 4.6).

The results of the qualitative detection of the total hardness of water are shown in Figure 4.7a. The device was dipped into the water samples at room temperature, and the color changes were observed in the detection zones after ~3 min. For the spiked water sample of a concentration 0.49 mM $CaCO_3$ equivalent (Figure 4.7a-i), the zones D.C. and D.S. turned pink while the remaining detection zones stayed blue. This observation showed that the water was soft, and the result was in accordance with the expectation. For the moderately hard water detection (Figure 4.7a-ii), a 0.81 mM spiked sample of $CaCO_3$ equivalent was used, and the zones D.C, D.S., and D.MH. turned pink. This moderately hard water also mimicked the expectation. For the classified hard water detection (Figure 4.7a-iii), a 1.35 mM spiked sample of $CaCO_3$ equivalent was used, and the expectation was for the zones D.C., D.S., D.MH. and D.H. to turn pink. The result of the actual device mimicked the expectation perfectly. This favorable result worked well for the very hard water detection as well, as shown in Figure 4.7a-iv using 2.5 mM spiked sample of $CaCO_3$ equivalent total hardness. The perfect synchronization between the expectation and the actual device's results proved that the device could qualitatively determine the total hardness of water using the classification given by the World Health Organization.

The fabricated device was also investigated to find out if it could test water samples that contain only a single ion. To do this, spiked samples of 0.81 mM calcium ion and 0.81 mM magnesium ion were utilized. At that concentration, the spiked sample falls into the moderately hard water category, and the expectation was for the zones D.C., D.S., and D.MH. to turn pink as shown in Figure 4.6b. The expectation was perfectly met since the zones D.C., D.S., and D.MH. turned pink as shown in Figure 4.8a and b. These results proved that the device is capable of testing for total hardness in water samples containing either or both magnesium and calcium ions.

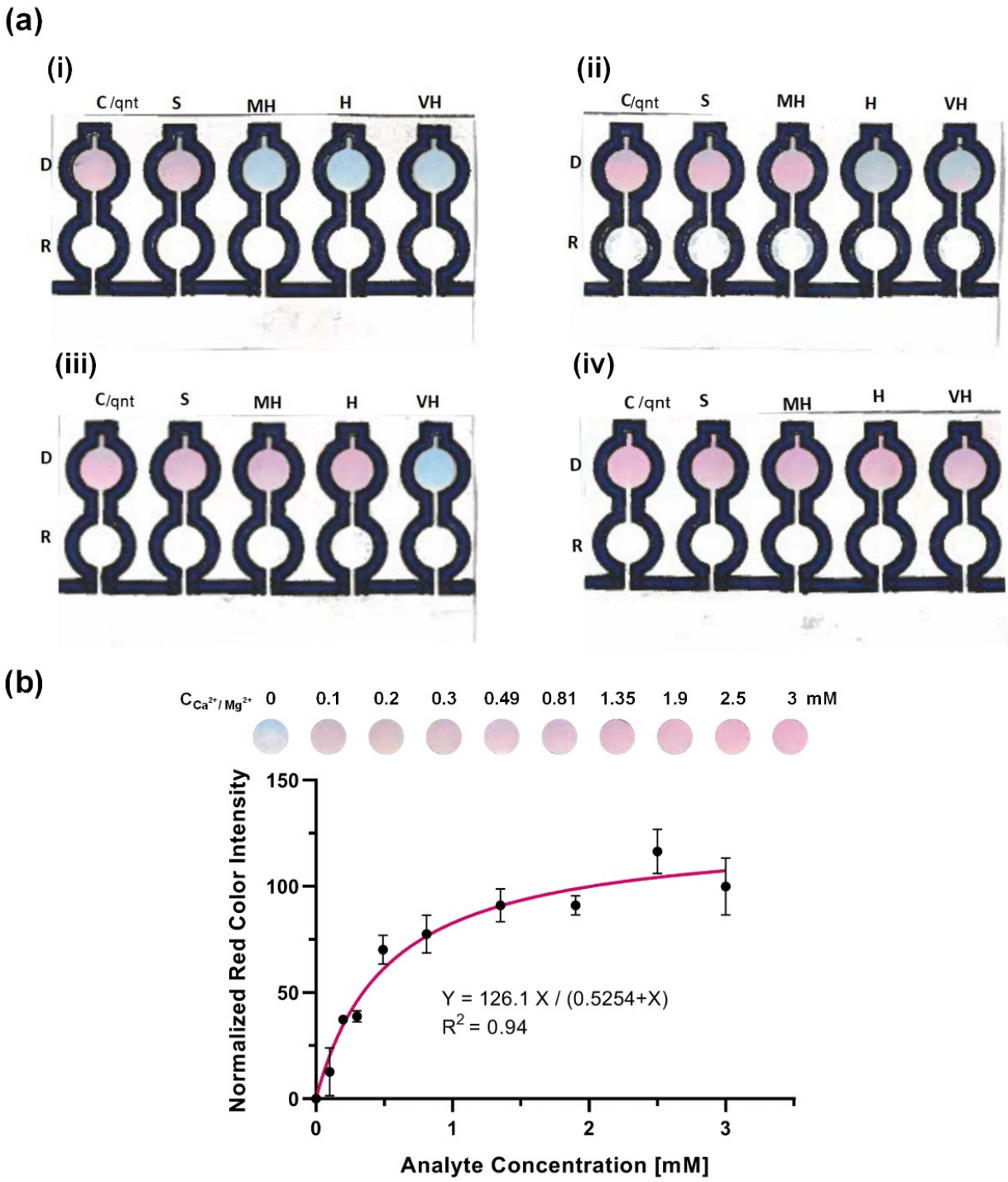

Figure 4-7 Qualitative and quantitative detection of the total hardness of water. (a) Qualitative detection of the total hardness of spiked samples of (i) soft water as in 0.49 mM equivalent $CaCO_3$ concentration, (ii) moderately hard water as in 0.81 mM equivalent $CaCO_3$ concentration, (iii) hard water as in 1.35 mM equivalent $CaCO_3$ concentration, and (iv) very hard water as in 2.5 mM equivalent $CaCO_3$ concentration. (b) Calibration curve for quantitative analysis using the paper-based analytical device. The control detection zone of the device changed from blue to pink in ~3

min in correspondence with different concentrations of the $CaCO_3$ equivalent to the total hardness of water. In the graph, the black data points represent the normalized average red color intensities of the control detection zone of the device at each concentration obtained by the ImageJ software after scanning. Each point is the mean of the three individual experiments at each concentration ± standard deviation. The solid line illustrates the best fitted Michaelis-Menten equation to the data.

4.1.6 Quantitative Determination of the Total Hardness of Water for Spiked Samples

To make the sensor quantitative (not semi-quantitative), we introduced an alternative colorimetric reaction. Here, unlike other existing works, we performed a reaction without utilizing EDTA. In this approach, the colorimetric signal is not easily distinguishable by naked eyes; however, using a smart-phone or a mobile scanner, the user can store an image of the sensing zone to be analyzed by ImageJ, a mobile phone application and software available for free. Thus, for quantitative detection, the result is determined by scanning the device after the completion of the qualitative detection and the complete drying of the device. The red color intensity of the control detection zone (D.C.) is then used to determine the concentration of the equivalent ion.

To be able to use the device for the quantification of the water hardness, we tested the μPAD in a series of standard concentrations of $CaCO_3$ equivalent of total hardness and obtained a calibration curve (Figure 4.7b). The concentrations 0.1, 0.2, 0.3, 0.49, 0.81, 1.35, 1.9, 2.5, and 3 mM were chosen such that they cover all types of water hardness according to the WHO classification. The quantitative detection was done through the control channel with the detection zone (DC) loaded with the indicator (EBT) and the reaction zone (RC) devoid of EDTA. The control detection zone was turned from blue to pink ~3 min after putting the device in the water samples due to the formation of calcium/magnesium–Eriochrome Black T complex. Then, the device was air dried, scanned with an office scanner, and the average red color intensity of the control detection zone

was obtained by the ImageJ software. This process of detection allowed the quantitative detection of the total hardness of water without the need of EDTA in the reaction zone.

As Figure 4.7b demonstrates, the red color intensities in the concentration range of the experiment show a saturation behavior. This observation is justifiable by the fact that there were only limited amounts of indicator molecules reacting with the analytes to form the pink complexes, eventually reaching a saturated state in color intensities. Accordingly, we fitted the Michaelis–Menten saturation equation to our calibration data. The high R-squared value of 0.94 showed that the fitted line properly predicted the trend of the data in the desired concentration range. Therefore, this equation was used for further quantification of water hardness in real-world samples.

In addition, the limit of detection of the fabricated μPAD using an existing equation ($LOD = X_{b1} + 3S_{b1}$, where X_{b1} is mean concentration of the blank and S_{b1} is the standard deviation of the blank) was calculated to be 0.02 mM. This low LOD improved on existing commercially available test strips (often with a LOD of 0.25 mM) and other reported μPADs in the literature. As shown in Figure 4.9, our fabricated μPAD improved the value of the LOD of water hardness devices by at least 80%, hence showing its greatly improved sensitivity.

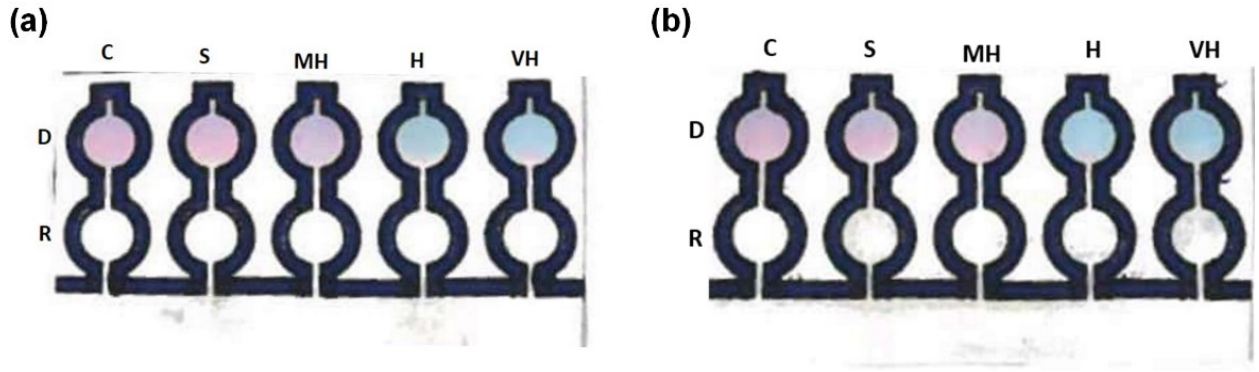

Figure 4-8 Qualitative detection of total hardness of water containing only a single ion of calcium and magnesium ion. (a) 0.81 mM calcium ion, and (b) 0.81 mM magnesium ion.

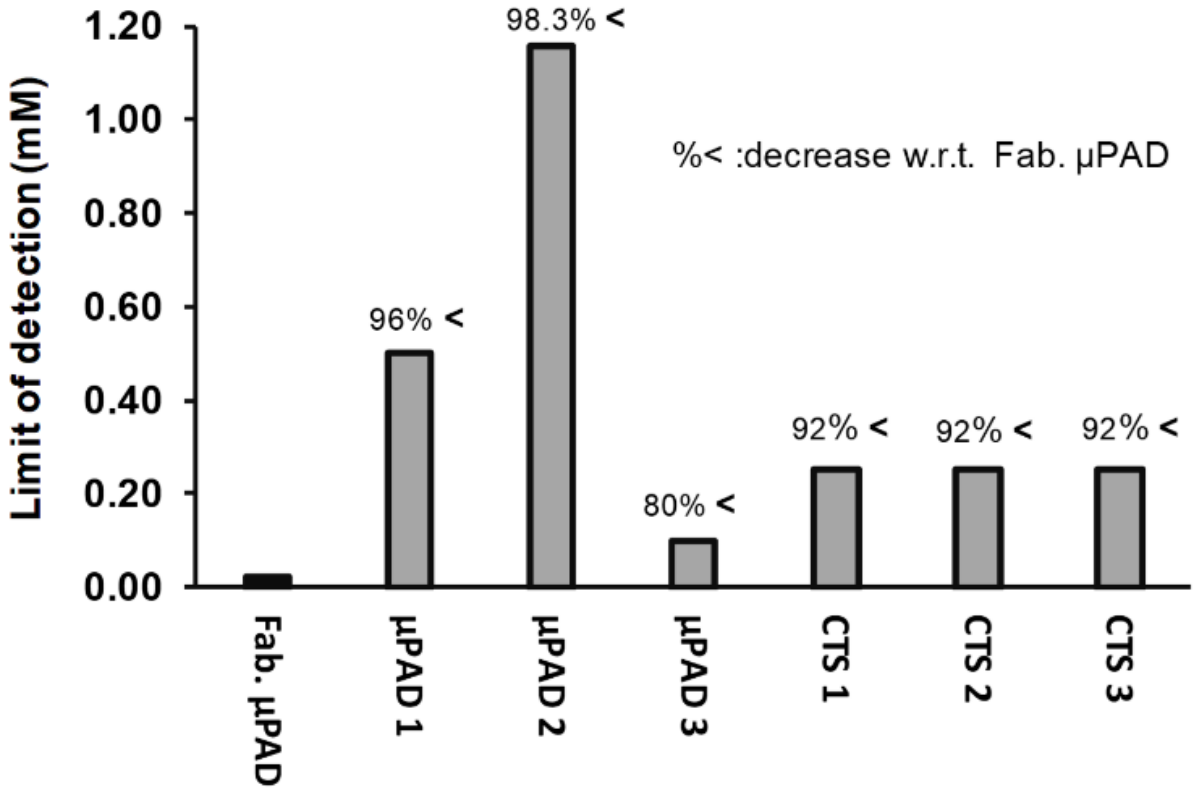

Figure 4-9 Comparison of the limit of detection (LOD) of the fabricated µPAD (Fab. µPAD) with µPAD 1 (fabricated by Karita and Kaneta (Karita and Kaneta, 2016)), µPAD 2 (fabricated by Shariati-Rad and Heidari (Shariati-Rad and Heidari, 2020)), µPAD 3 (fabricated by Ostad et al. (Ostad et al., 2017)), CTS 1 (Commercial Test Strip manufactured by Honeforest (HoneForest, n.d.)), CTS 2 (Commercial Test Strip manufactured by Health Metric (Health Metric, n.d.)), and CTS 3 (Commercial Test Strip manufactured by Thomas Scientific (Thomas Scientific, n.d.)).

4.1.7 Real-World Sample Analysis

To demonstrate the applicability of the paper-based device for the determination of water hardness in real samples, tap water samples from different municipal districts were collected and analyzed for their total hardness using both the paper-based device and the common traditional titration assay. The results of the qualitative and comparative quantitative analyses are shown in Figure 4.10 a and b, respectively. For the water sample from Abeokuta in Nigeria, the µPAD (quantitative) recorded a value of 0.37 mM, and the total hardness gotten from the traditional titration value was 0.37 mM (p = 0.932) (Figure 4.10b-iv). Qualitatively, the traditional titration predicted that the water was soft, and the µPAD also predicted the same (Figure 4.10a-iv). For the water sample from Cote des Neiges, Montreal, the total hardness gotten using the traditional titration was 1.19 mM, and the µPAD (quantitative) gave a total hardness value of 1.11 mM (p = 0.094) (Figure 4.10b-i). Qualitatively, the traditional titration predicted a moderately hard water sample, and the µPAD also predicted the same (Figure 4.10a-i). The analysis of the water samples gotten from Montreal East and the Concordia University Hall building in Montreal, Canada with the µPAD (quantitative) gave a total hardness concentration of 1.38 mM and 1.21 mM, respectively. The total hardness concentration gotten through the traditional titration for both locations were 1.29 (p = 0.052) and 1.27 mM (p = 0.222), respectively (Figure 4.10b-ii and iii). With the total hardness value gotten through the traditional titration means, both water samples were categorized as hard water, and the µPAD gave the same outcome (Figure 4.10a-ii and iii).

Overall, the device proved to be an accurate tool to test for the total hardness of water with error values less than 7% in comparison with the traditional titration means. This error may be mainly attributed to the non-uniformity and inconsistency in the Whatman filter paper's structure (Liu et al., 2014), which affects the repeatability and sensitivity of the assay.

Previously, μPADs have been reported for the semi-quantitative analysis of the total hardness of water using the chelate titration as the detection method (Karita and Kaneta, 2016). Nonetheless, the proposed approach here provides a number of advantages: (1) the dip-and-read lateral flow design makes the device ready-to-use, eliminating the need for any auxiliary equipment such as volume-calibrated pipettes or droppers; (2) the design based on the WHO classification makes it easier for the final consumer to readily determine how high the total hardness of water is; and (3) the inclusion of a control zone in the design allows for the quantification of the total hardness of water for more accurate analysis.

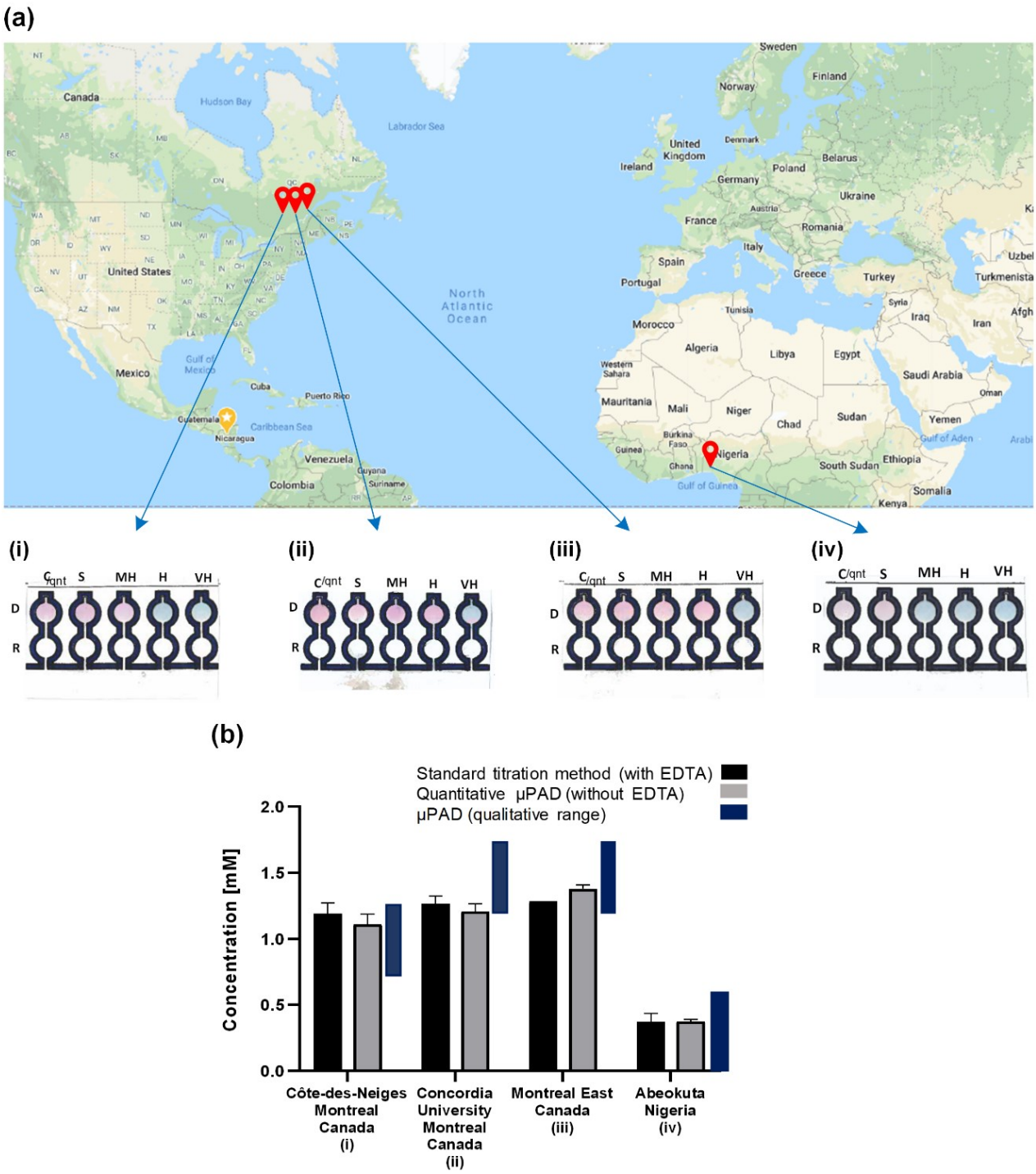

Figure 4-10 Real-world tap water samples and comparison with the conventional detection method. ***(a)*** *Qualitative analysis of the total hardness for the real-world tap water samples from (i) Cote-des-Neiges, Montreal, Canada. Moderately hard water was qualitatively predicted by the µPAD. (ii) Concordia University, Montreal, Canada. Hard water was qualitatively predicted by the µPAD. (iii) Montreal East, Canada. Hard water was qualitatively predicted by the µPAD. (iv)*

Abeokuta, Nigeria. Soft water was qualitatively predicted by the μPAD. (b) Quantitative analysis of the water hardness of the real-world samples with the μPAD and their comparison with the traditional titration method. Each bar represents the mean of the three individual experiments for each water sample ± standard deviation. The statistical analysis showed no significant difference between the μPAD results and those of the traditional titration.

4.1.8 Stability Test

Next, shelf-life investigations were performed to further demonstrate practical utility. To evaluate the long-term stability of the device, the colorimetric response of the reagents on the μPAD to spiked water sample concentrations was monitored upon storage at room temperature, and in the fridge for up to eight weeks. As shown in Figure 4.11a, after monitoring the retained activity, the device was stable for at least eight weeks at room temperature and at 4 °C. Furthermore, the retained activity of the device on exposure to varying harsh temperatures over 20 min was also investigated. Figure 4.11b shows the stability of the device across different temperatures ranging from 25–100 °C. These stability results show the excellent shelf-life of the device at varying conditions.

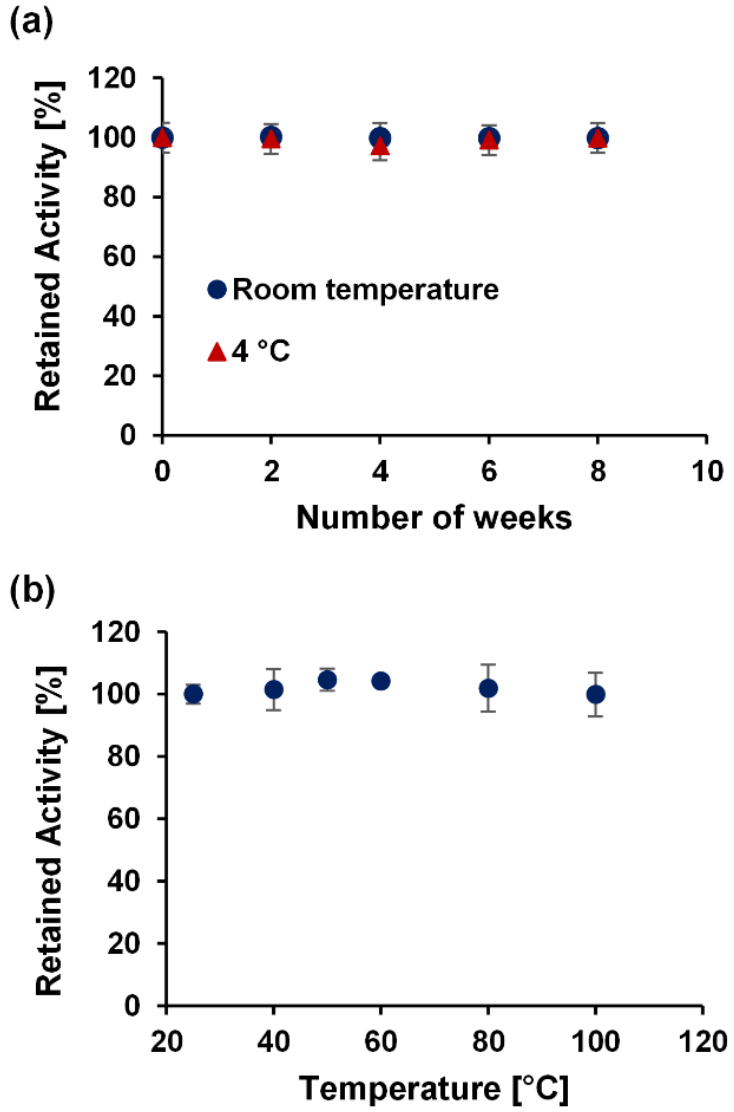

Figure 4-11 Stability test on µPAD at varying time intervals and conditions. Retained activity of the test kit (a) over a period of 2 months (8 weeks) at room temperature and at 4 °C and (b) after 20 min at varying temperatures from 25 °C to 100 °C. Each data point is the mean of the three individual experiments ± standard deviation.

4.1.9 Interference Test

After the analytical performance comparison and shelf-life evaluation, the interference of common ions in water such as Mn^{2+}, Fe^{2+}, NH^{4+}, Cl^{-}, F^{-}, and Cu^{2+} was investigated. The maximum allowable concentration (MAC) by Health Canada (Health Canada, 2019) for the studied ions is

given in Table 4.2. The MAC of each of the ions is less than 80 µM; hence, the interference of 100 µM (0.1 mM) of each ion was compared with the limit of detection of the device (0.1 mM) for the total water hardness. Figure 4.12 shows the average red color intensity value of 214 when the device began to quantitatively detect the presence of ions (Mg^{2+} & Ca^{2+}) in the water samples (LOD), and the red color intensity of the tested interference ions were largely lower than this value. Hence, each of the ions had no significant interference with the usage of the device for the detection of the total hardness of water at the maximum allowable concentration set by Health Canada.

Table 4.2 Maximum allowable concentration (MAC) of ions in water by Health Canada (Health Canada, 2019)

S/N	Definition	MAC (mg/L)	MAC (µM)
1	Mn^{2+}	0.12	2.19
2	Fe^{2+}	0.3	5.38
3	NH^{4+}	0.1	5.56
4	Cl^{-}	2	56.34
5	F^{-}	1.5	78.95
6	Cu^{2+}	2	31.25

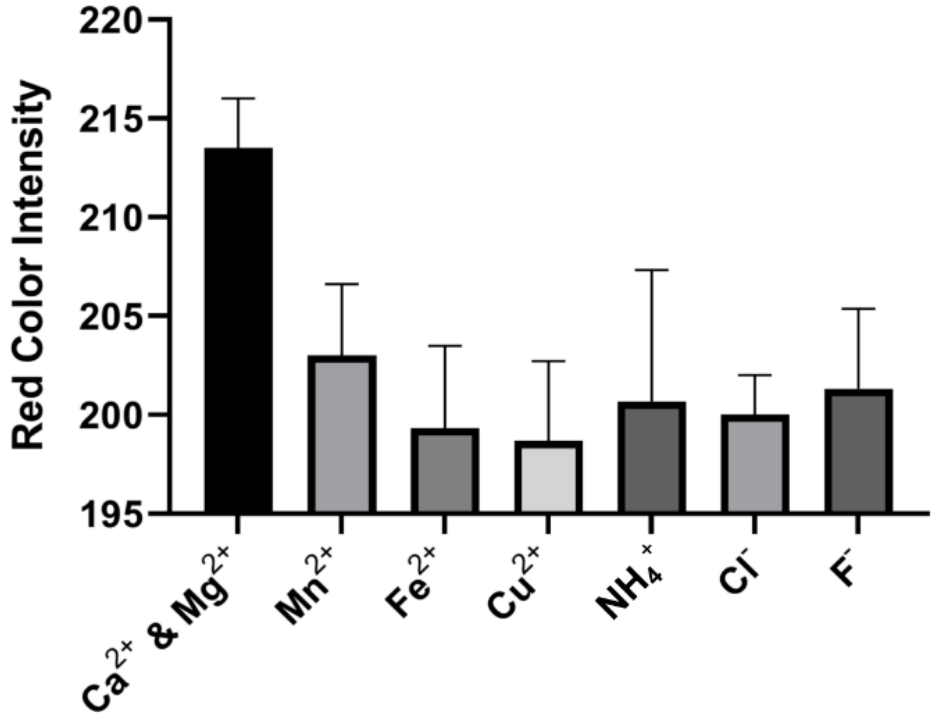

Figure 4-12 Interference test of the common ions in water in comparison with the limit of detection (0.1 mM) of the combined calcium and magnesium ions by the device. For each of the interference ions, the concentration of 0.1 mM was used for the comparison. Each data point is the mean of the three individual experiments ± standard deviation.

4.2 Pullulan tablet for the determination of the total water hardness

4.2.1 Analysis of water using the pullulan tablet

After publishing the results on the developed paper-based sensor for detection of water hardness, the scope of the project was extended to explore a tablet-based platform. Pullulan as a natural water-soluble polysaccharide was used to encapsulate all the assay reagents. The pullulan tablets were fabricated as described in section 3.2.14, with the average weight of each tablet being 13 mg ± 0.1, and it takes about 5 minutes to dissolve in water after some level of agitation of the vessel. For the determination of the total water hardness using the tablet sensor, the tablet only needs to be dropped in the water sample, allowed to dissolve with some agitation, and the red color intensity is computed and analysed (Figure 4.13).

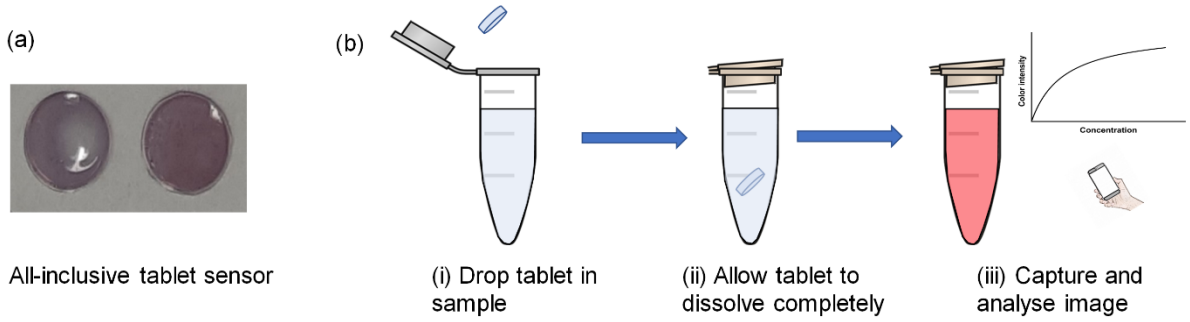

Figure 4-13 Tablet assay kit for total water hardness. (a) solidified tablet comprising of EBT, CAPS buffer and pullulan. (b)The application steps of the tablet sensor for the determination of the total water hardness.

4.2.2 Determination of the amount of pullulan tablets for each test

In order to determine the amount of pullulan tablets to use for each assay, a study into the quantity of tablets per volume of water was done. For this experiment, varying number of tablets (1 – 5 tablets) were introduced into different microtubes containing 1.4 mL of water (hardness of 0.49 mM). All the tablets in each microtubes were then allowed to dissolve to cause a color change to pink spectrum. On full dissolution, the color intensity of the solution in each microtubes is computed using the image-J software and graphed as shown in Figure 4.14. The figure shows a gentle slope beginning from two doses of tablets and upwards. Due to this, a dosage ration of 2 tablets per 1.4 ml of water was utilized consequently. These 2 tablets can however be merged into one single tablet by utilizing a combined ratio of EBT.

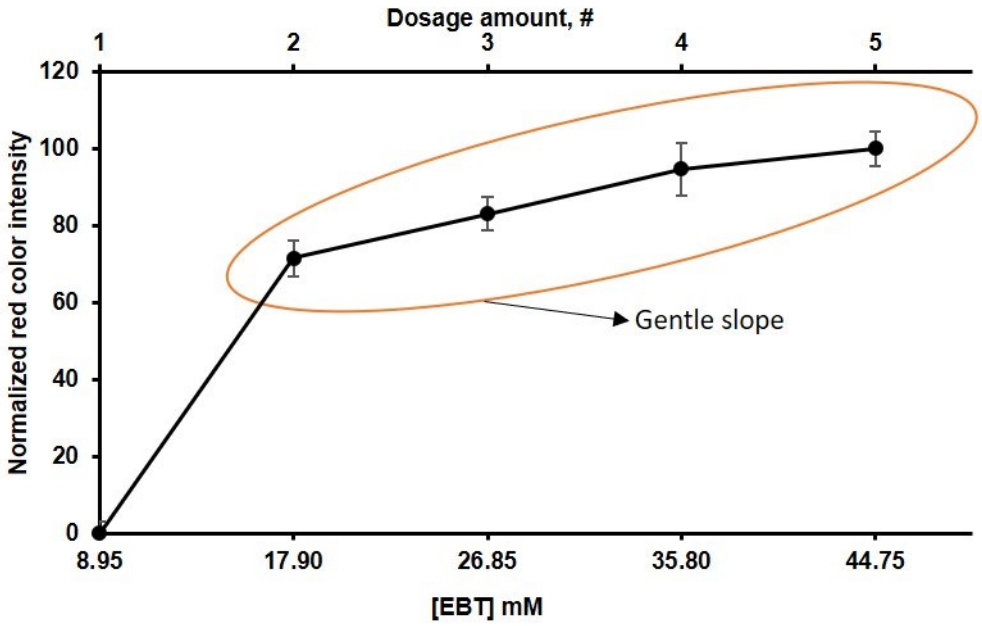

Figure 4-14 Dosage ration of the pullulan table and eriochrome black T (EBT) concentration for the detection of the total water hardness per volume of water. The dosage amount of the tablet is varied from one to five in different 1.4 mL of water (hardness of 0.49 mM), and each tablet contains about 8.95 mM EBT.

4.2.3 Quantitative detection of the total water hardness with pullulan tablets

After the optimization of the amount of tablet dose per liter of water, a calibration curve for the quantification of the total water hardness using the pullulan tablets was generated (Figure 4.15). In order to generate the curve, two sensor tablets were dropped into 1.4 mL of water with varying water hardness, and the red color intensity of the resulting solution was plotted with the total hardness concentration. As shown in Figure 4.15, the red color intensity of the resulting solution increased as the total hardness concentration of the water sample increased. The limit of detection of the tablet assay was determined to be 0.0140 mM using the LOD equation ($LOD = X_{b1} + 3S_{b1}$, where X_{b1} is mean concentration of the blank and S_{b1} is the standard deviation of the blank).

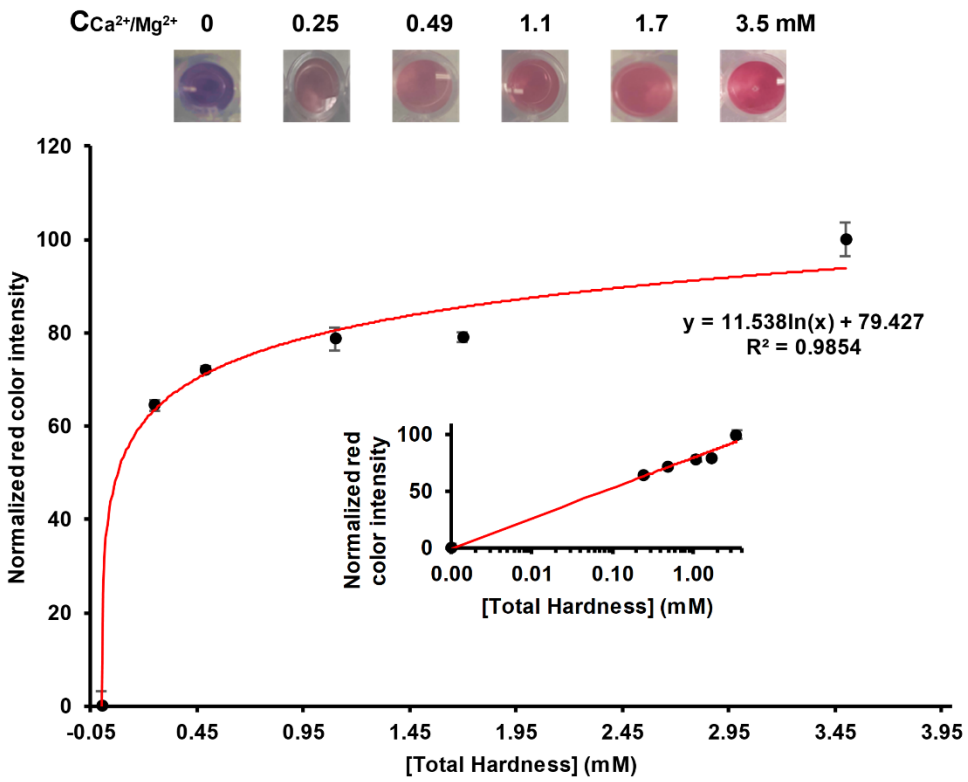

Figure 4-15 Calibration curve for quantitative analysis using the tablet-based sensor. In the graph, the black data points represent the normalized average red color intensities of the assay at each concentration obtained by the ImageJ software. Each point is the mean of the three individual experiments at each concentration ± standard deviation. The smaller linear plot represents the same calibration curve using a logarithm scale on the abscissa.

5.1 Conclusion

Developing low-cost and portable analytical devices are of high importance, especially for remote places, developing countries, and point-of-use testing. Here, we developed a paper-based analytical device with off-the-shelf permanent markers (Sharpie©) along with a regular office printer which together cost less than $1 CAD for the creation of 100 devices. The proposed approach can be of particular interest to laboratories with a very limited budget and/or minimal space to accommodate more advanced equipment such as a laser cutter, XY plotter, photolithography, hot embossing, etc. In addition, in established laboratories that are already equipped with one of those (recently discontinued) Xerox solid ink printers plus the required oven, in case the printer breaks down the presented approach can be considered to resume the experiments instantly without delay. The dip-and-read design of the device also eliminates any requirements for auxiliary equipment. We have demonstrated that the fabricated paper-based analytical device can appropriately detect the total hardness of water quantitatively and qualitatively in accordance with the classification given by the World Health Organization. Using such classification in the design helps the final user to simply determine whether the water is soft, moderately hard, hard, or very hard in about 3 min with the naked eye, and if needs be, quantitative analysis can be conducted to have a numeric value of the total hardness by making use of the calibration curve that was generated. This quantitative calibration curve was generated using a new alternative reaction without the use of EDTA as a standard solution for the detection on the μPAD. To determine the exact value of the water hardness, a smart-phone or a mobile scanner can be used

to analyze the color intensity of the designated sensing zone. The developed μPAD showed a calculated limit of detection (LOD) of 0.02 mM, which is at least 80% less than those of the commercially available test strip and other reported μPADs. In addition, the μPAD demonstrated an excellent stability over a long time at varying temperature conditions and resistance to interference from common water interference ions.

The computation of the fabricated microfluidic paper-based analytical device showed that the response time of the device can be estimated using a geometrically modified Lucas-Washburn equation. The estimation predicted perfectly the flow of liquid water through the hydrophilic channel of the device which makes it feasible to be tailored to various usage by modifying the elution distance. Varying the hydrophilic channel of the fabricated μPAD proved to have no effect on the relation between elution distance and time, hence the design of the device can be utilized for diagnostic analysis involving various numbers of hydrophilic channels. In addition, the μPAD can be utilized for diagnostic analysis on blood samples with accurate predictions based on the modified mathematical equation.

Furthermore, the fabricated pullulan tablets proved to be an effective analytical for the quantification of the total water hardness. This assay brings a testing platform which solves the disadvantages of using paper as substrate and gives results in about five minutes. Also, the limit of detection of the tablet assay was computed to be 0.0140 mM total water hardness.

5.2 Recommendation/Future study

This research was an investigation into the use of commercially available permanent market for the fabrication of μPADs for the detection of the total hardness of water. In additions, pullulan

tablets were utilized for the detection of the total hardness of water which still need some experimental validations. Overall, further investigation into the research can be extended by:

- Performing a wider real-life test analysis from multiple water sources (river, lakes, well, etc) to further validate the performance of the μPAD.
- Reducing the result output time from the present 3 mins, either by optimizing the geometry of the μPAD, or by retrofitting a miniaturized pump system into the μPAD which will allow fast flow of water sample along the hydrophilic channels and without compromising the proper reaction between analytes.
- Electrochemical detection method can be incorporated into the μPAD to further enhance the sensitivity of the device. However, the electrochemical setup should be miniaturized so that the device can still maintain its portability and simplicity.
- Further validation of the all-inclusive pullulan tablets to test for interference ions, real-life sample analysis, sensitivity test, and stability analysis.

REFERENCES

Abe, K., Kotera, K., Suzuki, K., Citterio, D., 2010. Inkjet-printed paperfluidic immuno-chemical sensing device. Anal Bioanal Chem 398, 885–893. https://doi.org/10.1007/s00216-010-4011-2

Abe, K., Suzuki, K., Citterio, D., 2008. Inkjet-printed microfluidic multianalyte chemical sensing paper. Anal. Chem. 80, 6928–6934. https://doi.org/10.1021/ac800604v

Abeliotis, K., Candan, C., Amberg, C., Ferri, A., Osset, M., Owens, J., Stamminger, R., 2015. Impact of water hardness on consumers' perception of laundry washing result in five European countries: Consumer water hardness. International Journal of Consumer Studies 39, 60–66. https://doi.org/10.1111/ijcs.12149

Aksorn, J., Teepoo, S., 2020. Development of the simultaneous colorimetric enzymatic detection of sucrose, fructose and glucose using a microfluidic paper-based analytical device. Talanta 207, 120302. https://doi.org/10.1016/j.talanta.2019.120302

Akyazi, T., Basabe-Desmonts, L., Benito-Lopez, F., 2018. Review on microfluidic paper-based analytical devices towards commercialisation. Analytica Chimica Acta 1001, 1–17. https://doi.org/10.1016/j.aca.2017.11.010

Akyazi, T., Saez, J., Elizalde, J., Benito-Lopez, F., 2016. Fluidic flow delay by ionogel passive pumps in microfluidic paper-based analytical devices. Sensors and Actuators B: Chemical 233, 402–408. https://doi.org/10.1016/j.snb.2016.04.116

Alahmad, W., Uraisin, K., Nacapricha, D., Kaneta, T., 2016. A miniaturized chemiluminescence detection system for a microfluidic paper-based analytical device and its application to the determination of chromium (III). Anal. Methods 8, 5414–5420. https://doi.org/10.1039/C6AY00954A

Allen, P.B., Arshad, S.A., Li, B., Chen, X., Ellington, A.D., 2012. DNA circuits as amplifiers for the detection of nucleic acids on a paperfluidic platform. Lab Chip 12, 2951. https://doi.org/10.1039/c2lc40373k

Almeida, M.I.G.S., Jayawardane, B.M., Kolev, S.D., McKelvie, I.D., 2018. Developments of microfluidic paper-based analytical devices (μPADs) for water analysis: A review. Talanta 177, 176–190. https://doi.org/10.1016/j.talanta.2017.08.072

Apilux, A., Dungchai, W., Siangproh, W., Praphairaksit, N., Henry, C.S., Chailapakul, O., 2010. Lab-on-paper with dual electrochemical/colorimetric detection for simultaneous determination of gold and iron. Anal. Chem. 82, 1727–1732. https://doi.org/10.1021/ac9022555

Arciuli, M., Palazzo, G., Gallone, A., Mallardi, A., 2013. Bioactive paper platform for colorimetric phenols detection. Sensors and Actuators B: Chemical 186, 557–562. https://doi.org/10.1016/j.snb.2013.06.042

Bakker, E., 2018. ion-selective electrodes, in: reference module in chemistry, Molecular Sciences and Chemical Engineering. Elsevier, p. B9780124095472144000. https://doi.org/10.1016/B978-0-12-409547-2.14364-1

Bhattacharjee, T., Jiang, H., Behdad, N., 2013. Sensor design for water hardness detection, in: 2013 IEEE Sensors. Presented at the 2013 IEEE Sensors, IEEE, Baltimore, MD, USA, pp. 1–4. https://doi.org/10.1109/ICSENS.2013.6688443

Boodaghi, M., Shamloo, A., 2020. A comparison of different geometrical elements to model fluid wicking in paper-based microfluidic devices. AIChE J 66. https://doi.org/10.1002/aic.16756

Bruzewicz, D.A., Reches, M., Whitesides, G.M., 2008. Low-Cost Printing of Poly(dimethylsiloxane) Barriers To Define Microchannels in Paper. Anal. Chem. 80, 3387–3392. https://doi.org/10.1021/ac702605a

Butcher, D.J., 2010. Advances in inductively coupled plasma optical emission spectrometry for environmental analysis. instrumentation science & technology 38, 458–469. https://doi.org/10.1080/10739149.2010.517884

Caglayan, M.G., Sheykhi, S., Mosca, L., Anzenbacher, P., 2016. Fluorescent zinc and copper complexes for detection of adrafinil in paper-based microfluidic devices. Chem. Commun. 52, 8279–8282. https://doi.org/10.1039/C6CC03640F

Cai, L., Xu, C., Lin, S., Luo, J., Wu, M., Yang, F., 2014. A simple paper-based sensor fabricated by selective wet etching of silanized filter paper using a paper mask. Biomicrofluidics 8, 056504. https://doi.org/10.1063/1.4898096

Cao, L., Han, G.-C., Xiao, H., Chen, Z., Fang, C., 2020. A novel 3D paper-based microfluidic electrochemical glucose biosensor based on rGO-TEPA/PB sensitive film. Analytica Chimica Acta 1096, 34–43. https://doi.org/10.1016/j.aca.2019.10.049

Carrilho, E., Martinez, A.W., Whitesides, G.M., 2009. Understanding Wax Printing: A Simple Micropatterning Process for Paper-Based Microfluidics. Anal. Chem. 81, 7091–7095. https://doi.org/10.1021/ac901071p

Cassano, C.L., Fan, Z.H., 2013. Laminated paper-based analytical devices (LPAD): fabrication, characterization, and assays. Microfluid Nanofluid 15, 173–181. https://doi.org/10.1007/s10404-013-1140-x

Cate, D.M., Dungchai, W., Cunningham, J.C., Volckens, J., Henry, C.S., 2013. Simple, distance-based measurement for paper analytical devices. Lab Chip 13, 2397. https://doi.org/10.1039/c3lc50072a

Chabaud, K.R., Thomas, J.L., Torres, M.N., Oliveira, S., McCord, B.R., 2018. Simultaneous colorimetric detection of metallic salts contained in low explosives residue using a microfluidic paper-based analytical device (μPAD). Forensic Chemistry 9, 35–41. https://doi.org/10.1016/j.forc.2018.03.008

Chaiyo, S., Apiluk, A., Siangproh, W., Chailapakul, O., 2016. High sensitivity and specificity simultaneous determination of lead, cadmium and copper using μPAD with dual electrochemical and colorimetric detection. Sensors and Actuators B: Chemical 233, 540–549. https://doi.org/10.1016/j.snb.2016.04.109

Channon, R.B., Yang, Y., Feibelman, K.M., Geiss, B.J., Dandy, D.S., Henry, C.S., 2018. Development of an electrochemical paper-based analytical device for trace detection of virus particles. Anal. Chem. 90, 7777–7783. https://doi.org/10.1021/acs.analchem.8b02042

Chen, G.-H., Chen, W.-Y., Yen, Y.-C., Wang, C.-W., Chang, H.-T., Chen, C.-F., 2014. Detection of mercury(ii) ions using colorimetric gold nanoparticles on paper-based analytical devices. Anal. Chem. 86, 6843–6849. https://doi.org/10.1021/ac5008688

Chiang, C.-K., Kurniawan, A., Kao, C.-Y., Wang, M.-J., 2019. Single step and mask-free 3D wax printing of microfluidic paper-based analytical devices for glucose and nitrite assays. Talanta 194, 837–845. https://doi.org/10.1016/j.talanta.2018.10.104

Ching, T., Li, Y., Karyappa, R., Ohno, A., Toh, Y.-C., Hashimoto, M., 2019. Fabrication of integrated microfluidic devices by direct ink writing (DIW) 3D printing. Sensors and Actuators B: Chemical 297, 126609. https://doi.org/10.1016/j.snb.2019.05.086

Cotruvo, J.A., Costello, R., Weglicki, W.B., 2017. Public health -- magnesium, hard water, and health. jawwa 109, 62–68. https://doi.org/10.5942/jawwa.2017.109.0146

Credou, J., Berthelot, T., 2014. Cellulose: from biocompatible to bioactive material. J. Mater. Chem. B 2, 4767–4788. https://doi.org/10.1039/C4TB00431K

Criscuolo, F., Taurino, I., Stradolini, F., Carrara, S., De Micheli, G., 2018. Highly-stable Li+ ion-selective electrodes based on noble metal nanostructured layers as solid-contacts. Analytica Chimica Acta 1027, 22–32. https://doi.org/10.1016/j.aca.2018.04.062

Cunningham, J.C., Brenes, N.J., Crooks, R.M., 2014. Paper electrochemical device for detection of dna and thrombin by target-induced conformational switching. Anal. Chem. 86, 6166–6170. https://doi.org/10.1021/ac501438y

Curto, V.F., Lopez-Ruiz, N., Capitan-Vallvey, L.F., Palma, A.J., Benito-Lopez, F., Diamond, D., 2013. Fast prototyping of paper-based microfluidic devices by contact stamping using indelible ink. RSC Adv. 3, 18811. https://doi.org/10.1039/c3ra43825b

de Oliveira, T.R., Fonseca, W.T., de Oliveira Setti, G., Faria, R.C., 2019. Fast and flexible strategy to produce electrochemical paper-based analytical devices using a craft cutter printer to create wax barrier and screen-printed electrodes. Talanta 195, 480–489. https://doi.org/10.1016/j.talanta.2018.11.047

De Schampheleire, S., De Kerpel, K., Ameel, B., De Jaeger, P., Bagci, O., De Paepe, M., 2016. A discussion on the interpretation of the darcy equation in case of open-cell metal foam based on numerical simulations. Materials 9, 409. https://doi.org/10.3390/ma9060409

de Tarso Garcia, P., Garcia Cardoso, T.M., Garcia, C.D., Carrilho, E., Tomazelli Coltro, W.K., 2014. A handheld stamping process to fabricate microfluidic paper-based analytical devices with chemically modified surface for clinical assays. RSC Adv. 4, 37637–37644. https://doi.org/10.1039/C4RA07112C

Delaney, J.L., Hogan, C.F., Tian, J., Shen, W., 2011. Electrogenerated chemiluminescence detection in paper-based microfluidic sensors. Anal. Chem. 83, 1300–1306. https://doi.org/10.1021/ac102392t

Demirel, G., Babur, E., 2014. Vapor-phase deposition of polymers as a simple and versatile technique to generate paper-based microfluidic platforms for bioassay applications. Analyst 139, 2326–2331. https://doi.org/10.1039/C4AN00022F

Devadhasan, J.P., Kim, J., 2018. A chemically functionalized paper-based microfluidic platform for multiplex heavy metal detection. Sensors and Actuators B: Chemical 273, 18–24. https://doi.org/10.1016/j.snb.2018.06.005

Dornelas, K.L., Dossi, N., Piccin, E., 2015. A simple method for patterning poly(dimethylsiloxane) barriers in paper using contact-printing with low-cost rubber stamps. Analytica Chimica Acta 858, 82–90. https://doi.org/10.1016/j.aca.2014.11.025

Dossi, N., Toniolo, R., Pizzariello, A., Impellizzieri, F., Piccin, E., Bontempelli, G., 2013. Pencil-drawn paper supported electrodes as simple electrochemical detectors for paper-based fluidic devices: Microfluidics and Miniaturization. ELECTROPHORESIS 34, 2085–2091. https://doi.org/10.1002/elps.201200425

Dungchai, W., Chailapakul, O., Henry, C.S., 2011. A low-cost, simple, and rapid fabrication method for paper-based microfluidics using wax screen-printing. Analyst 136, 77–82. https://doi.org/10.1039/C0AN00406E

e Silva, R.F., Longo Cesar Paixão, T.R., Der Torossian Torres, M., de Araujo, W.R., 2020. Simple and inexpensive electrochemical paper-based analytical device for sensitive detection of Pseudomonas aeruginosa. Sensors and Actuators B: Chemical 308, 127669. https://doi.org/10.1016/j.snb.2020.127669

Evans, E., Gabriel, E.F.M., Coltro, W.K.T., Garcia, C.D., 2014. Rational selection of substrates to improve color intensity and uniformity on microfluidic paper-based analytical devices. Analyst 139, 2127–2132. https://doi.org/10.1039/C4AN00230J

Fan, Y., Huang, Y., Linthicum, W., Liu, F., Beringhs, A.O., Dang, Y., Xu, Z., Chang, S.-Y., Ling, J., Huey, B.D., Suib, S.L., Ma, A.W.K., Gao, P.-X., Lu, X., Lei, Y., Shaw, M.T., Li, B., 2020. Toward long-term accurate and continuous monitoring of nitrate in wastewater using poly(tetrafluoroethylene) (PTFE)–solid-state ion-selective electrodes (S-ISEs). ACS Sens. 5, 3182–3193. https://doi.org/10.1021/acssensors.0c01422

Fenton, E.M., Mascarenas, M.R., López, G.P., Sibbett, S.S., 2009. Multiplex lateral-flow test strips fabricated by two-dimensional shaping. ACS Appl. Mater. Interfaces 1, 124–129. https://doi.org/10.1021/am800043z

Firdaus, M.L., Aprian, A., Meileza, N., Hitsmi, M., Elvia, R., Rahmidar, L., Khaydarov, R., 2019. Smartphone coupled with a paper-based colorimetric device for sensitive and portable mercury ion sensing. Chemosensors 7, 25. https://doi.org/10.3390/chemosensors7020025

Gao, C., Su, M., Wang, Y., Ge, S., Yu, J., 2015. A disposable paper-based electrochemiluminescence device for ultrasensitive monitoring of CEA based on $Ru(bpy)_3^{2+}$@Au nanocages. RSC Adv. 5, 28324–28331. https://doi.org/10.1039/C5RA00393H

Garcia-Cordero, J.L., Fan, Z.H., 2017. Sessile droplets for chemical and biological assays. Lab Chip 17, 2150–2166. https://doi.org/10.1039/C7LC00366H

Ge, L., Yan, J., Song, X., Yan, M., Ge, S., Yu, J., 2012. Three-dimensional paper-based electrochemiluminescence immunodevice for multiplexed measurement of biomarkers and point-of-care testing. Biomaterials 33, 1024–1031. https://doi.org/10.1016/j.biomaterials.2011.10.065

Haller, P.D., Flowers, C.A., Gupta, M., 2011. Three-dimensional patterning of porous materials using vapor phase polymerization. Soft Matter 7, 2428. https://doi.org/10.1039/c0sm01214a

He, P.J.W., Katis, I.N., Eason, R.W., Sones, C.L., 2015. Laser-based patterning for fluidic devices in nitrocellulose. Biomicrofluidics 9, 026503. https://doi.org/10.1063/1.4919629

He, Q., Ma, C., Hu, X., Chen, H., 2013. Method for fabrication of paper-based microfluidic devices by alkylsilane self-assembling and uv/o $_3$ -patterning. Anal. Chem. 85, 1327–1331. https://doi.org/10.1021/ac303138x

Health Canada, 2019. Guidelines for canadian drinking water quality—summary table. Water and Air Quality Bureau, Healthy Environments and Consumer Safety Branch, Health Canada, Ottawa, Ontario.

Health Metric, n.d. URL https://www.health-metric.com/products/well-water-test-kit (accessed 9.7.20).

Henares, T.G., Yamada, K., Takaki, S., Suzuki, K., Citterio, D., 2017. “Drop-slip” bulk sample flow on fully inkjet-printed microfluidic paper-based analytical device. Sensors and Actuators B: Chemical 244, 1129–1137. https://doi.org/10.1016/j.snb.2017.01.088

Hildebrand, G.P., Reilley, C.N., 1957. New indicator for complexometric titration of calcium in presence of magnesium. Anal. Chem. 29, 258–264. https://doi.org/10.1021/ac60122a025

HoneForest, n.d. URL http://www.honeforest.net/product/water-hardness-test-strips/ (accessed 9.7.20).

Hsieh, P.-Y., Monsur Ali, M., Tram, K., Jahanshahi-Anbuhi, S., Brown, C.L., Brennan, J.D., Filipe, C.D.M., Li, Y., 2017. RNA protection is effectively achieved by pullulan film formation. ChemBioChem 18, 502–505. https://doi.org/10.1002/cbic.201600643

Hsu, H., 2010. Particle Movement in Paper Porous Media: Influence Factors and Model.

Jahanshahi-Anbuhi, S., Chavan, P., Sicard, C., Leung, V., Hossain, S.M.Z., Pelton, R., Brennan, J.D., Filipe, C.D.M., 2012. Creating fast flow channels in paper fluidic devices to control timing of sequential reactions. Lab Chip 12, 5079. https://doi.org/10.1039/c2lc41005b

Jahanshahi-Anbuhi, S., Henry, A., Leung, V., Sicard, C., Pennings, K., Pelton, R., Brennan, J.D., Filipe, C.D.M., 2014a. Paper-based microfluidics with an erodible polymeric bridge giving controlled release and timed flow shutoff. Lab Chip 14, 229–236. https://doi.org/10.1039/C3LC50762A

Jahanshahi-Anbuhi, S., Pennings, K., Leung, V., Kannan, B., Brennan, J.D., Filipe, C.D.M., Pelton, R.H., 2015. Design rules for fluorocarbon-free omniphobic solvent barriers in paper-based devices. ACS Applied Materials & Interfaces 7, 25434–25440. https://doi.org/10.1021/acsami.5b08301

Jahanshahi-Anbuhi, S., Pennings, K., Leung, V., Liu, M., Carrasquilla, C., Kannan, B., Li, Y., Pelton, R., Brennan, J.D., Filipe, C.D.M., 2014b. Pullulan encapsulation of labile biomolecules to give stable bioassay tablets. Angew. Chem. Int. Ed. 53, 6155–6158. https://doi.org/10.1002/anie.201403222

Jahanshahi-Anbuhi, S., Pennings, K., Leung, V., Liu, M., Carrasquilla, C., Kannan, B., Li, Y., Pelton, R., Brennan, J.D., Filipe, C.D.M., 2014c. Pullulan encapsulation of labile biomolecules to give stable bioassay tablets. Angewandte Chemie International Edition 53, 6155–6158. https://doi.org/10.1002/anie.201403222

Jarujamrus, P., Meelapsom, R., Naksen, P., Ditcharoen, N., Anutrasakda, W., Siripinyanond, A., Amatatongchai, M., Supasorn, S., 2019. Screen-printed microfluidic paper-based analytical device (μPAD) as a barcode sensor for magnesium detection using rubber latex waste as a novel hydrophobic reagent. Analytica Chimica Acta 1082, 66–77. https://doi.org/10.1016/j.aca.2019.06.058

Jayawardane, B.M., McKelvie, I.D., Kolev, S.D., 2012. A paper-based device for measurement of reactive phosphate in water. Talanta 100, 454–460. https://doi.org/10.1016/j.talanta.2012.08.021

Jayawardane, B.M., Wei, S., McKelvie, I.D., Kolev, S.D., 2014a. Microfluidic paper-based analytical device for the determination of nitrite and nitrate. Anal. Chem. 86, 7274–7279. https://doi.org/10.1021/ac5013249

Jayawardane, B.M., Wongwilai, W., Grudpan, K., Kolev, S.D., Heaven, M.W., Nash, D.M., McKelvie, I.D., 2014b. Evaluation and application of a paper-based device for the determination of reactive phosphate in soil solution. J. Environ. Qual. 43, 1081–1085. https://doi.org/10.2134/jeq2013.08.0336

Jeong, S.-G., Lee, S.-H., Choi, C.-H., Kim, J., Lee, C.-S., 2015. Toward instrument-free digital measurements: a three-dimensional microfluidic device fabricated in a single sheet of paper by double-sided printing and lamination. Lab Chip 15, 1188–1194. https://doi.org/10.1039/C4LC01382D

Jiang, Y., Hao, Z., He, Q., Chen, H., 2016. A simple method for fabrication of microfluidic paper-based analytical devices and on-device fluid control with a portable corona generator. RSC Adv. 6, 2888–2894. https://doi.org/10.1039/C5RA23470K

Juang, Y.-J., Chen, P.-S., Wang, Y., 2019. Rapid fabrication of microfluidic paper-based analytical devices by microembossing. Sensors and Actuators B: Chemical 283, 87–92. https://doi.org/10.1016/j.snb.2018.12.004

Juang, Y.-J., Li, W.-S., Chen, P.-S., 2017. Fabrication of microfluidic paper-based analytical devices by filtration-assisted screen printing. Journal of the Taiwan Institute of Chemical Engineers 80, 71–75. https://doi.org/10.1016/j.jtice.2017.08.007

Kannan, B., Jahanshahi-Anbuhi, S., Pelton, R.H., Li, Y., Filipe, C.D.M., Brennan, J.D., 2015a. Printed paper sensors for serum lactate dehydrogenase using pullulan-based inks to immobilize reagents. Analytical Chemistry 87, 9288–9293. https://doi.org/10.1021/acs.analchem.5b01923

Kannan, B., Jahanshahi-Anbuhi, S., Pelton, R.H., Li, Y., Filipe, C.D.M., Brennan, J.D., 2015b. Printed paper sensors for serum lactate dehydrogenase using pullulan-based inks to immobilize reagents. Anal. Chem. 87, 9288–9293. https://doi.org/10.1021/acs.analchem.5b01923

Kao, P.-K., Hsu, C.-C., 2014. One-step rapid fabrication of paper-based microfluidic devices using fluorocarbon plasma polymerization. Microfluid Nanofluid 16, 811–818. https://doi.org/10.1007/s10404-014-1347-5

Karita, S., Kaneta, T., 2016. Chelate titrations of Ca^{2+} and Mg^{2+} using microfluidic paper-based analytical devices. Analytica Chimica Acta 924, 60–67. https://doi.org/10.1016/j.aca.2016.04.019

Kelly, B.C., Gobas, F.A.P.C., McLachlan, M.S., 2004. Intestinal absorption and biomagnification of organic contaminants in fish, wildlife, and humans. Environ Toxicol Chem 23, 2324. https://doi.org/10.1897/03-545

Kim, S.C., Jalal, U.M., Im, S.B., Ko, S., Shim, J.S., 2017. A smartphone-based optical platform for colorimetric analysis of microfluidic device. Sensors and Actuators B: Chemical 239, 52–59. https://doi.org/10.1016/j.snb.2016.07.159

Koop, S.H.A., van Leeuwen, C.J., 2017. The challenges of water, waste and climate change in cities. Environ Dev Sustain 19, 385–418. https://doi.org/10.1007/s10668-016-9760-4

Kudo, H., Yamada, K., Watanabe, D., Suzuki, K., Citterio, D., 2017. Paper-based analytical device for zinc ion quantification in water samples with power-free analyte concentration. Micromachines 8, 127. https://doi.org/10.3390/mi8040127

Kwong, P., Gupta, M., 2012. Vapor phase deposition of functional polymers onto paper-based microfluidic devices for advanced unit operations. Anal. Chem. 84, 10129–10135. https://doi.org/10.1021/ac302861v

Lerga, T.M., O'Sullivan, C.K., 2008. Rapid determination of total hardness in water using fluorescent molecular aptamer beacon. Analytica Chimica Acta 610, 105–111. https://doi.org/10.1016/j.aca.2008.01.031

Leung, V., Mapletoft, J., Zhang, A., Lee, A., Vahedi, F., Chew, M., Szewczyk, A., Jahanshahi-Anbuhi, S., Ang, J., Cowbrough, B., Miller, M.S., Ashkar, A., Filipe, C.D.M., 2019. Thermal stabilization of viral vaccines in low-cost sugar films. Scientific Reports 9, 7631. https://doi.org/10.1038/s41598-019-44020-w

Leung, V., Shehata, A.-A.M., Filipe, C.D.M., Pelton, R., 2010. Streaming potential sensing in paper-based microfluidic channels. Colloids and Surfaces A: Physicochemical and Engineering Aspects 364, 16–18. https://doi.org/10.1016/j.colsurfa.2010.04.008

Leurs, L.J., Schouten, L.J., Mons, M.N., Goldbohm, R.A., van den Brandt, P.A., 2010. Relationship between tap water hardness, magnesium, and calcium concentration and mortality due to ischemic heart disease or stroke in the Netherlands. Environmental Health Perspectives 118, 414–420. https://doi.org/10.1289/ehp.0900782

Li, H., Fang, X., Cao, H., Kong, J., 2016. Paper-based fluorescence resonance energy transfer assay for directly detecting nucleic acids and proteins. Biosensors and Bioelectronics 80, 79–83. https://doi.org/10.1016/j.bios.2015.12.065

Li, L., Zhang, Y., Liu, F., Su, M., Liang, L., Ge, S., Yu, J., 2015. Real-time visual determination of the flux of hydrogen sulphide using a hollow-channel paper electrode. Chem. Commun. 51, 14030–14033. https://doi.org/10.1039/C5CC05710H

Li, W., Qian, D., Wang, Q., Li, Y., Bao, N., Gu, H., Yu, C., 2016. Fully drawn origami paper analytical device for electrochemical detection of glucose. Sensors and Actuators B: Chemical 231, 230–238. https://doi.org/10.1016/j.snb.2016.03.031

Li, X., Liu, X., 2014. Fabrication of three-dimensional microfluidic channels in a single layer of cellulose paper. Microfluid Nanofluid 16, 819–827. https://doi.org/10.1007/s10404-014-1340-z

Li, X., Tian, J., Garnier, G., Shen, W., 2010a. Fabrication of paper-based microfluidic sensors by printing. Colloids and Surfaces B: Biointerfaces 76, 564–570. https://doi.org/10.1016/j.colsurfb.2009.12.023

Li, X., Tian, J., Nguyen, T., Shen, W., 2008. Paper-Based Microfluidic Devices by Plasma Treatment. Anal. Chem. 80, 9131–9134. https://doi.org/10.1021/ac801729t

Li, X., Tian, J., Shen, W., 2010b. Progress in patterned paper sizing for fabrication of paper-based microfluidic sensors. Cellulose 17, 649–659. https://doi.org/10.1007/s10570-010-9401-2

Liang, J., Huang, Y., Zhang, F., Zhang, Y., Li, N., Chen, Y., 2014. The use of graphene oxide membranes for the softening of hard water. Sci. China Technol. Sci. 57, 284–287. https://doi.org/10.1007/s11431-014-5467-7

Liang, L., Su, M., Li, L., Lan, F., Yang, G., Ge, S., Yu, J., Song, X., 2016. Aptamer-based fluorescent and visual biosensor for multiplexed monitoring of cancer cells in microfluidic paper-based analytical devices. Sensors and Actuators B: Chemical 229, 347–354. https://doi.org/10.1016/j.snb.2016.01.137

Liu, C., Gomez, F.A., Miao, Y., Cui, P., Lee, W., 2019. A colorimetric assay system for dopamine using microfluidic paper-based analytical devices. Talanta 194, 171–176. https://doi.org/10.1016/j.talanta.2018.10.039

Liu, H., Crooks, R.M., 2011. Three-dimensional paper microfluidic devices assembled using the principles of origami. J. Am. Chem. Soc. 133, 17564–17566. https://doi.org/10.1021/ja2071779

Liu, W., Kou, J., Xing, H., Li, B., 2014. Paper-based chromatographic chemiluminescence chip for the detection of dichlorvos in vegetables. Biosensors and Bioelectronics 52, 76–81. https://doi.org/10.1016/j.bios.2013.08.024

Liu, Z., Hu, J., Zhao, Y., Qu, Z., Xu, F., 2015. Experimental and numerical studies on liquid wicking into filter papers for paper-based diagnostics. Applied Thermal Engineering 88, 280–287. https://doi.org/10.1016/j.applthermaleng.2014.09.057

Lu, J., Ge, S., Ge, L., Yan, M., Yu, J., 2012. Electrochemical DNA sensor based on three-dimensional folding paper device for specific and sensitive point-of-care testing. Electrochimica Acta 80, 334–341. https://doi.org/10.1016/j.electacta.2012.07.024

Lu, Y., Shi, W., Jiang, L., Qin, J., Lin, B., 2009. Rapid prototyping of paper-based microfluidics with wax for low-cost, portable bioassay. Electrophoresis 30, 1497–1500. https://doi.org/10.1002/elps.200800563

Mace, C.R., Deraney, R.N., 2014. Manufacturing prototypes for paper-based diagnostic devices. Microfluid Nanofluid 16, 801–809. https://doi.org/10.1007/s10404-013-1314-6

Madhu, N.T., Resmi, P.E., Pradeep, A., Satheesh Babu, T.G., 2019. Design and simulation of fluid flow in paper based microfluidic platforms. IOP Conf. Ser.: Mater. Sci. Eng. 577, 012104. https://doi.org/10.1088/1757-899X/577/1/012104

Maejima, K., Tomikawa, S., Suzuki, K., Citterio, D., 2013. Inkjet printing: an integrated and green chemical approach to microfluidic paper-based analytical devices. RSC Adv. 3, 9258. https://doi.org/10.1039/c3ra40828k

Maj-Zurawska, M., Rouilly, M., Morf, W.E., Simon, W., 1989. Determination of magnesium and calcium in water with ion-selective electrodes. Analytica Chimica Acta 218, 47–59. https://doi.org/10.1016/S0003-2670(00)80281-0

Mani, V., Kadimisetty, K., Malla, S., Joshi, A.A., Rusling, J.F., 2013. Paper-based electrochemiluminescent screening for genotoxic activity in the environment. Environ. Sci. Technol. 47, 1937–1944. https://doi.org/10.1021/es304426j

Marquez, S., Liu, J., Morales-Narváez, E., 2019. Paper-based analytical devices in environmental applications and their integration with portable technologies. Current Opinion in Environmental Science & Health 10, 1–8. https://doi.org/10.1016/j.coesh.2019.08.002

Martinez, A.W., Phillips, S.T., Butte, M.J., Whitesides, G.M., 2007. Patterned paper as a platform for inexpensive, low-volume, portable bioassays. Angew. Chem. Int. Ed. 46, 1318–1320. https://doi.org/10.1002/anie.200603817

Masoodi, R., Pillai, K.M., 2010. Darcy's law-based model for wicking in paper-like swelling porous media. AIChE J. NA-NA. https://doi.org/10.1002/aic.12163

Maxwell, E.J., Mazzeo, A.D., Whitesides, G.M., 2013. Paper-based electroanalytical devices for accessible diagnostic testing. MRS Bull. 38, 309–314. https://doi.org/10.1557/mrs.2013.56

Meier, P.C., Erne, D., Cimerman, Z., Ammann, D., Simon, W., 1980. Direct potentiometric water hardness determination using ion-selective electrodes. Mikrochim Acta 73, 317–327. https://doi.org/10.1007/BF01196318

Mohammadi, S., Maeki, M., Mohamadi, R.M., Ishida, A., Tani, H., Tokeshi, M., 2015. An instrument-free, screen-printed paper microfluidic device that enables bio and chemical sensing. Analyst 140, 6493–6499. https://doi.org/10.1039/C5AN00909J

Mora, M.F., Garcia, C.D., Schaumburg, F., Kler, P.A., Berli, C.L.A., Hashimoto, M., Carrilho, E., 2019. Patterning and modeling three-dimensional microfluidic devices fabricated on a single sheet of paper. Anal. Chem. 91, 8298–8303. https://doi.org/10.1021/acs.analchem.9b01020

Mott, C.R., Walnutport Pa., 1992. Aqueous permanent coloring composition for a marker. United States Patent 8.

Müller, R.H., Clegg, D.L., 1949. Automatic paper chromatography. Anal. Chem. 21, 1123–1125. https://doi.org/10.1021/ac60033a032

Myers, N.M., Kernisan, E.N., Lieberman, M., 2015. Lab on paper: iodometric titration on a printed card. Anal. Chem. 87, 3764–3770. https://doi.org/10.1021/ac504269q

Nantaphol, S., Kava, A.A., Channon, R.B., Kondo, T., Siangproh, W., Chailapakul, O., Henry, C.S., 2019. Janus electrochemistry: simultaneous electrochemical detection at multiple working conditions in a paper-based analytical device. Analytica Chimica Acta 1056, 88–95. https://doi.org/10.1016/j.aca.2019.01.026

Nguyen, M.P., Meredith, N.A., Kelly, S.P., Henry, C.S., 2018. Design considerations for reducing sample loss in microfluidic paper-based analytical devices. Analytica Chimica Acta 1017, 20–25. https://doi.org/10.1016/j.aca.2018.01.036

Nguyen, V.-T., Song, S., Park, S., Joo, C., 2020. Recent advances in high-sensitivity detection methods for paper-based lateral-flow assay. Biosensors and Bioelectronics 152, 112015. https://doi.org/10.1016/j.bios.2020.112015

Nogueira, S.A., Lemes, A.D., Chagas, A.C., Vieira, M.L., Talhavini, M., Morais, P.A.O., Coltro, W.K.T., 2019. Redox titration on foldable paper-based analytical devices for the visual determination of alcohol content in whiskey samples. Talanta 194, 363–369. https://doi.org/10.1016/j.talanta.2018.10.036

Nuchtavorn, N., Macka, M., 2016. A novel highly flexible, simple, rapid and low-cost fabrication tool for paper-based microfluidic devices (μPADs) using technical drawing

pens and in-house formulated aqueous inks. Analytica Chimica Acta 919, 70–77. https://doi.org/10.1016/j.aca.2016.03.018

Ohzawa, Y., Nomura, K., Sugiyama, K., 1998. Relation between porosity and pore size or pressure drop of fibrous SiC filter prepared from carbonized cellulose-powder preforms. Materials Science and Engineering: A 255, 33–38. https://doi.org/10.1016/S0921-5093(98)00773-4

Olkkonen, J., Lehtinen, K., Erho, T., 2010. Flexographically printed fluidic structures in paper. Anal. Chem. 82, 10246–10250. https://doi.org/10.1021/ac1027066

Ostad, M.A., Hajinia, A., Heidari, T., 2017. A novel direct and cost-effective method for fabricating paper-based microfluidic device by commercial eye pencil and its application for determining simultaneous calcium and magnesium. Microchemical Journal 133, 545–550. https://doi.org/10.1016/j.microc.2017.04.031

OuYang, L., Wang, C., Du, F., Zheng, T., Liang, H., 2014. Electrochromatographic separations of multi-component metal complexes on a microfluidic paper-based device with a simplified photolithography. RSC Adv. 4, 1093–1101. https://doi.org/10.1039/C3RA43625J

Rahbar, M., Wheeler, A.R., Paull, B., Macka, M., 2019. Ion-exchange based immobilization of chromogenic reagents on microfluidic paper analytical devices. Anal. Chem. 91, 8756–8761. https://doi.org/10.1021/acs.analchem.9b01288

Rattanarat, P., Dungchai, W., Cate, D.M., Siangproh, W., Volckens, J., Chailapakul, O., Henry, C.S., 2013. A microfluidic paper-based analytical device for rapid quantification of particulate chromium. Analytica Chimica Acta 800, 50–55. https://doi.org/10.1016/j.aca.2013.09.008

Rosa, A.M.M., Louro, A.F., Martins, S.A.M., Inácio, J., Azevedo, A.M., Prazeres, D.M.F., 2014. Capture and detection of dna hybrids on paper via the anchoring of antibodies with fusions of carbohydrate binding modules and zz-domains. Anal. Chem. 86, 4340–4347. https://doi.org/10.1021/ac5001288

Rosenson, R.S., McCormick, A., Uretz, E.F., 1996. Distribution of blood viscosity values and biochemical correlates in healthy adults. Clin. Chem. 42, 1189–1195.

Rosina, J., Kvasnák, E., Suta, D., Kolárová, H., Málek, J., Krajci, L., 2007. Temperature dependence of blood surface tension. Physiol Res 56 Suppl 1, S93-98.

Ruecha, N., Rodthongkum, N., Cate, D.M., Volckens, J., Chailapakul, O., Henry, C.S., 2015. Sensitive electrochemical sensor using a graphene–polyaniline nanocomposite for simultaneous detection of Zn(II), Cd(II), and Pb(II). Analytica Chimica Acta 874, 40–48. https://doi.org/10.1016/j.aca.2015.02.064

Saleh, M.A., Ewane, E., Jones, J., Wilson, B.L., 2000. Monitoring Wadi El Raiyan lakes of the egyptian desert for inorganic pollutants by ion-selective electrodes, ion chromatography, and inductively coupled plasma spectroscopy. Ecotoxicology and Environmental Safety 45, 310–316. https://doi.org/10.1006/eesa.1999.1881

Sanborn, K.B., Loftin, R.M., 1998. Permanent aqueous marker inks. United States Patent 4.

Santhiago, M., Henry, C.S., Kubota, L.T., 2014. Low cost, simple three-dimensional electrochemical paper-based analytical device for determination of p-nitrophenol. Electrochimica Acta 130, 771–777. https://doi.org/10.1016/j.electacta.2014.03.109

Satarpai, T., Shiowatana, J., Siripinyanond, A., 2016. Paper-based analytical device for sampling, on-site preconcentration and detection of ppb lead in water. Talanta 154, 504–510. https://doi.org/10.1016/j.talanta.2016.04.017

Sengupta, P., 2013. Potential health impacts of hard water. Int J Prev Med 4, 866–875.

Shariati-Rad, M., Heidari, S., 2020. Classification and determination of total hardness of water using silver nanoparticles. Talanta 219, 121297. https://doi.org/10.1016/j.talanta.2020.121297

Shih, W.-C., Yang, M.-C., Lin, M.S., 2009. Development of disposable lipid biosensor for the determination of total cholesterol. Biosensors and Bioelectronics 24, 1679–1684. https://doi.org/10.1016/j.bios.2008.08.055

Sicard, C., Glen, C., Aubie, B., Wallace, D., Jahanshahi-Anbuhi, S., Pennings, K., Daigger, G.T., Pelton, R., Brennan, J.D., Filipe, C.D.M., 2015. Tools for water quality monitoring and mapping using paper-based sensors and cell phones. Water Research 70, 360–369. https://doi.org/10.1016/j.watres.2014.12.005

Silveira, C., Monteiro, T., Almeida, M., 2016. Biosensing with paper-based miniaturized printed electrodes–a modern trend. Biosensors 6, 51. https://doi.org/10.3390/bios6040051

Sones, C.L., Katis, I.N., He, P.J.W., Mills, B., Namiq, M.F., Shardlow, P., Ibsen, M., Eason, R.W., 2014. Laser-induced photo-polymerisation for creation of paper-based fluidic devices. Lab Chip 14, 4567–4574. https://doi.org/10.1039/C4LC00850B

Songjaroen, T., Dungchai, W., Chailapakul, O., Henry, C.S., Laiwattanapaisal, W., 2012. Blood separation on microfluidic paper-based analytical devices. Lab Chip 12, 3392. https://doi.org/10.1039/c2lc21299d

Songjaroen, T., Dungchai, W., Chailapakul, O., Laiwattanapaisal, W., 2011. Novel, simple and low-cost alternative method for fabrication of paper-based microfluidics by wax dipping. Talanta 85, 2587–2593. https://doi.org/10.1016/j.talanta.2011.08.024

Spicar-Mihalic, P., Toley, B., Houghtaling, J., Liang, T., Yager, P., Fu, E., 2013. CO $_2$ laser cutting and ablative etching for the fabrication of paper-based devices. J. Micromech. Microeng. 23, 067003. https://doi.org/10.1088/0960-1317/23/6/067003

Sun, G., Wang, P., Ge, S., Ge, L., Yu, J., Yan, M., 2014. Photoelectrochemical sensor for pentachlorophenol on microfluidic paper-based analytical device based on the molecular imprinting technique. Biosensors and Bioelectronics 56, 97–103. https://doi.org/10.1016/j.bios.2014.01.001

Sun, H., Li, W., Dong, Z.-Z., Hu, C., Leung, C.-H., Ma, D.-L., Ren, K., 2018. A suspending-droplet mode paper-based microfluidic platform for low-cost, rapid, and convenient detection of lead (II) ions in liquid solution. Biosensors and Bioelectronics 99, 361–367. https://doi.org/10.1016/j.bios.2017.07.073

Sun, J.-Y., Cheng, C.-M., Liao, Y.-C., 2015. Screen printed paper-based diagnostic devices with polymeric inks. Anal. Sci. 31, 145–151. https://doi.org/10.2116/analsci.31.145

Szűcs, J., Gyurcsányi, R.E., 2012. Towards protein assays on paper platforms with potentiometric detection. electroanalysis 24, 146–152. https://doi.org/10.1002/elan.201100522

Tabani, H., Dorabadi Zare, F., Alahmad, W., Varanusupakul, P., 2020. Determination of Cr (III) and Cr (VI) in water by dual-gel electromembrane extraction and a microfluidic paper-based device. Environ Chem Lett 18, 187–196. https://doi.org/10.1007/s10311-019-00921-w

Tan, W., Zhang, L., Doery, J.C.G., Shen, W., 2020. Three-dimensional microfluidic tape-paper-based sensing device for blood total bilirubin measurement in jaundiced neonates. Lab Chip 20, 394–404. https://doi.org/10.1039/C9LC00939F

Tasaengtong, B., Sameenoi, Y., 2020. A one-step polymer screen-printing method for fabrication of microfluidic cloth-based analytical devices. Microchemical Journal 105078. https://doi.org/10.1016/j.microc.2020.105078

Thomas Scientific, n.d. URL https://www.thomassci.com/Laboratory-Supplies/Water-Quality-Test-Strips/_/Total-Hardness-Test-Strips?q=Test%20Strips%20Total%20Hardness (accessed 9.7.20).

Tóth, K., Lindner, E., Horváth, M., Jeney, J., Pungor, E., Bitter, I., Ágai, B., Töke, L., 1993. Analytical performances of lipophilic diamides based alkaline earth ion-selective electrodes. Electroanalysis 5, 781–790. https://doi.org/10.1002/elan.1140050911

Tsunogai, S., 1968. Complexometric titration of calcium in the presence of larger amounts of magnesium. Talanta 15, 385–390. https://doi.org/10.1016/0039-9140(68)80247-4

van der Werf, I.D., Germinario, G., Palmisano, F., Sabbatini, L., 2011. Characterisation of permanent markers by pyrolysis gas chromatography–mass spectrometry. Anal Bioanal Chem 399, 3483–3490. https://doi.org/10.1007/s00216-011-4714-z

Verissimo, M., Oliveira, J., Gomes, M., 2007. Determination of the total hardness in tap water using acoustic wave sensors. Sensors and Actuators B: Chemical 127, 102–106. https://doi.org/10.1016/j.snb.2007.07.006

Wang, J., Monton, M.R.N., Zhang, X., Filipe, C.D.M., Pelton, R., Brennan, J.D., 2014. Hydrophobic sol–gel channel patterning strategies for paper-based microfluidics. Lab Chip 14, 691–695. https://doi.org/10.1039/C3LC51313K

Wang, S., Ge, L., Zhang, Y., Song, X., Li, N., Ge, S., Yu, J., 2012. Battery-triggered microfluidic paper-based multiplex electrochemiluminescence immunodevice based on potential-resolution strategy. Lab Chip 12, 4489. https://doi.org/10.1039/c2lc40707h

Wang, Y., Xu, H., Luo, J., Liu, J., Wang, L., Fan, Y., Yan, S., Yang, Y., Cai, X., 2016. A novel label-free microfluidic paper-based immunosensor for highly sensitive electrochemical detection of carcinoembryonic antigen. Biosensors and Bioelectronics 83, 319–326. https://doi.org/10.1016/j.bios.2016.04.062

World Health Organization, 2010. Hardness in drinking water: background document for development of WHO guidelines for drinking water quality.

Wu, Q., He, J., Meng, H., Wang, Y., Zhang, Y., Li, H., Feng, L., 2019. A paper-based microfluidic analytical device combined with home-made SPE column for the colorimetric determination of copper (II) ion. Talanta 204, 518–524. https://doi.org/10.1016/j.talanta.2019.06.006

Wu, X., Kuang, H., Hao, C., Xing, C., Wang, L., Xu, C., 2012. Paper supported immunosensor for detection of antibiotics. Biosensors and Bioelectronics 33, 309–312. https://doi.org/10.1016/j.bios.2012.01.017

Xerox Inc., n.d. URL https://www.xerox.com/en-us/office/solid-ink (accessed 3.17.20).

Xia, Y., Si, J., Li, Z., 2016. Fabrication techniques for microfluidic paper-based analytical devices and their applications for biological testing: A review. Biosensors and Bioelectronics 77, 774–789. https://doi.org/10.1016/j.bios.2015.10.032

Xu, C., Cai, L., Zhong, M., Zheng, S., 2015. Low-cost and rapid prototyping of microfluidic paper-based analytical devices by inkjet printing of permanent marker ink. RSC Adv. 5, 4770–4773. https://doi.org/10.1039/C4RA13195A

Yamada, K., Citterio, D., Henry, C.S., 2018. “Dip-and-read” paper-based analytical devices using distance-based detection with color screening. Lab Chip 18, 1485–1493. https://doi.org/10.1039/C8LC00168E

Yamada, K., Takaki, S., Komuro, N., Suzuki, K., Citterio, D., 2014. An antibody-free microfluidic paper-based analytical device for the determination of tear fluid lactoferrin by fluorescence sensitization of Tb3+. Analyst 139, 1637. https://doi.org/10.1039/c3an01926h

Yang, C.-H., Shi, X.-H., Yuan, J.-H., 2014. Study on the Application of Raman Spectroscopy on Detecting Water Hardness. water environ res 86, 417–420. https://doi.org/10.2175/106143013X13807328849936

Yehia, A.M., Farag, M.A., Tantawy, M.A., 2020. A novel trimodal system on a paper-based microfluidic device for on-site detection of the date rape drug "ketamine." Analytica Chimica Acta 1104, 95–104. https://doi.org/10.1016/j.aca.2020.01.002

Yu, J., Ge, L., Huang, J., Wang, S., Ge, S., 2011a. Microfluidic paper-based chemiluminescence biosensor for simultaneous determination of glucose and uric acid. Lab Chip 11, 1286. https://doi.org/10.1039/c0lc00524j

Yu, J., Wang, S., Ge, L., Ge, S., 2011b. A novel chemiluminescence paper microfluidic biosensor based on enzymatic reaction for uric acid determination. Biosensors and Bioelectronics 26, 3284–3289. https://doi.org/10.1016/j.bios.2010.12.044

Zangheri, M., Cevenini, L., Anfossi, L., Baggiani, C., Simoni, P., Di Nardo, F., Roda, A., 2015. A simple and compact smartphone accessory for quantitative chemiluminescence-based lateral flow immunoassay for salivary cortisol detection. Biosensors and Bioelectronics 64, 63–68. https://doi.org/10.1016/j.bios.2014.08.048

Zhu, X., Xiong, S., Zhang, J., Zhang, X., Tong, X., Kong, S., 2018. Improving paper-based ELISA performance through covalent immobilization of antibodies. Sensors and Actuators B: Chemical 255, 598–604. https://doi.org/10.1016/j.snb.2017.08.090

APPENDICES

A. Estimation of the response time of the paper-based device

A.1 Estimating the signal time for the microfluidics paper-based analytical device

The voluntary absorption of liquid up a paper matrix is known as wicking. It is accomplished through capillary force interaction between the paper media and the liquid molecules. This capillary force is spontaneous, without the need for an external force. The capillary force during wicking is as a result of capillary suction buildup on the interface of dry and wet matrix of the paper media. The wicking predominantly occurs when the interaction of the liquid molecules and the molecules of the paper medium is greater than the mutual interaction between the liquid molecules (Masoodi and Pillai, 2010; Ohzawa et al., 1998). Examples of wicking phenomenon includes the soaking of liquid with cotton towels, tissue paper, washing sponge, wipes and napkins. Industrially, wicking is used in cleaning of industrial spills by absorbing pads and towels, addition of moisture to fabrics in the fabric manufacturing plants etc. This phenomenon is also greatly used in the pulp and paper industry during the manufacturing processes (Masoodi and Pillai, 2010).

The wicking efficiency of different kinds of paper is of great importance in the pulp and paper industry. Furthermore, in the fabrication of paper-based analytical devices, the wicking efficiency of the used paper type contributes greatly to the overall efficiency of the device (Madhu et al., 2019). Several scientists and research groups have reported the use of several grades and types of paper for the manufacturing of sensors. The grades commonly used are the Whatman® grade 4 filter paper, the Whatman® grade 4 chromatography paper, the Whatman® grade 1 filter paper, the Whatman® grade 2 filter paper and the Whatman® grade 3 filter paper. All these grades and

types of paper have different pore sizes and thickness which contributes greatly to the wicking ability of the paper.

Wicking in paper is categorized to be in the laminar flow region as the fluid moves gently across the matrix of the paper (Boodaghi and Shamloo, 2020; Madhu et al., 2019; Masoodi and Pillai, 2010). This makes it less complex to mathematically model the flow regime using available flow regime equations. The Lucas-Washburn equation and the Darcy equation are the two traditional methods that have been used to mathematically model the wicking phenomenon in paper. The Lucas-Washburn equation assumes a paper to be made of capillary tubes arranged sequentially in parallel to make up a paper matrix, and flow in one dimension. The Lucas-Washburn equation is designed specifically for simple paper strips with regular rectangular prism geometry as shown in Figure A.1. Hence, the equation will need modifications in order to use it for irregular geometries apart from the rectangular prism paper strip. The Darcy's law on the other hand relates the average velocity of liquid flow to the pressure gradient within the paper. Wicking is generally dependent on liquid property, macro and microstructure of the porous media and wicking time (Boodaghi and Shamloo, 2020; De Schampheleire et al., 2016; Madhu et al., 2019; Masoodi and Pillai, 2010).

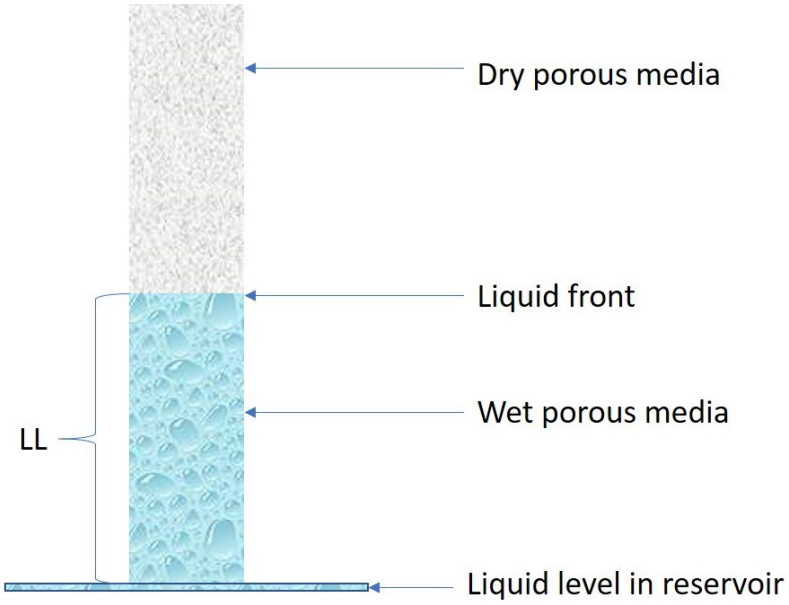

Figure A.1 Schematic diagram of a porous media rectangular strip modelled by the Lucas – Washburn's equation.

Due to the laminar flow regime along paper matrix of the Whatman© filter paper used for fabricating the paper-based analytical device utilized in this project, the Lucas-Washburn equation was used to perform the time estimation analysis. Since the equation assumes a bundle of capillary tubes, the Hagen -Poiseuille equation is used to model the flow along the tubes, neglecting gravity.

$$\frac{4 \cdot \gamma \cdot Cos(\theta)}{D_c} = \frac{32 \cdot \mu \cdot LL}{D_h^2} \frac{dL}{dt} \tag{A.1}$$

$$D_e = \frac{D_h^2}{D_c} \tag{A.2}$$

$$r = \frac{D_e}{2} \tag{A.3}$$

Where μ = Viscosity of liquid [Pa.s]

γ = Surface tension of liquid [N/m]

L = Height of the rising liquid font in the paper [m]

θ = The contact angle of liquid with the paper substrate [deg.]

t = Time taken for liquid to rise the capillary tubes [s]

D_c = Capillary pore diameter [m]

D_h = Hydraulic pore diameter [m]

D_e = Effective pore diameter [m]

r = Effective radius [m]

Hence mathematical integration of equation (A.1) and incorporating equations (A.2) and (A.3) gives Equation (A.4) below.

$$L = \sqrt{\frac{\gamma \cdot r \cdot \cos(\theta) \cdot t}{4 \cdot \mu}} \tag{A.4}$$

In order to allow the use of the design of the fabricated μPAD (Fig. 3.1a) for other testing applications, the Lucas-Washburn equation was utilized. The time it takes the device to give the result output was computed using the Lucas-Washburn equation. The Lucas-Washburn equation however works for regular shaped paper strip (Figure A.1). Since the design of the μPAD is irregular, the Lucas-Washburn equation was modified to fit the present design of the μPAD. In order to achieve this, a geometric correction factor constant was computed and introduced into the

Lucas Washburn's equation to account for the irregular geometry of the μPAD. The modified Lucas-Washburn equation is given in equation A.5. below;

$$L = \Psi \sqrt{\frac{\gamma \cdot r \cdot \cos(\theta) \cdot t}{4 \cdot \mu}} \tag{A.5}$$

Where Ψ = Geometric correction factor [-]

μ = Viscosity of liquid [Pa.s]

γ = Surface tension of liquid [N/m]

L = Height of the rising liquid font in the paper [m]

θ = The contact angle of liquid with the paper substrate [deg.]

t = Time taken for liquid to rise the capillary tubes [s]

r = Effective radius of paper substrate [m]

The liquid used for this analysis is HPLC grade water and its properties are assumed to be the same with deionized water. The viscosity (μ) is assumed to be 8.49×10^{-4} Pa.s. The surface tension (γ) is taken to be 72×10^{-3} N/m. The contact angle (θ) of the water on the Whatman® grade 4 filter paper is assumed to be zero since the water molecule travels along the hydrophilic matrix of the paper. The relative humidity of the experiment surrounding was between 30 – 40 % which according to the study done by Hsu (Hsu, 2010) has no significant effect on the elution distance at that range of relative humidity. Also, the effect of evaporation was neglected due to the small height of the hydrophilic channel of the μPAD (Hsu, 2010; Liu et al., 2015).

A.2 Determination of the effective radius and the correction factor.

In order to determine the value of the geometric correction factor (Ψ) of the fabricated device, the effective radius of the Whatman® grade 4 filter paper is needed. The pore diameter given by the manufacture is 20- 25 µm, which often varies from the effective dimension needed to be utilized for mathematical calculations. In order to determine the effective radius of the Whatman® grade 4 filter paper, the result of the elution distance as shown in Figure 4.1 was utilized with the Lucas – Washburn equation. As shown in Figure 4.1, the average elution velocity of HPLC grade water in Whatman® grade 4 filter paper (paper strip of dimensions 4 cm × 0.5 cm) is 269.66 ± 4.3 µm/s. Hence, the average time taken for the HPLC grade water to move up the 4 cm mark is 148 s. These known values of elution distance and time with other known liquid properties was incorporated into the Lucas - Washburn equation to compute an effective radius (r) of 2.55×10^{-7} m (Appendix B). This value of effective radius is then used for subsequent calculations. In this Investigation, the 'plain µPAD' is defined as the µPAD without EDTA and EBT in the reaction and detection zones respectively, and the 'full µPAD' is defined as the µPAD with EDTA and EBT in the reaction and detection zones respectively.

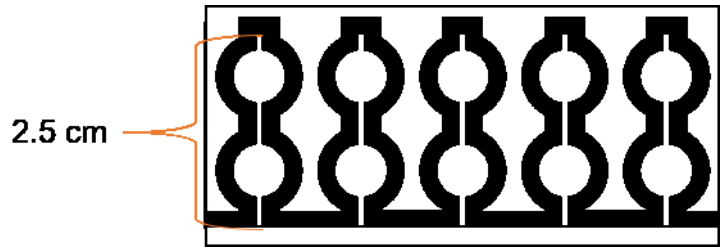

Figure A.2 Schematic diagram of microfluidic paper-based analytical device showing the height of the hydrophilic channels.

Furthermore, the average time for HPLC grade water to completely fill up the hydrophilic channel of the plain µPAD (without EDTA and EBT) of height 2.5 cm (Figure A.2) was determined

experimentally. It was determined that it takes 113 seconds to fill up the plain μPAD channels. Hence, using the value of the height of the μPAD channels as the elution distance, the average time to completely fill up the channels (113 s) as the time, and the value of the computed effective radius (2.55×10^{-7} m), the geometric correction factor (Ψ) was calculated using the Modified Lucas–Washburn equation (Equation A.5). The value of the geometric correction factor (Ψ) was then determined to be 0.7152 (Appendix B), that is $\Psi = 0.7152$.

A.3 Application of Modified Lucas Washburn's Equation to the Fabricated Device.

The Lucas-Washburn equation (without the geometric correction factor) was computed using the effective radius value already determined and other properties of the liquid and paper substrate given in section A.1 (viscosity of liquid, surface tension of liquid, the contact angle of the liquid on the paper substrate). Figure A.3(a) shows the relationship between the time and elution distance of the paper strip computed by the Lucas - Washburn equation without the correction factor. Figure A.3(c) on the other hand shows the experimental values gotten from the μPAD for the relationship between the elution distance and time. The large discrepancy between the data gotten from the paper strip and that of the experimental values of the μPAD shows that the Lucas – Washburn equation (without the geometry correction factor) cannot accurately predict the elution distance versus time relationship of the fabricated μPAD. This is due to the irregular geometry of the fabricated μPAD as against the regular geometry of the paper strip.

On the other hand, Figure A.3(b) shows the relation between elution distance versus time as computed with the modified Lucas – Washburn's equation. This modified-version data follows perfectly the trend gotten through the experimental values. Hence the modified Lucas – Washburn's equation predicted accurately the flow of HPLC grade water along the hydrophobic

channel of the µPAD. This showed that the geometric correction factor accurately modified the Lucas-Washburn equation to predict the behaviour of fabricated µPAD.

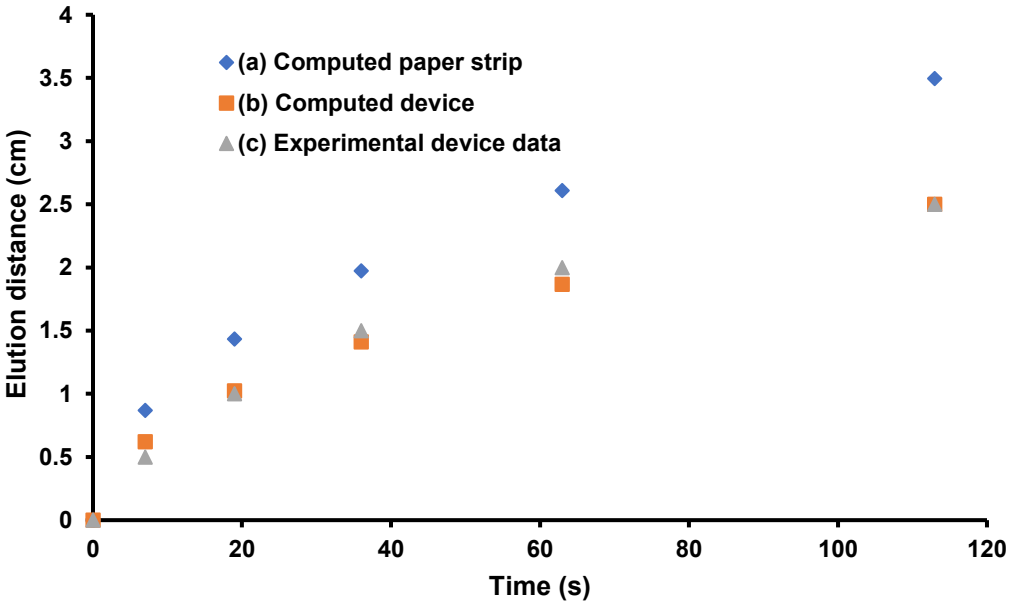

Figure A.3 Graph showing the relationship between elution distance and time determined with the (a) Lucas –Washburn equation on the computed paper strip,(b) Modified Lucas-Washburn equation on the µPAD,(c) experimental observation of the wicking of the µPAD.

A.4 Effect of bulk channel on the microfluidic paper-based analytical device.

The µPAD design utilized in this study contains 5 channels. The effect of combination of these channels over time taken for HPLC grade water to fill up the device completely was investigated. Hence, the time taken to fill the µPAD containing one channel (Figure A.4a), two Channels (Figure A.4b), three channels (Figure A.4c), four channels (Figure A.4d) and five channels (Figure A.4e) were studied. This was achieved by dipping the µPAD of varying channel into HPLC grade water, and the time it takes to fill up the device was recorded.

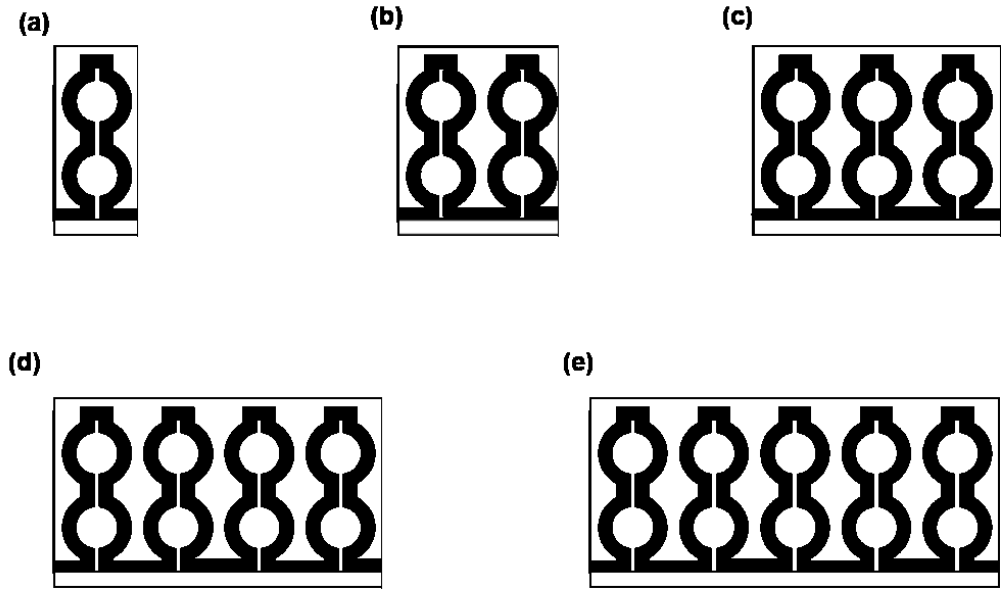

Figure A.4 Design of microfluidic paper-based analytical device with (a) one hydrophilic channel, (b) two hydrophilic channels, (c) three hydrophilic channels, (d) four hydrophilic channels, (e) five hydrophilic channels.

As shown in Figure A.5, the μPAD having varying channels from one to five have similar elution distance versus time curve. This evidently proved that varying the number of channels in the design of the μPAD doesn't change the elution distance versus time response. Hence, the number of channels of the device can be manipulated and adapted for other usages apart from the afore studied total hardness detection and still retain its elution distance versus time response.

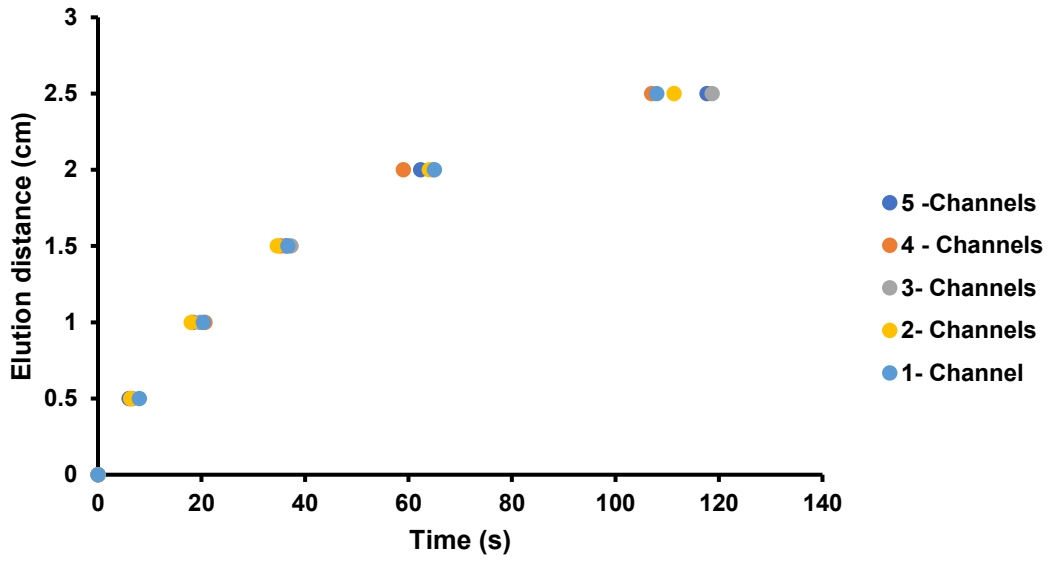

Figure A.5 Graph showing the effect of varying the number of hydrophilic channels in the microfluidic paper-based analytic device on the time it takes to fill up the device.

A.5 Determination of the Actual Signal Time on the Device for the Detection of the Total Hardness of Water

The time delay caused by the presence of analytes on the µPAD was investigated. This was achieved by comparative analysis between time taken to fill up the empty µPAD (without EDTA and EBT at the reactions and the detection zones) with HPLC grade water only, the empty µPAD with spiked water sample of 3.0 mM $CaCO_3$ equivalent total hardness only, and the full µPAD (with EDTA and EBT at the reactions and the detection zones) with spiked sample of 3.0 mM $CaCO_3$ equivalent water.

It took 113 s to fill up the empty µPAD with HPLC grade water only and 114 s with the spiked water sample of 3.0 mM $CaCO_3$ equivalent total hardness. In addition, it takes 172 s to fill up the full µPAD with the spiked water sample of 3.0 mM $CaCO_3$ equivalent total hardness. Hence, the time lag caused by the analytes present and the reactions that took place in the µPAD was calculated as the difference between the time taken to fill up the empty µPAD with HPLC grade

water only and the time taken to fill up the full μPAD with the spiked water sample of 3.0 mM $CaCO_3$ equivalent total hardness. This gave a value of 59 s. Therefore, using the simulation graph given in Figure A.3 and the lag time caused by the analytes and the complexometric titration on the μPAD, the actual signal time of the device can be determined; which is 113 s + 59 s = 172 s (≈ 3 minutes). This computed signal time of ≈ 3 minutes correlates with the eye-observed time of about 3 minutes reported in section 4.1.3 and Figure 4.5.

A.6 Reliability for biological assay

The usage of the fabricated μPAD for biological diagnostic was computed by considering the flow of blood serum on the device. The modified Lucas – Washburn equation was used for the simulation by incorporating pre-existing data determined in the previous sections.

For the analysis, the viscosity of blood serum was taken to be 1.5×10^{-3} Pa.s (Rosenson et al., 1996), the surface tension of blood serum was taken to be 52×10^{-3} N/m (Rosina et al., 2007), the contact angle of blood serum on the hydrophilic channel of the device was assumed to be zero, the effective radius of the Whatman® grade 4 filter paper was 2.55×10^{-7} m, and the geometric correction factor was 0.7154.

As shown in Fig. A.6, the time it will take to fill up the device with blood serum is 275 s (4 min 45 s), which apparently takes longer when compared to the case of HPLC grade water. This longer time can be largely attributed to the higher viscosity of blood serum (1.5×10^{-3} Pa.s) in comparison to the HPLC grade water (8.49×10^{-4} Pa.s). This 275 s time serves as the least waiting time for result output by colorimetric display when blood serum is used as the sample liquid. Any additional time will be the time delay caused by the reactions occurring at the different zones and the amount of analytes on the hydrophilic channel. These 275 s time can be reduced by decreasing the height

of the hydrophilic channel of the µPAD. If the height of the hydrophilic channel of the µPAD is reduced to 1.5 cm, then it will take about 113 s seconds for blood serum to fill up the device as shown in Figure A.6. Hence, the height of the hydrophilic channel of the device can be reduced in order to have a shorter response time.

Therefore, this computation makes it possible to predict the least time for the µPAD to display a colorimetric result if used for biological diagnostics with blood serum as the sample.

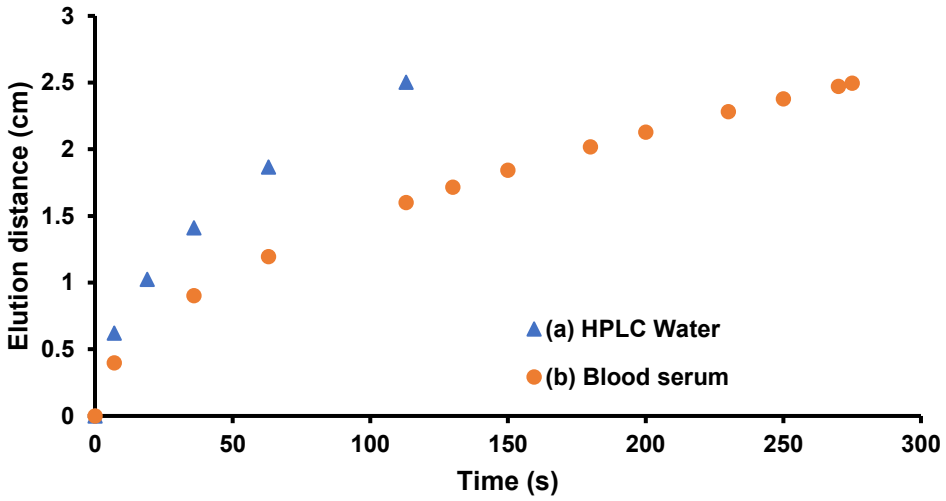

Figure A.6 Graph showing the relationship between elution distance versus time for the fabricated µPAD using (a) HPLC grade water as the sample and (b) human blood serum as the sample.

B. SAMPLE CALCULATION OF THE EFFECTIVE RADIUS AND THE GEOMETRIC CORRECTION FACTOR

I. Calculation of the effective radius 'r'

$$L = \sqrt{\frac{\gamma \cdot r \cdot \cos(\theta) \cdot t}{4 \cdot \mu}}$$

µ = Viscosity of liquid [Pa.s] = 72 $\times 10^{-3}$ N/m

γ = Surface tension of liquid [N/m] = 8.49 $\times$ 10^{-4} Pa.s

L = Height of the rising liquid font in the paper (paper strip) [m]= 4 cm

θ = The contact angle of liquid with the paper substrate [deg.] = 0 °

t = Time taken for liquid to rise the capillary tubes [s] = 148 s

r = Effective radius of paper substrate [m] = ?

$$4 \times 10^{-2}\ \text{m} = \sqrt{\frac{(8.49 \times 10^{-4}\ \text{Pa.s}) \cdot (r) \cdot (\cos(0)) \cdot (148\ s)}{4 \cdot (72 \times 10^{-3}\ \text{N/m})}}$$

$$\therefore r = 2.55 \times 10^{-7}\ m$$

II. Calculation of the Geometric correction factor 'Ψ'

$$L = \Psi \sqrt{\frac{\gamma \cdot r \cdot \cos(\theta) \cdot t}{4 \cdot \mu}}$$

Ψ = Geometric correction factor [-] = ?

μ = Viscosity of liquid [Pa.s] = 72 ×10^{-3} N/m

γ = Surface tension of liquid [N/m] = 8.49 × 10^{-4} Pa.s

L = Height of the rising liquid font in the paper (Device channel) [m] = 2.5 cm

θ = The contact angle of liquid with the paper substrate [deg.] = 0 °

t = Time taken for liquid to rise the capillary tubes [s] = 113 s

r = Effective radius of paper substrate [m] = $2.55 \times 10^{-7}\ m$

$$2.5 \times 10^{-2}\ \text{m} = \Psi \sqrt{\frac{(8.49 \times 10^{-4}\ \text{Pa.s}) \cdot (2.55 \times 10^{-7}\ m) \cdot (\cos(0)) \cdot (113\ s)}{4 \cdot (72 \times 10^{-3}\ \text{N/m})}}$$

$$\therefore \Psi = 0.7152$$